MAYFLOWER WIND

Appendix F3. Hydrodynamic and Sediment Transport Modeling for the Brayton Point Export Cable Burial Assessment

Document Revision A

Issue Date March 2022

Hydrodynamic and Sediment Transport Modeling for the Brayton Point Export Cable Burial Assessment

Mayflower Wind Energy LLC | USA

01 March 2022 - Final Report

Daniel L. Mendelsohn, Innovative Environmental Science
J. Craig Swanson, Swanson Environmental

Swanson Environmental

IES Innovative Environmental Science

EXECUTIVE SUMMARY

Mayflower Wind Energy LLC (Mayflower Wind) is in the process of developing an offshore wind renewable energy generation project (Project) located in federal waters off the southern coast of Massachusetts in the Outer Continental Shelf (OCS) Lease Area OCS-A 0521 (Lease Area). The Project will deliver electricity to the grid via subsea export cables installed within the Brayton Point Export Cable Corridor (ECC) that will make landfall at Brayton Point in Somerset, Massachusetts and via subsea export cables installed within the Falmouth ECC that will make landfall in Falmouth, Massachusetts.

The Brayton Point ECC, which is the focus of this report, has been defined through which the export cables will run from the Lease Area to landfall at Brayton Point. For this study, it is assumed that the cables will be buried with a trench depth of approximately 3 m (9.8 ft) using one or more of several burial methods, which may include use of jet trenching and mechanical trenching. For purposes of this study, jet trenching is considered as the worst-case representative burial scenario. A jet-trencher uses high pressure jets to fluidize the seabed sediments forcing some fraction of them into the water column through the burial process. This report presents an assessment of sediment plume dispersion (Total Suspended Solids [TSS] in the water column and seabed deposits) associated with the installation of the export cables between the Lease Area and Brayton Point landing(s), including the nearshore horizontal directional drilling (HDD) entry points that will be used to bring the cable ashore. In alignment with the Bureau of Ocean Energy Management (BOEM) guidelines, for the Construction and Operations Plan (COP) (BOEM, 2020), this study addresses the following:

- Concentrations of excess sediment suspended in the water column (as total suspended solids) following seafloor disturbance during cable installation
- Extent and thickness of sediment re-deposited to the seafloor following suspension.

A regional and local high-resolution, site-specific hydrodynamic model application was developed to simulate the metocean conditions over the extent of the offshore and nearshore / Narragansett Bay segments (i.e Mount Hope Bay and the Sakonnet River) of the Brayton Point ECC. The model was verified and validated against site-specific measurements and then applied to drive scenarios of the sediment plume dispersion from trenching and HDD-related dredging activities.

Surface sediment grab sample data was collected along the ECC at 23 sites used in the modeling. The data showed that the nearshore / Narragansett Bay segments were mostly characterized by high fractions of the fine grade silt and clay sediment classes. Offshore, the sediments tended to have higher fractions of fine sand to coarse sand classes with an occasional pocket of silt or very fine sand.

The results of the sediment dispersion modeling indicated that the water column concentration (TSS) and the sediment deposition pattern and thickness were most heavily influenced by the properties of the trench sediments (i.e. grain size distribution) disturbed during the jet trenching operations and localized current velocities. The dimensions of the trench, the advance rate, and the loss rate (a conservative loss rate of 25 percent representative of the jetting or mechanical trenching and 100 percent for the HDD pit dredging) to the water column, specified the total amount of sediments re-suspended, but the response was short lived for all but the finest grade sediments (silts and clays).

Suspended Sediment Concentrations

The fine- grained classes settle more slowly than the larger grain size sediments meaning that the suspended silt and clay sediments tend to be transported farther with the tidal currents than coarser sediments, increasing higher water column concentrations and durations of plumes. The Mount Hope Bay and the Sakonnet River segments, where higher fractions of fine-grained silt and clay are found in the sediments, exhibit this impact. The higher- level concentrations (100 mg/L and up) were somewhat contained in the Sakonnet River but covered a larger area in Mount Hope Bay where a part of the export cables ran perpendicular to the currents which, combined with the fine grade resuspended sediments, increased the overall material transport extending the maximum 100 mg/L concentration a little over 1 km (0.62 mi). Concentrations reached levels of 500 mg/L but were short lived and persist for approximately 30 minutes to an hour. Concentrations in the range of 200 mg/L or more were not expected to endure for longer than about 2 hours, while the lowest concentrations, in the 10 mg/L range may last many hours after re-suspension.

In regions with large grain sizes, sediments quickly dropped back to the sea floor keeping concentrations low, and within a few meters of the Trenching tool. The associated deposition footprint area was also small. Concentrations of 100mg/L were predicted to be within 50 m (160 ft) of the route centerline and decreased rapidly (less than 15 minutes). The sections of the offshore ECC segment that had higher fractions of the fine grade sediments had higher transport of the model predicted TSS concentrations showing the 100 mg/L concentration extending to 300 m (984 ft). The 100 mg/L TSS concentration level or greater covered a total of 2,457 ha (6,070 ac) along the 152 km (94 mi) length of the Brayton Point ECC.

The HDD exit pit dredging impacts were smaller compared with the impact resulting from cable installation. The source was assumed to be at a single point and continuous over a 1-hour period, releasing 100 percent of the dredged material into the water column. The TSS concentrations exceeding 100 mg/L travelled a maximum distance of 0.32 km (0.2 mi) and dissipated in a little over an hour at the Brayton Point site but were half that at the Aquidneck Island sites. The area coverage of the 100 mg/L or greater level was contained within an average of 5 ha (12 ac).

Sediment Deposition Coverage and Thickness

The sediment deposition footprint resulting from the cable installation activities occurred relatively locally along the majority of the ECC route where the mass settles out quickly. Deposition thicknesses of 1 mm (0.04 in) and greater are generally limited to a corridor with a maximum width of 30 - 35 m (100 – 115 ft) around the cable centerline. In the areas where there are finer grain sediments, the 1 mm (0.04 in) thickness contour distance can increase locally to 165 m (540 ft) from the ECC indicative centerline .

The sedimentation footprint for HDD sites was very small with a maximum coverage of the 1 mm (0.04 in) thickness contour of only 0.5 ha (1.2 ac), extending a maximum distance of 95 m (312 ft) and 1 ha (2.5 ac) for the 0.5 mm (0.02 in) thickness contour, extending a maximum distance of 158 m (518 ft) from the HDD site. Deposition thicknesses are greater if the location of the release is fixed. Cable burial operations are mobile, and thus will produce smaller maximum deposit thicknesses. The total coverage of the 1 mm (0.04 in) and 0.5 mm (0.02 in) thickness levels along the entire ECC route was 361 ha (892 ac) and 531 ha (1,312 ac), respectively.

New sediment data received since the completion of the sediment transport and dispersion study indicates that in the lower Mount Hope Bay and upper Sakonnet River areas there is a divergence from the surface grabs used in the present study. New data points where vertical profiles of the sediments were taken near the East Passage entrance to Mount Hope Bay show considerably coarser material. The same is true for stations near the mid- to upper-mid portion of the Sakonnet River. The increased prevalence of coarser grain sizes in the distribution would have the effect of reducing the amount of material transported and therefore area of higher concentrations, also reducing deposition and thickness as reported in Section 4 and therefore have less of an impact. Model results should be considered very conservative for these areas.

In summary, despite conservative model assumptions, water column TSS concentrations and seabed deposition sediment thickness and extent as a result of the cable installation/burial operations and HDD exit pit dredging remain generally localized and of short duration.

TABLE OF CONTENTS

Executive Summary iii

1 Introduction 1-1

1.1 Project Objective 1-1

1.2 Project Description 1-1

2 Methodology 2-1

2.1 Hydrodynamic Model 2-2

2.2 Hydrodynamic Model Technical Description 2-2

2.3 Sediment Transport Model 2-4

2.4 Sediment Model Technical Description 2-4

3 Hydrodynamic Modeling 3-1

3.1 Hydrodynamic Model Application 3-1

3.2 Environmental Forcing 3-3

3.3 Model Validation Results 3-5

3.4 Validation of Model Predicted Water Surface Elevations 3-5

3.5 Validation of Model Predicted Currents 3-11

3.6 Project Scenario 3-16

4 Sediment Transport Modeling 4-1

4.1 Brayton Point Export Cable Corridor Description 4-1

4.2 Sediment Source Terms 4-3

4.3 Export Cable Corridor Sediment Characteristics 4-4

4.4 Brayton Point ECC Sediment Model Application 4-6

4.5 Sediment Transport Model Results 4-7

4.6 Water Column Concentration 4-8

4.7 Sediment Deposition on the Seabed 4-21

5 Discussion and Conclusions 5-1

6 References 6-1

Appendix 1 - Brayton Point ECC Surface Sediment Grab Sample Grain Size Distribution 6-1

LIST OF FIGURES

Figure 1-1. Overview of the Project Area and Brayton Point Export Cable Corridor. 1-2
Figure 3-1. Large Grid and Bathymetry DeVeloped for the Hydrodynamic Model Application. 3-1
Figure 3-2. Higher Resolution Nested Grid of Narragansett Bay with a Focus on the Sakonnet River and Mount Hope Bay also Showing the Gridded Bathymetry. 3-2
Figure 3-3. Time Series of Wind Speeds During the Hydrodynamic Model Validation Period. 3-3
Figure 3-4. Wind Rose for the Hydrodynamic Model Validation Period. Data from the Mayflower Wind Offshore Metocean Buoy. 3-4
Figure 3-5. Observation Stations Used for Developing Model Forcing and Model Validation. Inset Shows A SUBSET of kilometer (KP) Markers Along Brayton Point ECC Indicative Centerline. 3-5
Figure 3-6. Comparison of Modeled and Observed Water Surface Elevations at NOAA Sandy Hook, Montauk, Woods Hole, and Nantucket Tide Stations. Water Surface Elevations are Plotted Relative to MSL. 3-8
Figure 3-7. Comparison of Modeled and Observed Water Surface Elevations at NOAA Newport, Providence, Quonset Point, and Fall River Tide Stations. Water Surface Elevations are Plotted Relative to MSL. 3-9
Figure 3-8. CComparison of Modeled and NOAA Predicted Current Speed at Fall River. 3-12
Figure 3-9. Comparison of Modeled and Observed Bottom Current Speed at the Offshore Mayflower Wind Metocean Buoy. 3-13
Figure 3-10. Comparison of Modeled and Observed Bottom Direction at the Offshore Mayflower Wind Metocean Buoy. 3-13
Figure 3-11. Peak Ebb (Top) and Flood (Bottom) Current Speeds. 3-15
Figure 3-12. Current Roses from Model PredIcted Bottom Currents At Points Along ECC. 3-17
Figure 4-1. Map of the Brayton Point ECC Showing the Segments Used for Results Discussion and the Locations of the HDD Connection Sites Analyzed. 4-2
Figure 4-2. Grain Size Distribution Along the Brayton Point Export Cable Corridor. (MAYFLOWER WIND, 2021A) 4-5
Figure 4-3. Map of Maximum Sediment Concentration in the Mount Hope Bay Portion of the Export Cable Installation, KP0 to KP10. 4-9
Figure 4-4. Map of Maximum Sediment Concentration in the Sakonnet River Portion of the Export Cable Installation, KP15 to KP34. 4-10
Figure 4-5. Map of an Example Instantaneous Sediment Concentration at in the Sakonnet River Portion of the Export Cable Installation, KP15 to KP34. 4-11
Figure 4-6. Map of Maximum Sediment Concentration Associated with the Offshore Export Cable Installation, KP34 to KP55. 4-14
Figure 4-7. Map of Maximum Sediment Concentration Associated with the Offshore Export Cable Installation, KP55 to KP78. 4-15
Figure 4-8. Map of Maximum Sediment Concentration Associated with the Offshore Export Cable Installation, KP78 to KP105. 4-16
Figure 4-9. Map of Maximum Sediment Concentration Associated with the Offshore Export Cable Installation, KP105 to KP125. 4-17

Figure 4-10. Map of Maximum Sediment Concentration Associated with the Offshore Export Cable Installation, KP125 to KP152. 4-18
Figure 4-11. Map of Maximum Sediment Concentration Associated with the Excavation Activities at the Three HDD Connection Pits at Brayton Point (Left Map), and Mount Hope Bridge and Aquidneck Island (Right Map). 4-20
Figure 4-12. Map of Maximum Seabed Sediment Deposition Thickness in the Mount Hope Bay Portion of the Export Cable Installation, KP0 to KP10 4-23
Figure 4-13. Map of Maximum Seabed Sediment Deposition Thickness in the Sakonnet River Portion of the Export Cable Installation, KP15 to KP34 4-24
Figure 4-14. Map of Maximum Seabed Sediment Deposition Along the First Part of Offshore Segment 1 of the Export Cable Installation, KP34 to KP55. 4-26
Figure 4-15. Map of Maximum Seabed Sediment Deposition Along the Second Part of Offshore Segment 1 of the Export Cable Installation, KP55 to KP78. 4-27
Figure 4-16. Map of Maximum Seabed Sediment Deposition Along the First Third of Offshore Segment 2 of the Export Cable Installation, KP78 to KP105. 4-28
Figure 4-17. Map of Maximum Seabed Sediment Deposition Along the Middle Third of Offshore Segment 2 of the Export Cable Installation, KP105 to KP125 4-29
Figure 4-18. Map of Maximum Seabed Sediment Deposition Along the Last Third of Offshore Segment 2 of the Export Cable Installation, KP125 to KP152. 4-30
Figure 4-19. Map of Maximum Seabed Sediment Deposition Associated with the Excavation Activities at the Three HDD Connection Pits at Brayton Point (Left Map), and Mount Hope Bridge and Aquidneck Island (Right Map) 4-32

LIST OF TABLES

Table 2-1. Breakdown of Sediment Classifications by Particle Diameter. 2-6
Table 3-1. Percentiles of Wind Speeds During the Hydrodynamic Model Validation Period as Recorded at the Mayflower Wind Offshore Metocean Buoy. 3-4
Table 3-2. Tidal Harmonic Constituent Characteristics (NOAA, 2007). 3-6
Table 3-3. Summary of Statistics at Water Surface Elevation Observation Stations Based on Comparison of Model Predicted to Observed Time Series of Data. 3-10
Table 3-4. Summary of Comparison of Harmonic Analysis Output of Constituent Amplitude for Both Modeled and Observed Data from Observation Stations Within the Model Domain. 3-10
Table 3-5. Summary of Comparison of Harmonic Analysis Output of Constituent Phase for Both Modeled and Observed Data from Observation Stations Within the Model Domain. 3-11
Table 3-6. Summary of Current Speed Statistics at Fall River. 3-12
Table 3-7. Summary of Current Speed Statistics at the Mayflower Wind Metocean Buoy. 3-14
Table 3-8. Summary of Current Speed Statistics Along the ECC. 3-16
Table 4-1. Distance and Surface Area of Each Trench Section. 4-2
Table 4-2. Summary of Export Cable Burial Activities Simulated. 4-4
Table 4-3. Summary of HDD Pit Excavation Activities Simulated. 4-4
Table 4-4. Area Coverage for Selected TSS Concentration Thresholds in Mount Hope Bay and the Sakonnet River (KP0 – KP34). 4-12
Table 4-5. Area Coverage for Selected TSS Concentration Thresholds for the Offshore Export Cable Segments (KP34 – KP152). 4-13
Table 4-6. Summary of Total Area Coverage for Selected TSS Concentration Thresholds Over the Length of the ECC. 4-17
Table 4-7. Time for TSS Concentrations to Drop Below Selected Levels Along the ECC After the End of the Cable Installation Activities 4-19
Table 4-8. Area Coverage for Selected TSS Concentration Thresholds for the Three HDD Pit Excavation Activities. 4-20
Table 4-9. Time for TSS to Drop Below Selected Levels at the HDD Sites After the End of the Release. 4-21
Table 4-10. Area Coverage for Seabed Sedimentation Thickness Thresholds in Mount HHope Bay and the Sakonnet River (KP0 – KP34). 4-22
Table 4-11. Area Coverage for Seabed Sedimentation Thickness Thresholds Along the Offshore Export Cable Segments (KP34 – KP152). 4-25
Table 4-12. Summary of Total Area Coverage for Selected Sediment Deposition Thresholds Over the Length of the Export Cable Corridor. 4-31
Table 4-13. Area Coverage for Seabed Sedimentation Thickness Thresholds for the Three HDD Pit Excavation Activities. 4-32

Abbreviations and Acronyms

ac	Acre(s)
BOEM	Bureau of Ocean Energy Management
CFR	Code of Federal Regulations
COP	Construction and Operations Plan
ECC	Export Cable Corridor
ft	Foot/feet
ha	Hectare(s)
HDD	Horizontal Directional Drilling
km	Kilometer(s)
KP	Kilometer Point
kts	Knots
LiDAR	Light Detection And Ranging
m	Meter(s)
mi	Statute mile(s)
MLLW	Mean Lower Low Water
m^3/hr	Cubic meters per hour
mm	millimeter
mi/hr	Miles per hour
m/s	Meters per second
mg/L	Milligrams per liter
NCEP CFSR	National Centers for Environmental Prediction Climate Forecast System Reanalysis
NOAA	National Oceanic and Atmospheric Administration
nm	Nautical mile(s)
N/m^2	Newtons per meter squared
OCS	Outer Continental Shelf
OSP(s)	Offshore Substation Platform(s)
PSD	Particle Size Distribution
QQ	Quantile-Quantile
TSS	Total Suspended Solids
WTG	Wind Turbine Generator

1 INTRODUCTION

Mayflower Wind Energy LLC (Mayflower Wind) proposes to develop an offshore wind renewable energy generation project (Project) located in federal waters off the southern coast of Massachusetts in the Outer Continental Shelf (OCS) Lease Area OCS-A 0521 (Lease Area). The Project will deliver electricity to the grid via subsea export cables installed within the Brayton Point Export Cable Corridor (ECC) that will make landfall at Brayton Point in Somerset, Massachusetts and via subsea export cables installed within the Falmouth ECC that will make landfall in Falmouth, Massachusetts.

The Brayton Point ECC, which is the focus of this report, has been defined through which export cables will run from the Lease Area to landfall at Brayton Point. The cables will be buried with a trench depth of approximately 3 m (9.8 ft) using one or more of several burial methods, which may include use of jet trenching and mechanical trenching which are considered as representative worst case burial scenarios for this study. A jet trenching system uses high pressure jets to fluidize the seabed sediments releasing some fraction of the sediments into the water column through the burial process and the stinger (arm with water jets along its length that is lowered into the sediment to create the trench) of the jet-trencher creates the trench within the bed to lay the cable. A similar process occurs with the mechanical trenching however a chain cutter is used instead of water jets. This report presents an assessment of sediment plume dispersion (Total Suspended Solids [TSS] and deposits) associated with the installation of the export cables between the Lease Area and landing(s), and the nearshore HDD entry/exit points used for subsurface cable installation for the shoreline landings.

1.1 PROJECT OBJECTIVE

The Bureau of Ocean Energy Management (BOEM) produced regulations and guidelines for preparing the Construction and Operations Plan (COP) and conducting specific technical studies to support COP development.

Consistent with BOEM's *Information Guidelines for a Renewable Energy Construction and Operations Plan (COP)* (BOEM, 2020), the objectives of this sediment plume dispersion assessment are to:

- Model disturbances associated with cable installation, including near shore HDD entry,and specifically the resulting:
  - Suspended sediments in the water column (TSS)
  - Redeposition of disturbed and suspended sediments including thickness and extenton the seabed

Results from the sediment plume dispersion assessment provide quantitative and qualitative information to support the Mayflower Wind COP.

1.2 PROJECT DESCRIPTION

The Mayflower Wind Lease Area is located offshore of the southern coast of Massachusetts, approximately 49 kilometers (km) [26 nautical miles (nm)] south of Martha's Vineyard and 37 km (20 nm) south of Nantucket shown in Figure 1-1.

The Project layout will align to a 1 nm x 1 nm grid with an east-west and north-south orientation, as agreed upon across the entire Massachusetts/Rhode Island (MA/RI) Wind Energy Areas. The Project will consist of up to 149 positions within the Lease Area, to be occupied by Wind Turbine Generators (WTGs) and Offshore Substation Platforms (OSPs), connected with inter-array cables. Power will be transmitted to shore via submarine offshore export cables installed within two export cable corridors, the Brayton Point ECC and the Falmouth ECC. Falmouth modeling is covered in a separate report.

The offshore export cables within the Brayton Point ECC will travel from the Lease Area in Federal waters, through Rhode Island Sound, and up the Sakonnet River to make an intermediate landfall at the north end of Aquidneck Island (Portsmouth, RI). The cables will then cross Aquidneck Island (Portsmouth, RI) onshore and exit the island in Mount Hope Bay to ultimately reach the Brayton Point landfall. The cables are planned to be buried within the seabed along the Brayton Point ECC.

Additional details regarding the Project description and construction and installation methods are available in Section 3 of the COP. Specific details regarding construction methods used in this assessment are provided in Section 4 of this report.

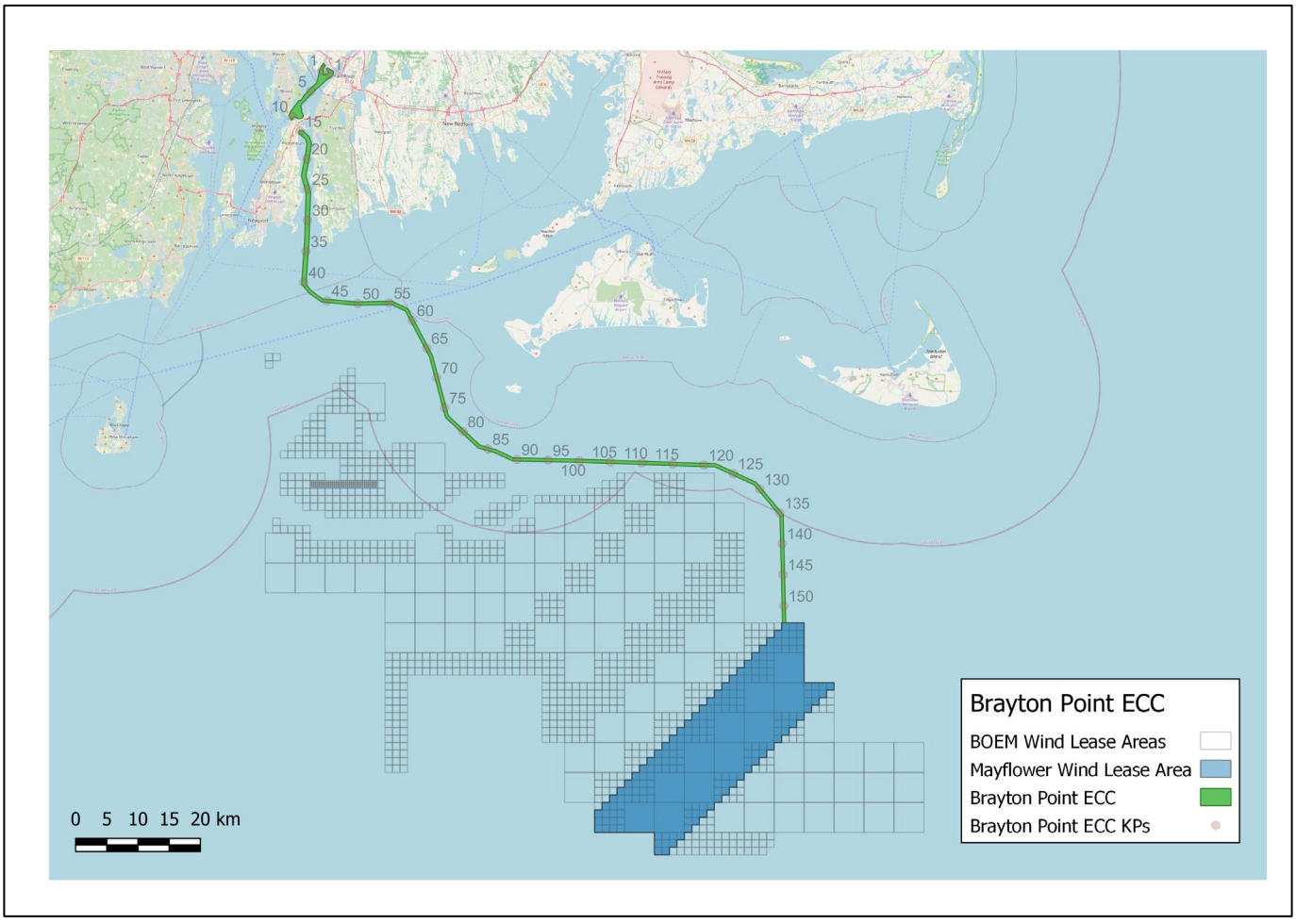

FIGURE 1-1. OVERVIEW OF THE PROJECT AREA AND BRAYTON POINT EXPORT CABLE CORRIDOR.

2 METHODOLOGY

The goal of this study was to determine the impacts of Mayflower Wind's proposed Brayton Point ECC export cable installation activities on the environment. The impacts were evaluated in terms of excess suspended sediment water column concentrations and sediment deposition footprint and thickness. The approach to evaluate the concentration and deposition impacts was to use two numerical models to simulate the hydrodynamics in the study area and the transport and dispersion of sediments resuspended from the cable burial activities during the construction phase of the Project, respectively.

The two models used have been developed over many years to perform this specific type of evaluation. The hydrodynamic model used was the Delft3D-FLOW model system (Deltaris, 2018a) which was applied to develop currents and circulation from the tides, winds, and river flow. The model was applied in two parts; a large-scale application to the offshore area from the New York Bight to east of Cape Cod to capture the dynamics along the Brayton Point ECC from the Mayflower Wind Lease Area to the entrance of the Sakonnet River and a second fine grid nested model application to Narragansett Bay with a focus on the Sakonnet River and Mount Hope Bay cable corridor portions. A more detailed description of the Delft3D model and its application is provided in Section 3.

The sediment transport model used was the Delft3D, D-WAQ PART (Deltaris, 2018b), particle transport model system. The PART model is integrated with the FLOW model allowing direct input of the hydrodynamic model predicted currents into the transport model. The model was used to simulate excess suspended sediment transport and dispersion, predicting the water column concentration and sediment deposition, resulting from the proposed cable embedment activities. A description of the D-WAQ PART model and its application is provided in Section 4.

The hydrodynamic model was set up and run to predict the tidal and wind driven currents in the region. A time period was selected that would be consistent with the likely allowable dredge windows, commonly during the late fall/early winter months, and where both currents and water surface elevation observations were available for comparison with the model predictions. The product of the hydrodynamic modeling was a time and space varying current field, predicted from the tide and wind forcing, capturing several spring (higher tidal amplitude/more energy) and neap (lower tidal amplitude/lower energy) conditions as well as weather systems passages. The simulations were run long enough to generate current predictions that would encompass the duration of the proposed cable burial activities.

Time series of model predicted water surface elevation was collected at the nested grid interface with the large-scale model and used to drive the Narragansett Bay fine resolution application to generate currents in the bay. The simulation was run for the same time period as the offshore large scale application simulation.

The simulations were specified to take the sediment characteristics (sediment grain size distribution as sampled along the route) and cable burial tool characteristics representative of jet trenching/mechanical trenching (volume of source sediments resuspended, cable burial advance rate etc.) as well as the environmental conditions (water depth, currents), into account. The cable burial simulations were initiated at the Brayton Point terminus of the ECC and run seaward. Because of the ECC design where the cable crosses land at the northern end of Aquidneck Island, the simulation was split in two sections; the Mount Hope Bay section and the Sakonnet River to offshore section. The analysis was performed assuming that all concentrations and deposited sediments were

"excess sediments", i.e. in excess of natural conditions. Therefore, the effects are presented as isolated effects of the construction that occur, which would be added to the natural conditions.

The results of the sediment transport and dispersion simulations were predictions of the extent and duration of suspended sediment concentrations within the water column along the route and the final sediment deposition characteristics (pattern and thickness) associated with each proposed activity.

2.1 HYDRODYNAMIC MODEL

The circulation characteristics are an important input to the sediment transport modeling. A hydrodynamic model application of the study area was developed using Delft3D-FLOW, a multi-dimensional model system that has been applied successfully in numerous circulation studies around the world. This section provides details of the Delft3D-FLOW model system.

2.2 HYDRODYNAMIC MODEL TECHNICAL DESCRIPTION

The numerical hydrodynamic modeling system Delft3D-FLOW solves the unsteady shallow water equations in two (depth-averaged) or three dimensions. The systems of equations are based on the full Navier-Stokes equations with the shallow water approximation applied and consist of the horizontal equations of motion, the continuity equation, and the transport equations for conservative constituents. The equations are formulated in orthogonal curvilinear co-ordinates or in spherical co-ordinates on the globe.

In Delft3D-FLOW models with a rectangular grid (Cartesian frame of reference) are considered as a simplified form of a curvilinear grid. The hydrodynamic module applies the sigma co-ordinate transformation in the vertical, which maps both the water surface and bottom topography to the upper and lower grid boundaries, resulting in a smooth representation of each. This also results in a high computing efficiency because of the constant number of vertical layers over the whole computational domain.

The flow is forced by tide at the open boundaries, wind stress at the free surface, pressure gradients due to free surface gradients (barotropic) or density gradients (baroclinic). Source and sink terms are included in the equations to model the discharge and withdrawal of water.

The hydrodynamic module is based on the full Navier-Stokes equations with the shallow water approximation applied. The equations are solved with a highly accurate unconditionally stable solution procedure. The supported features are:

- two co-ordinate systems, i.e. Cartesian and spherical, in the horizontal directions;
- two grid systems in the vertical direction; the boundary fitted sigma grid and the horizontal layer Z-grid;
- domain decomposition both in the horizontal and vertical direction;
- tide generating forces (only in combination with spherical grids);
- simulation of drying and flooding of inter-tidal flats (moving boundaries);
- density gradients due to a non-uniform temperature and salinity concentration distribution (density driven flows);
- for 2D horizontal large eddy simulations the horizontal exchange coefficients due to circulations on a sub-grid scale (Smagorinsky concept);

- turbulence model to account for the vertical turbulent viscosity and diffusivity based on the eddy viscosity concept;
- selection from four turbulence closure models: k-", k-L, algebraic and constant coefficient;
- the effect of the Earth's rotation (Coriolis force).
- shear stresses exerted by the turbulent flow on the bottom based on a Chézy, Manning or White-Colebrook formulation;
- enhancement of the bottom stresses due to waves;
- automatic conversion of the 2D bottom-stress coefficient into a 3D coefficient;
- wind stresses on the water surface modelled by a quadratic friction law;
- space varying wind and barometric pressure (specified on the flow grid or on a coarser meteo grid), including the hydrostatic pressure correction at open boundaries (optional);
- simulation of the thermal discharge, effluent discharge and the intake of cooling water at any location and any depth in the computational field (advection-diffusion module);
- the effect of the heat flux through the free surface;
- online analysis of model parameters in terms of Fourier amplitudes and phases enabling the generation of co-tidal maps;
- drogue tracks;
- advection-diffusion of substances with a first order decay rate;
- online simulation of the transport of sediment (silt or sand) including formulations for erosion and deposition and feedback to the flow by the baroclinic pressure term, the turbulence closure model and the bed changes;
- the influence of spiral motion in the flow (i.e. in river bends). This phenomenon is especially important when sedimentation and erosion studies are performed;
- modeling of obstacles like 2D spillways, weirs, 3D gates, porous plates and floating structures;
- wave-current interaction, taking into account the distribution over the vertical;
- many options for boundary conditions, such as water level, velocity, discharge and weakly reflective conditions;
- several options to define boundary conditions, such as time series, harmonic and astronomical constituents;
- option for linear decay of conservative substances, and
- online visualization of model parameters enabling the production of animations.

2.3 SEDIMENT TRANSPORT MODEL

Sediment transport associated with the cable burial activities was simulated using the Deltares Delft3D D-WAQ PART model. The model requires inputs defining the environment (e.g. water depths, currents) and the construction activity loading (e.g. sediment grain size, resuspended volume) and produces predictions of the associated sediment plume and seabed deposition. Details of the model and theory are provided in the following sections.

The particle tracking module, D-WAQ PART, is a 3-dimensional far-field water quality model. It estimates a dynamic concentration distribution by following the tracks of thousands of particles in time and space (in the water column). The model calculates TSS concentrations and sedimentation patterns resulting from activities that cause sediment resuspension. The model requires a spatial and time varying circulation field (typically from hydrodynamic model output as described in the last section), definition of the water column bathymetry, and parameterization of the sediment disturbance (source). The model predicts the transport, dispersion and settling of suspended sediment released to the water column.

The focus of the model is on the far-field (i.e. beyond the initial disturbance) processes affecting the fate of suspended sediment. The model uses a specification of the suspended sediment source strength (i.e. material resuspension volume/mass flux), initial vertical distribution of sediments and the sediment grain-size distribution to represent losses (loads) to the water column. The losses are developed from a parameterization of different types of mechanical or hydraulic dredges, sediment dumping practices or other sediment activities such as jetting or mechanical trenching for cable or pipeline burial. Multiple sediment types or grain size fractions can be simulated simultaneously and are tracked separately but can impact each if specified. In addition, multiple loads and locations can be simulated as can discharges from moving sources.

2.4 SEDIMENT MODEL TECHNICAL DESCRIPTION

D-WAQ PART is a 3-dimensional particle tracking model that is particularly useful for mid- to far-field water quality modeling. It calculates a dynamic concentration distribution by following the tracks of thousands of particles with time. The model provides a detailed description of concentration distributions, resulting from instantaneous or continuous releases of materials such as salt, oil, temperature or sediments as in the present study. The materials can be simulated as conservative or simple decaying substances.

D-WAQ PART is a random walk particle tracking model, which is based on the principle that the movement of dissolved (or particulate) substances in water can be described by a limited (large) number of discrete particles that are subject to advection due to the currents and by horizontal and vertical dispersion. The movement of the particles consists therefore of two elements. For each time-step, the first step is the advection step due to the shear stresses from currents (bottom) and wind (surface). The second step is the random walk step in which the size and direction of the movement is a random process but is related to the horizontal and vertical dispersion.

The particle-based (Lagrangian) scheme represents the total mass of sediments suspended over time, and provides a method to track suspended sediment without any loss of mass as compared to Eulerian (continuous) models due to the nature of the numerical approximation used for the conservation equations. Thus, the method is not subject to artificial diffusion near sharp concentration gradients and can easily simulate all types of sediment sources.

In D-WAQ PART, two modules are available:

- Tracer module: simulation of conservative or first order decaying substances; and
- Oil spill module: simulation of oil spills with floating and dispersed oil fractions (special license required).

In this study only the tracer module was used. The tracer module is very flexible and is designed to be configured for sediment simulations of the user's design.

The physical components in the system are:

- discharges due to human activities or released naturally that may be instantaneous and/or continuous;
- settling and erosion of suspended matter;
- concentration- dependent settling velocity.

Physical processes or phenomena D-WAQ PART can represent include:

- the dynamics of patches close to an outfall location;
- simple first-order decay processes like the decay of several fractions of oil;
- vertical dispersion for well-mixed systems;
- horizontal dispersion due to turbulence. According to turbulence theory this dispersion increases in time.
- the effects of time-varying wind fields;
- the effects of bottom-friction;
- the existence of a plume at the outfall (rather than a point-source) by starting the simulation from a circular plume with an estimated or field-measured radius.
- settling of particles, where a concentration dependent settling, subject to a minimum and maximum settling velocity, can be specified;
- settled mass is collected in an additional bottom layer.

D-WAQ PART can in theory simulate an unlimited number of particles and substances. The only restriction is the available memory of the hardware. The coupling between the hydrodynamic module, Delft3D-FLOW, and D-WAQ PART is streamlined such that the current fields developed by the hydrodynamic model can be read directly into the particle model.

If detailed sediment data is available the sediments are broken out into 4 to 6 classes based on the grain size distribution, i.e. the fraction of the total sediment sample in each class. Each class is defined by a range of particle sizes and the density of that class material (Shelley, 1988; CERC, 1984; Wentworth, 1922). The system used in the sediment model is the Wentworth scale as presented in Table 2-1. Sediment grain size is important in determining the fall velocity (settling rate) of resuspended sediments. The fall velocity is determined from a form of the Stokes Law equation for common grains (rather than spheres) where the grain diameter is measured by the median sieve size (CERC, 1984.)

For a given activity and grain size distribution the amount of mass released in each class is calculated as a function of the volume of material resuspended, the fraction that is sediments, the density of the sediments and the fraction of the total mass in that class. A user input number of particles are released at each time step for each sediment class. The mass of each particle is determined as the mass in each sediment class divided by the number of particles.

Horizontal transport, settling, and turbulence-induced suspension of each particle is computed independently by the model for each time step. Particle advection is based on the relationship that a particle moves linearly (in 3-dimensions) with a local velocity obtained from the hydrodynamic field for a specified model time step. Diffusion is assumed to follow a simple random walk process defined as the square root of the product of an input diffusion coefficient and the time step.

TABLE 2-1. BREAKDOWN OF SEDIMENT CLASSIFICATIONS BY PARTICLE DIAMETER.

Sediment Classification	Particle Diameter (mm)
Clay	< 0.0039
Silt	0.0039 - 0.0625
Very Fine Sand	0.062 - 0.125
Fine Sand	0.125 - 0.25
Medium Sand	0.25 - 0.50
Coarse Sand	0.5 - 1.0

In a well-mixed, horizontally uniform flow, the vertical dispersion coefficient may be estimated from the mixing length and the turbulent kinetic energy. The empirical relationships for the turbulent kinetic energy at the bed and at the surface are taken from the k-L turbulence model used in Delft3D-FLOW, incorporating the shear stresses, resulting in a vertical dispersion model. The depth-dependency of the vertical dispersion coefficient is eliminated by depth-averaging to avoid particles gathering at the bottom or surface. D-WAQ PART allows linear scaling of the depth-averaged dispersion coefficient to allow for a reduction in vertical mixing due to stratification in the 3D models. Vertical diffusion is also scaled by an input coefficient and can be in the up or down direction.

Particle settling rates are calculated using Stokes equations based on the size and density of each particle class. Enhanced settling rates in the combined particle classes due to clumping are important for clay and fine-silt sized particles, bound by upper and lower concentration limits.

If the bed shear stress at any location is less than the critical shear stress for sedimentation, a particle that comes into contact with the bottom at that location will remain attached to the bottom (sedimentation). For sedimentation, D-WAQ PART creates an extra model layer for sediment at the bed. If the bed shear stress at any location is greater than the critical shear stress for sedimentation, a particle that comes in contact with the bottom at that location will be reflected back into the water column. If the bed shear stress at any location is greater than the critical shear stress for erosion, all deposited particles at that location (i.e. particles located in the extra bed-sediment layer) will be returned to the water column instantaneously.

For each model time step the suspended concentration of each sediment class as well as the total concentration is computed on a concentration grid. The concentration grid is a uniform rectangular grid with a user-specified cell size and overall area coverage that is independent of the resolution of the hydrodynamic data used to calculate transport. This allows for a finer resolution for determination of plume concentrations, avoiding concentration underestimation using the usually larger hydrodynamic model grid cells. The concentration grid is also used for sediment material deposited on the sea floor. Deposition is calculated as the sum of the mass of the sediment class particle that accumulates in a cell.

3 HYDRODYNAMIC MODELING

A hydrodynamic model application was developed to generate spatial and time varying currents for use in the sediment transport and dispersion modeling. The model application was validated against observations of water surface elevation and currents for the period of November 10, 2020 – December 22, 2020; this period was also used as the timeframe for simulating the cable installation in the sediment transport modeling scenarios.

3.1 HYDRODYNAMIC MODEL APPLICATION

The hydrodynamic model application to the Mayflower Wind Brayton Point ECC study area began with the development of a system of two grids, one overall large grid and a fine resolution nested grid. The large grid extended from New York Harbor through the New York Bight to an area approximately 40 km (25 mi) east of Cape Cod (and 60 km [37 mi] east of the Lease Area) covering the entire Brayton Point ECC with boundaries far removed from the Lease Area and Brayton Point ECC. Previous experience (Crowley and Mendelsohn, 2011) had shown that the extent of the large grid was necessary to capture the circulation and transport in the offshore areas associated with the BOEM MA/RI Lease Areas. The extent of the large grid and the gridded bathymetry is presented in Figure 3-1

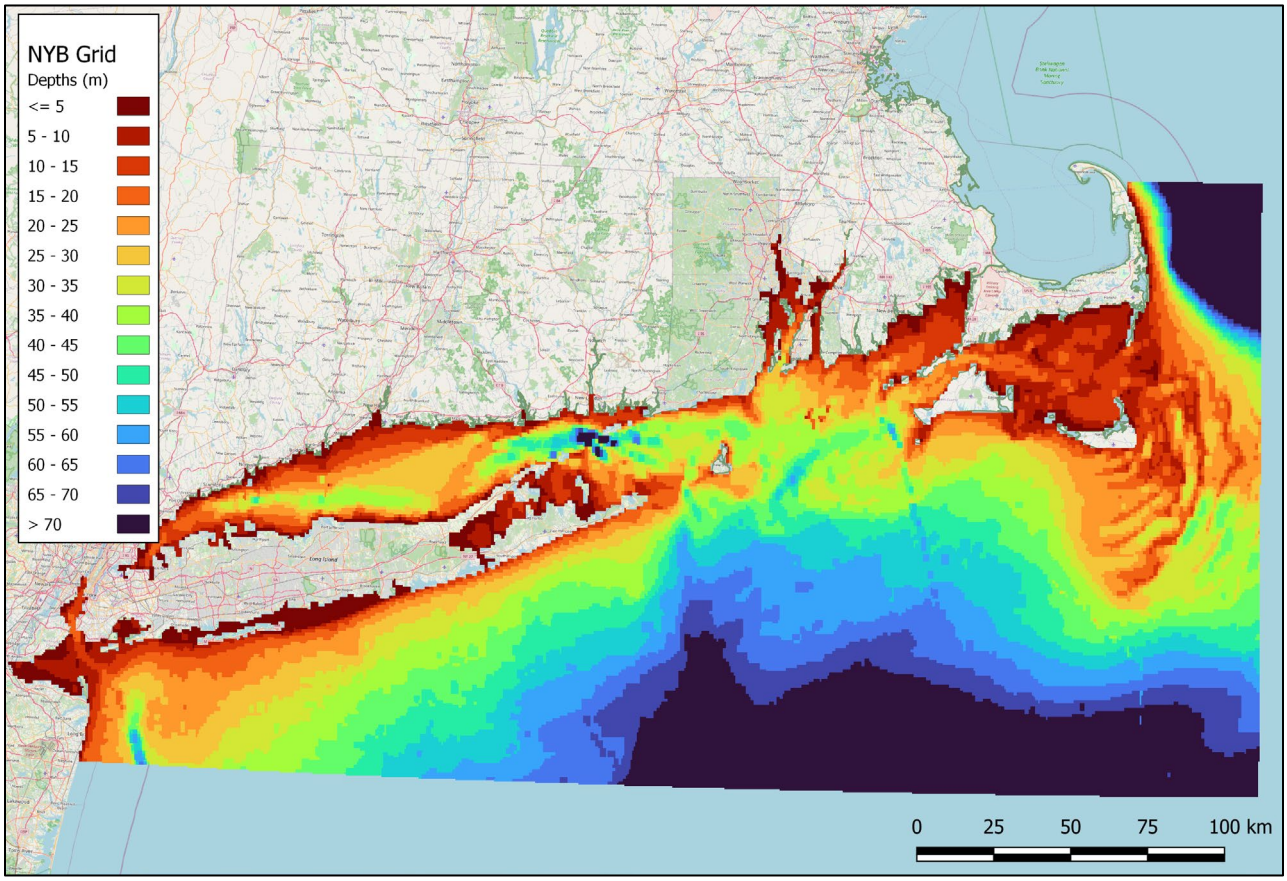

FIGURE 3-1. LARGE GRID AND BATHYMETRY DEVELOPED FOR THE HYDRODYNAMIC MODEL APPLICATION.

The nested grid was used to increase the resolution in Narragansett Bay with a focus on the Sakonnet River and Mount Hope Bay (Figure 3-2). The open boundaries extended offshore into Rhode Island Sound and were forced with time series output generated by the offshore large- scale grid.

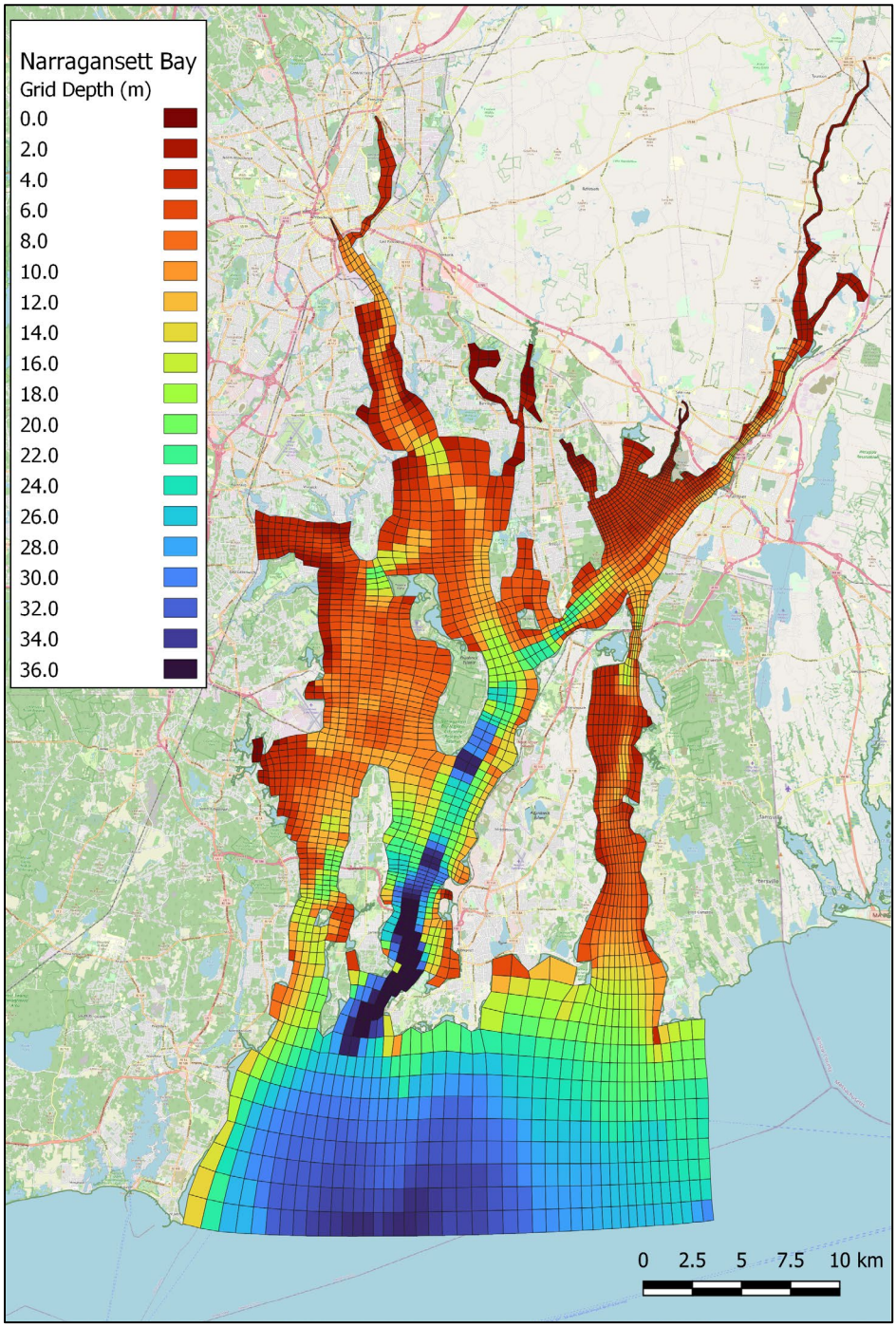

FIGURE 3-2. HIGHER RESOLUTION NESTED GRID OF NARRAGANSETT BAY WITH A FOCUS ON THE SAKONNET RIVER AND MOUNT HOPE BAY ALSO SHOWING THE GRIDDED BATHYMETRY.

The bathymetry for both grids was developed from a combination of sources including the General Bathymetric Chart of the Oceans GEBCO 08 Grid, NOAA Northeast Atlantic Coastal Relief Model (NOAA, 1999) and measurements along the ECC taken for the Project (Mayflower Wind G&G Survey, 2021a).

3.2 ENVIRONMENTAL FORCING

The model forcing included the open boundary specification of astronomic tides and surface winds. The tidal forcing was obtained from the TPXO 7.2 Global Inverse Tide Model (Egbert and Erofeeva, 2002) and was specified along the southern and eastern boundaries. Ocean currents and circulation in the study area are complex and influenced by several main factors. These include wind-driven processes, tides, and density gradients driven by offshore interaction with adjacent estuaries, and radiative and sensible heat flux through the air-sea interface (Codiga and Ullman, 2010). Throughout the domain however, tidal currents are the predominant force driving circulation (Spaulding and Gordon, 1982), with wind and density variations playing a smaller role. Further, the tides in this region are dominated by the M2 astronomical constituent (Spaulding and Swanson, 2008, Spaulding and White, 1990). Surface winds were applied based on the observations from the Mayflower Wind metocean buoy, available at 4 m (13 m) above mean sea level (MSL) at a 10-minute timestep and Quonset Point, RI - Station ID: 8454049, 2.1 m (6.97) ft. above MSL at a 6-minute timestep. A timeseries of the wind speeds for the validation timeframe is presented in Figure 3-3 and the wind rose is provided in Figure 3-4. The corresponding wind speed percentiles for this period are summarized in Table 3-1.

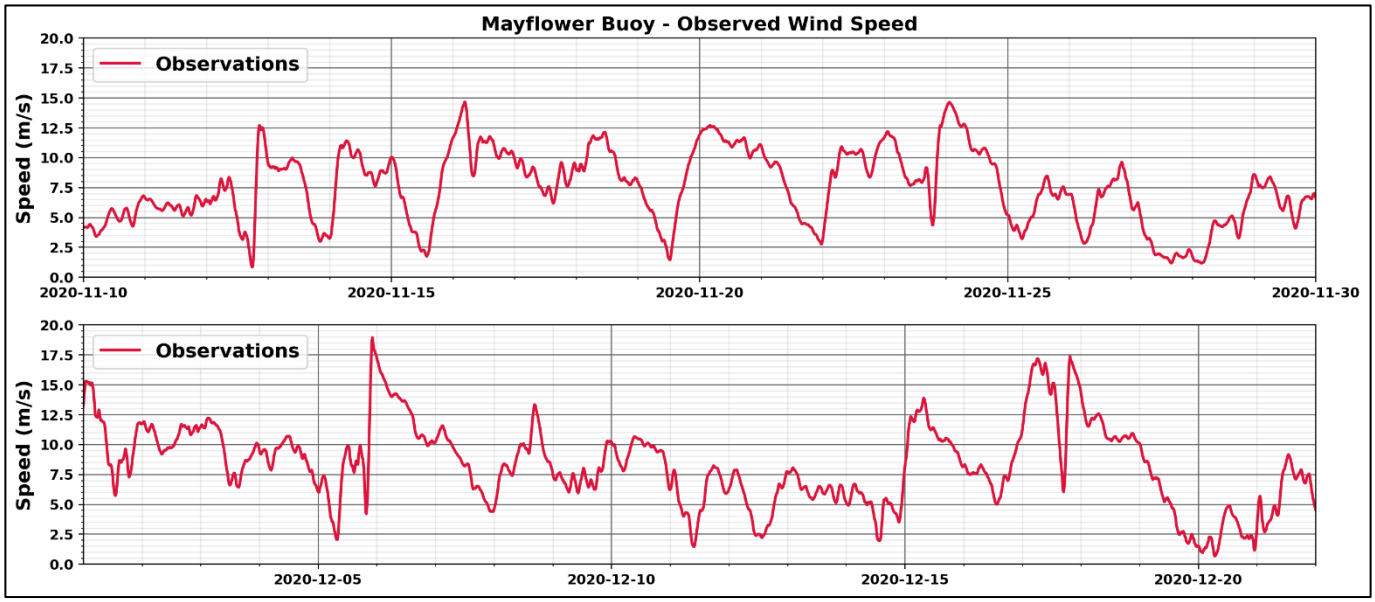

FIGURE 3-3. TIME SERIES OF WIND SPEEDS DURING THE HYDRODYNAMIC MODEL VALIDATION PERIOD.

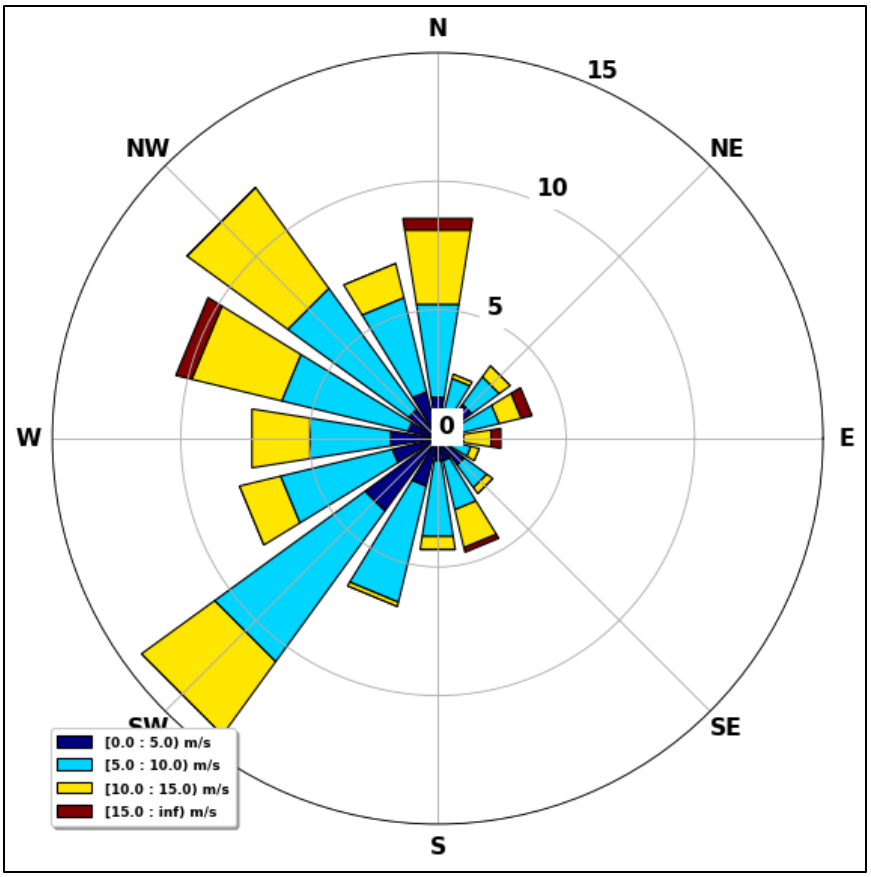

FIGURE 3-4. WIND ROSE FOR THE HYDRODYNAMIC MODEL VALIDATION PERIOD. DATA FROM THE MAYFLOWER WIND OFFSHORE METOCEAN BUOY.

TABLE 3-1. PERCENTILES OF WIND SPEEDS DURING THE HYDRODYNAMIC MODEL VALIDATION PERIOD AS RECORDED AT THE MAYFLOWER WIND OFFSHORE METOCEAN BUOY.

	Observed Wind Speed Statistics During Model Validation Period (m/s)
Minimum	0.19
Mean	7.78
Maximum	18.81
Percentiles	
5	2.12
10	3.16
25	5.34
50	7.74
75	10.27
90	12.00
95	13.31

3.3 MODEL VALIDATION RESULTS

The model application was validated against observations of water elevations and currents within the region. The locations of the various observation stations are shown in Figure 3-5.

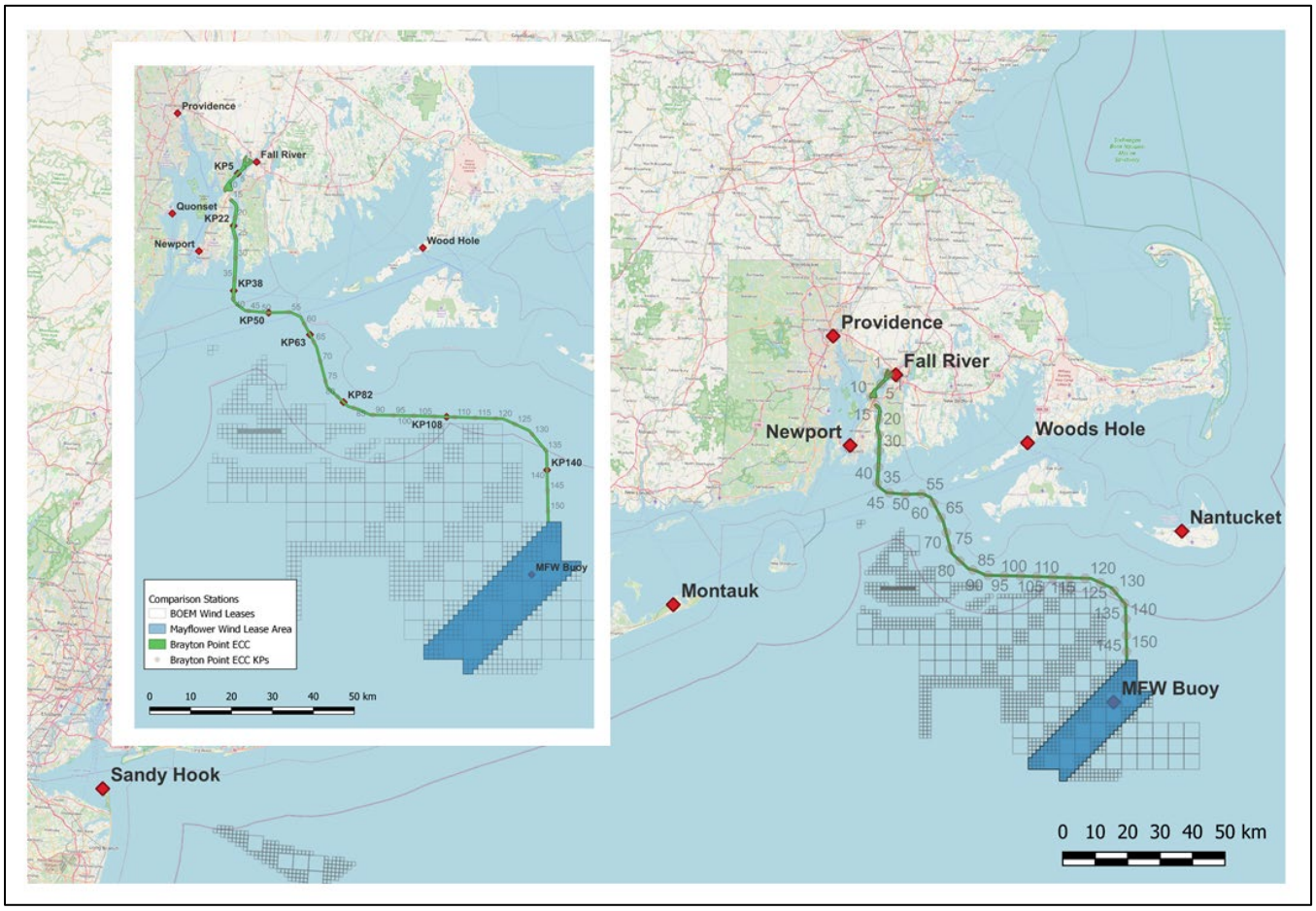

FIGURE 3-5. OBSERVATION STATIONS USED FOR DEVELOPING MODEL FORCING AND MODEL VALIDATION. INSET SHOWS A SUBSET OF KILOMETER (KP) MARKERS ALONG BRAYTON POINT ECC INDICATIVE CENTERLINE.

3.4 VALIDATION OF MODEL PREDICTED WATER SURFACE ELEVATIONS

Water surface elevations (WSEs) predominately reflect the influence of tides, though can also be affected by winds, wind driven waves, and offshore pressure related sea level variations, particularly in coastal areas during storms. Model predictions of water surface elevations were compared to observations to evaluate how well the model was capturing water level variation in the region, particularly the water level variation from tides since the area is known to be tidally dominated (Spaulding and Swanson, 2008, Spaulding and White, 1990). The validation included multiple components including: (1) a qualitative comparison of time series, (2) a statistical comparison of model vs observation time series statistics, (3) statistical comparison of the tidal harmonics developed through harmonic decomposition of observed and predicted time series data. Harmonic decomposition refers to the

output of a signal processing analysis that removes any non-periodic elements (such as set up or set down from winds) and then further breaks the tidal signal down in to its individual cyclical astronomical components (e.g. the semi-diurnal M2 component that dominates the tides in this region) that can be defined by their amplitude, period and phase. NOAA describes harmonic constituents as follows:

> *There are hundreds of periodic motions of the Earth, Sun, and Moon that are identified by astronomy. Each of these motions or "constituents" in a set of harmonic constants is a mathematical value describing the effect that cyclical motion of the Earth, Sun, Moon system has on the tides. There are 37 which normally have the greatest effect on tides and are used as the tidal harmonic constituents to predict tidal conditions for a location.*
>
> *A couple of examples:*
> - *M2 – The largest lunar constituent – is related to the direct gravitational effect of the Moon on the tides. The Earth rotates on its axis every 24-hours, but the Moon is orbiting in the same direction as the Earth's rotation. It takes a location on the Earth an additional 50 minutes to "catch up" to the Moon. This results in a tidal signal (M2) which has 2 peaks every 24-hours and 50 minutes.*
> - *S2 – The largest solar constituent – is related to the direct gravitational effect of the Sun on the tides. The Earth rotates on its axis every 24-hours. This results in a tidal signal (S2) which has 2 peaks every 24-hours.*

Water surface elevation data was obtained for the study time period from the following NOAA tide stations:

- Station 8531680: Sandy Hook, NJ
- Station 8510560: Montauk, NY
- Station 8452660: Newport, RI
- Station 8447930: Woods Hole, MA
- Station 8454000: Providence, RI
- Station 8454049: Quonset Point, RI
- Station 8447386: Fall River, MA

The five largest tidal harmonic components calculated from modeled and observed water surface elevation time series were compared at each of the NOAA tide stations (Figure 3-5). The five harmonic constituents compared were M2, S2, N2, K1, and O1 and their respective periods are presented in Table 3-2 below.

TABLE 3-2. TIDAL HARMONIC CONSTITUENT CHARACTERISTICS (NOAA, 2007).

Name	Constituent	Speed in degrees/hour	Period in hours
M2	Principal lunar semidiurnal constituent	28.98	12.42
S2	Principal solar semidiurnal constituent	30.00	12.00
N2	Larger lunar elliptic semidiurnal constituent	28.44	12.66
K1	Lunar diurnal constituent	15.04	23.93
O1	Lunar diurnal constituent	13.94	25.82

Plots of the model predicted and observed water surface elevation (WSE) time series are presented in Figure 3-6 through Figure 3-7 for stations located as shown in Figure 3-5. These plots illustrate that the model was able to capture the semi-diurnal nature of the tides, the shifts in water level due to storms and the variation of tidal range across the region. The tide range varies across the region, though the peak tidal amplitude is less than 1.25 m (4.10 ft) in most locations at most times.

The model predicted time series plotted in Figure 3-6 were generated by the large grid application and show that there is a large variation in tidal amplitudes and storm response across the domain which the model was able to predict. The Woods Hole station missed some of the variability likely due to complex coastal topography in the area. As will be shown below, the tidal harmonics are well represented at that station none the less.

The time series presented in Figure 3-7 were generated using the nested grid model application and again it can be seen that the model is able to adequately reproduce the tidal variability and the storm (wind) related offsets. This is a good indication that the model predictions are robust across the domain for many different types of areas as environmental conditions within the Brayton Point ECC study area.

The differences between model predictions and observations were evaluated quantitatively through the calculation of different statistical measures including the root mean square error (RMSE), and the correlation coefficient (R). Both of these measures are calculated on a point to point basis, i.e. the model predictions and the observations are compared one to one at every time step. As it essentially uses the absolute value of the differences, positive and negative differences do not average, making it an unforgiving measure of the difference between the model and the observations.

The root mean square error is a measure of the variance of the error (difference between the model prediction and the observation at a given time), defined by the equation is shown below.

$$RMSE = \sqrt{\overline{(model - obs)^2}}$$

The correlation coefficient is a measure of the variance of the error and is the standard of deviation of the difference between model predictions and observations, the equation is shown below.

$$R = \frac{covariance\ (model, obs)}{STD_{model} * STD_{obs}}$$

A summary of the statistics is shown in Table 3-3. With the exception of Woods Hole as was seen in the earlier comparison, the RMSE and correlation coefficient show an excellent fit between the model predictions and the observations, with a RMSE on the order of 0.1 m/s.

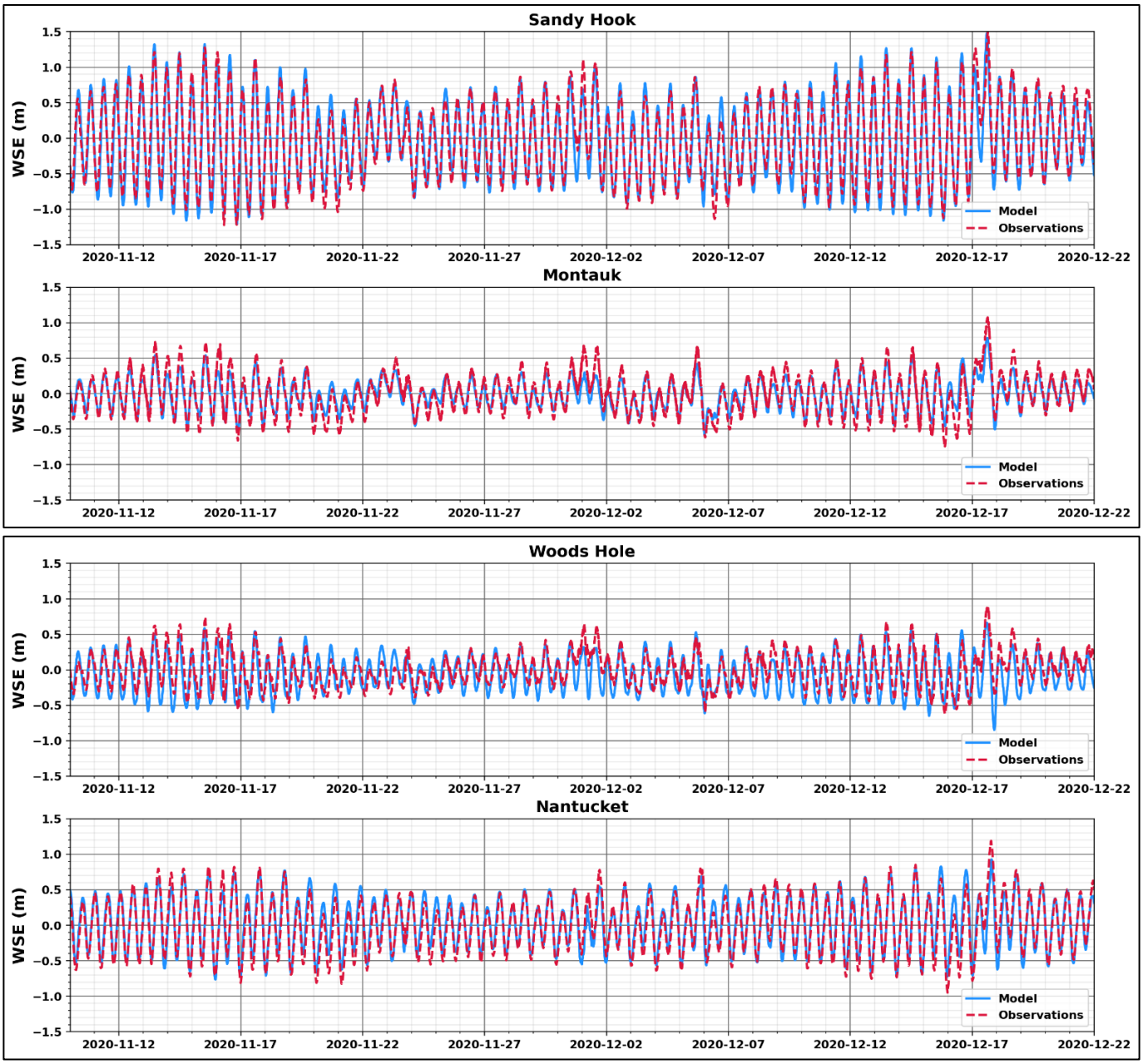

FIGURE 3-6. COMPARISON OF MODELED AND OBSERVED WATER SURFACE ELEVATIONS AT NOAA SANDY HOOK, MONTAUK, WOODS HOLE, AND NANTUCKET TIDE STATIONS. WATER SURFACE ELEVATIONS ARE PLOTTED RELATIVE TO MSL.

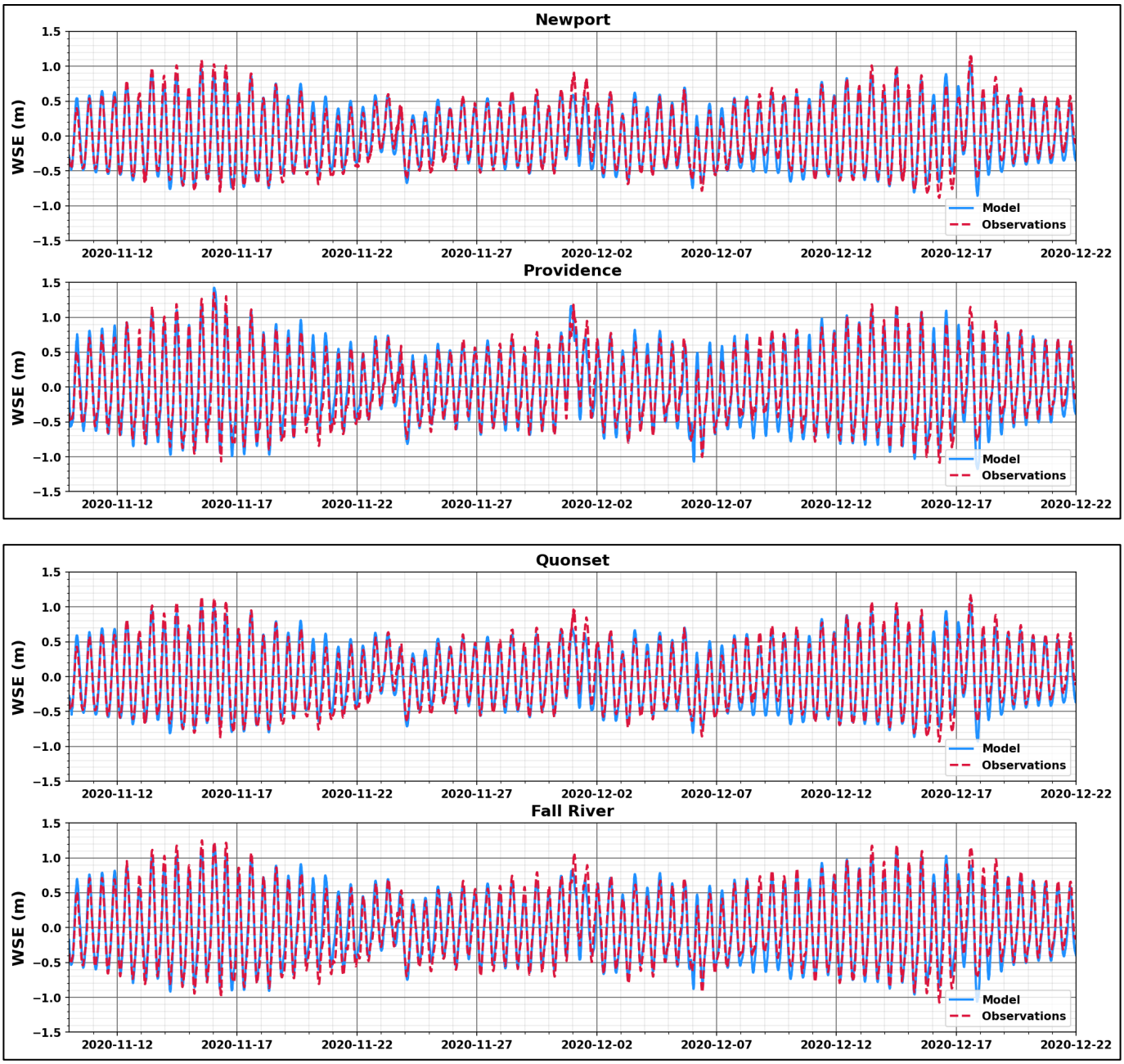

FIGURE 3-7. COMPARISON OF MODELED AND OBSERVED WATER SURFACE ELEVATIONS AT NOAA NEWPORT, PROVIDENCE, QUONSET POINT, AND FALL RIVER TIDE STATIONS. WATER SURFACE ELEVATIONS ARE PLOTTED RELATIVE TO MSL.

TABLE 3-3. SUMMARY OF STATISTICS AT WATER SURFACE ELEVATION OBSERVATION STATIONS BASED ON COMPARISON OF MODEL PREDICTED TO OBSERVED TIME SERIES OF DATA.

Station	RMSE (m/s)	R (-)
Sandy Hook	0.09	0.96
Montauk	0.13	0.92
Woods Hole	0.22	0.77
Nantucket	0.10	0.95
Newport	0.08	0.97
Fall River	0.09	0.96
Quonset Point	0.08	0.97
Providence	0.09	0.96

A harmonic decomposition was performed on both the observed and modeled time series at the observation locations. The harmonic constituents of the modeled and observed amplitude and phase at the eight comparison stations are summarized in Table 3-4 and Table 3-5, respectively. The results show that the M2 constituent dominates across all the sites and that the model is able to reproduce the variation in water surface elevation from the tides across the domain very well. The tables also provide the differences between model and observed characteristics. Differences in tidal amplitude vary up to a high of 0.09 m (2.95 ft) at Woods Hole, they are less than that in the majority.

TABLE 3-4. SUMMARY OF COMPARISON OF HARMONIC ANALYSIS OUTPUT OF CONSTITUENT AMPLITUDE FOR BOTH MODELED AND OBSERVED DATA FROM OBSERVATION STATIONS WITHIN THE MODEL DOMAIN.

		Amplitude (m)					
		Sandy Hook	Montauk	Woods Hole	Nantucket	Newport	Fall River
M2	**Model**	0.72	0.23	0.33	0.46	0.54	0.62
	Obs	0.69	0.30	0.24	0.46	0.52	0.61
	Difference	0.03	-0.07	0.09	0.00	0.02	0.01
N2	**Model**	0.20	0.07	0.08	0.11	0.13	0.14
	Obs	0.18	0.09	0.08	0.13	0.14	0.16
	Difference	0.03	-0.02	0.00	-0.01	-0.01	-0.02
K1	**Model**	0.17	0.08	0.07	0.11	0.07	0.06
	Obs	0.12	0.08	0.08	0.11	0.07	0.07
	Difference	0.05	-0.01	-0.01	0.00	-0.01	-0.01
S2	**Model**	0.13	0.06	0.06	0.04	0.09	0.10
	Obs	0.12	0.06	0.05	0.05	0.10	0.12
	Difference	0.01	0.01	0.01	0.00	-0.01	-0.01
O1	**Model**	0.04	0.04	0.05	0.08	0.04	0.03
	Obs	0.05	0.05	0.06	0.08	0.04	0.04
	Difference	-0.01	0.00	0.00	0.00	0.00	-0.01

TABLE 3-5. SUMMARY OF COMPARISON OF HARMONIC ANALYSIS OUTPUT OF CONSTITUENT PHASE FOR BOTH MODELED AND OBSERVED DATA FROM OBSERVATION STATIONS WITHIN THE MODEL DOMAIN.

		Constituent Phase (degrees)					
		Sandy Hook	Montauk	Woods Hole	Nantucket	Newport	Fall River
M2	Model	127	153	121	245	115	121
	Obs	122	163	151	249	117	124
	Difference	5	-10	-30	-4	-2	-2
N2	Model	327	348	321	69	314	322
	Obs	315	350	346	67	312	320
	Difference	12	-2	-26	2	1	1
K1	Model	14	183	192	216	177	186
	Obs	22	192	200	223	182	188
	Difference	-8	-9	-9	-7	-5	-2
S2	Model	174	32	359	161	6	12
	Obs	173	43	20	153	9	17
	Difference	1	-11	-21	8	-4	-5
O1	Model	291	304	295	314	297	301
	Obs	286	300	299	317	294	298
	Difference	5	4	-4	-3	3	3

3.5 VALIDATION OF MODEL PREDICTED CURRENTS

The model predictions of currents were validated to available observations. The objective of the comparison is to evaluate how well the model can recreate the magnitude and pattern of currents, particularly near the seabed where the sediments will be resuspended and transported by the currents during cable installation processes. Current data available to compare to the model predictions consisted of NOAA predictions of current velocities (along channel velocities) at the Fall River station, and current observations at the offshore Mayflower Wind metocean buoy in the Lease Area, both as located in Figure 3-5.

The Fall River bottom station is located adjacent to the dredged channel at a depth of approximately 9 m (30 ft) deep relative to MSL. The NOAA predicted current velocities, at that depth, were compared to model predictions at the corresponding depth. Figure 3-8 shows a comparison of current velocities. The NOAA predictions are provided as a singular directionless velocity, deemed to be aligned with the channel as there is little variability in current direction within channels in narrow waterways dominated by tides; as such the modeled speed plot shows the varying velocity in the along channel direction. The modeled current speeds match very well with the NOAA predicted speeds, with differences typically within a few centimeters per second in a total range of approximately 40 cm/s. The results of a statistical comparison between the model predictions and the observations at Fall River are presented in Table 3-6.

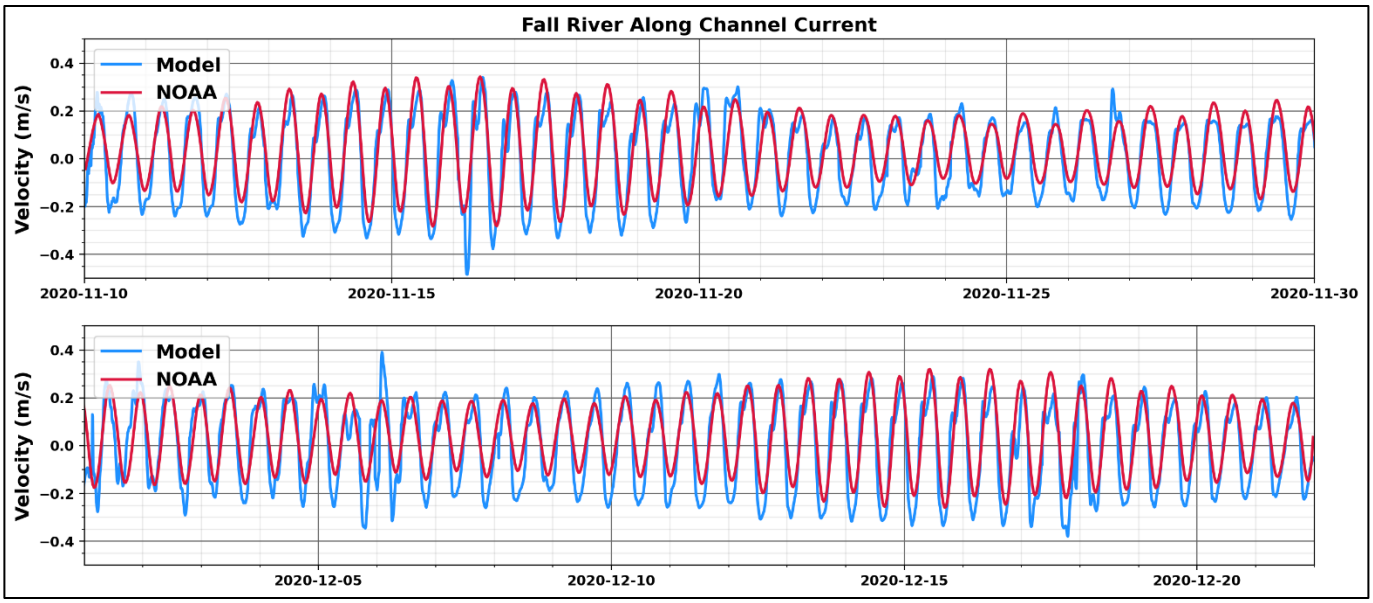

FIGURE 3-8. CCOMPARISON OF MODELED AND NOAA PREDICTED CURRENT SPEED AT FALL RIVER.

TABLE 3-6. SUMMARY OF CURRENT SPEED STATISTICS AT FALL RIVER.

	Model (m/s)	NOAA (m/s)	Difference (m/s)
Minimum	-0.48	-0.41	-0.07
Maximum	0.39	0.37	0.02
Percentiles			
5	-0.27	-0.27	0.00
10	-0.24	-0.22	-0.02
25	-0.16	-0.12	-0.05
50	0.05	0.09	-0.04
75	0.16	0.18	-0.02
90	0.22	0.24	-0.02
95	0.25	0.28	-0.03

The Mayflower Wind metocean buoy is located in approximately 47 m (154 ft) of water and has a vertical profile of current observations available, with observations extending to 41 m (135 ft). The near bottom observed currents were compared to model predictions near the bottom. Figure 3-9 shows a comparison of speeds at 39 m (128 ft) depth, and the associated observed and predicted current directions are shown in Figure 3-10. The comparison was made at the 39 m (128 ft) level as the signal in the observations was missing more data at the 41 m (135 ft) depth.

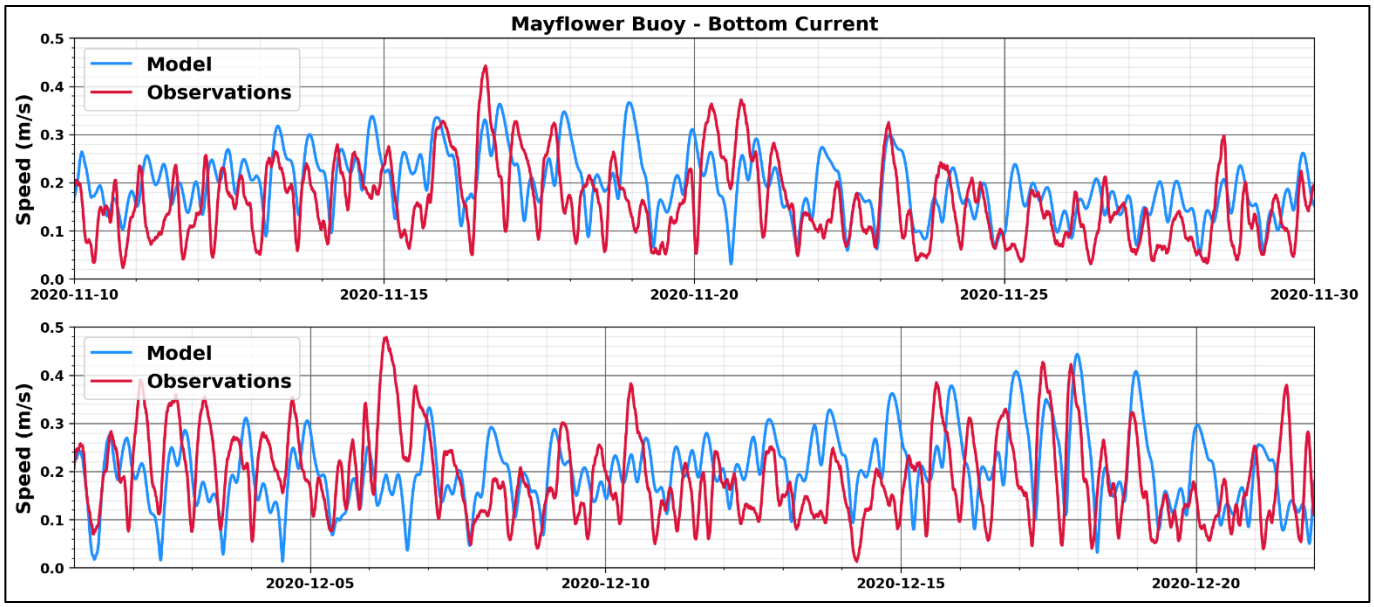

FIGURE 3-9. COMPARISON OF MODELED AND OBSERVED BOTTOM CURRENT SPEED AT THE OFFSHORE MAYFLOWER WIND METOCEAN BUOY.

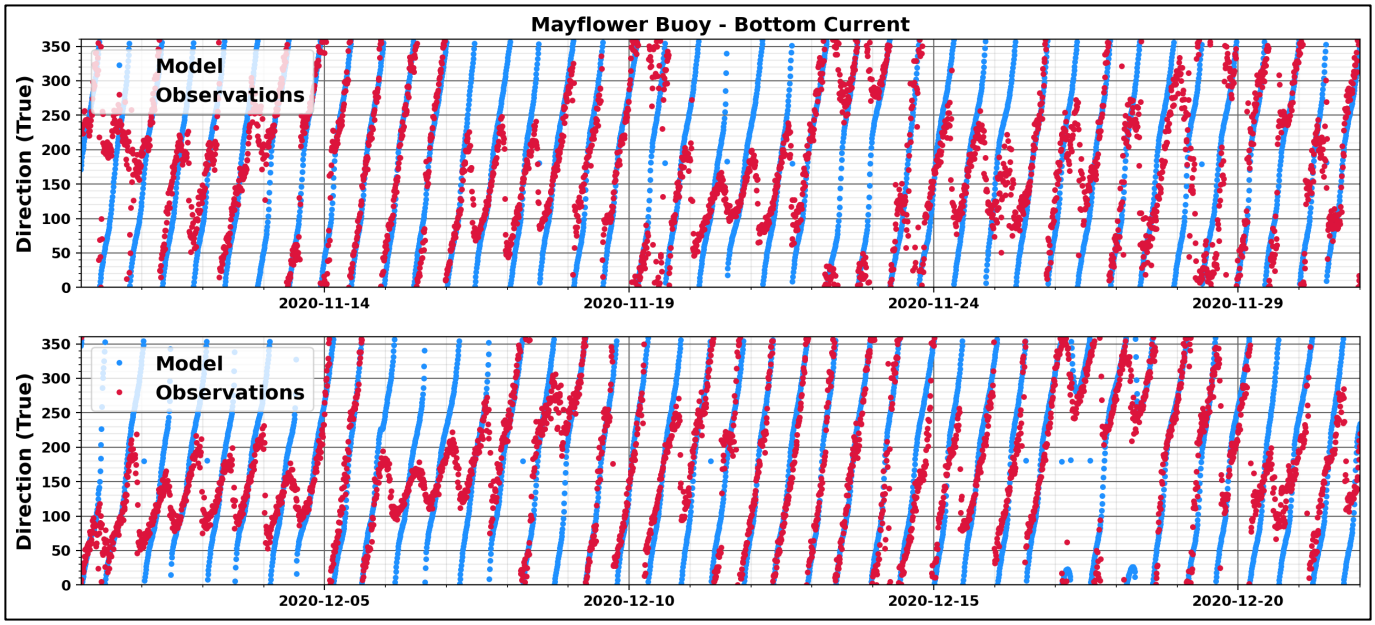

FIGURE 3-10. COMPARISON OF MODELED AND OBSERVED BOTTOM DIRECTION AT THE OFFSHORE MAYFLOWER WIND METOCEAN BUOY.

The figures show that the model recreates the overall magnitude and trends of the current speeds and the general rotary nature of the currents, however the model does not capture the directionality in all instances. The observed currents during this period show more tendency to flow towards the north and east, deviating from the more definite rotary characteristics than was captured by the model. This may be due to the currents during

storm events and also influences of larger offshore currents that are not included in the model. At locations closer to shore from this offshore location it is expected that the current regime is more tidally dominated and outside the influences of the larger scale circulation offshore.

A statistical analysis of the observed and model predicted currents was also performed for the Mayflower Wind metocean buoy location. The minimum, mean and maximum current speeds comparing the model predicted and observed are presented in Table 3-7 along with a range of current speed percentiles. The comparison of these statistics shows that the model is within 0.07 m/s (0.14 kts) on average and has a difference less than 0.05 m/s (0.1 kts) at all percentile levels indicating that while the direction may not always be aligned with the observations the model is predicting the correct proportion and variability of bottom current speeds.

TABLE 3-7. SUMMARY OF CURRENT SPEED STATISTICS AT THE MAYFLOWER WIND METOCEAN BUOY.

	Model (m/s)	Observation (m/s)	Difference (m/s)
Minimum	0.01	0.00	0.01
Maximum	0.44	0.51	-0.07
Percentiles			
5	0.09	0.05	0.04
10	0.11	0.07	0.05
25	0.15	0.11	0.04
50	0.19	0.16	0.03
75	0.24	0.23	0.01
90	0.29	0.30	-0.01
95	0.32	0.34	-0.02

The currents vary throughout a given day and vary day to day as a function of the solar and lunar cycles; most variability is captured in the spring/neap cycle which refers to a two-week period where there are periods of larger tidal amplitudes (spring tides) and smaller amplitudes (neap tides) and these periods are connected by transitional or mean tides. The northeast is dominated by semi-diurnal M2 tides, which results in two high tides and two low tides per day. As a result of these tides, the currents ebb (flow out) and flood (flow in) twice a day. This causes current speeds to continuously ramp up and down in intensity and the directions to oscillate by 180 degrees (e.g. in and out of Narragansett Bay).

In some places the tidal currents are rectilinear, meaning primarily a singular flood and ebb direction with little time at directions between the two, whereas other regions have more rotary like currents which still have predominant ebb and flood however also have a more gradual transition between the two. Plots of the near bottom current speeds across the entire domain for peak ebb and peak flood currents are provided in Figure 3-9. While each plot represents an instant in time, they illustrate the relative spatial variability of peak current speeds across the region. Along the majority of the ECC, the peak current speeds are relatively low (<0.3 m/s), with a few regions with higher peaks such as near the Lease Area termination, a small portion southwest of Martha's Vineyard and then within the Sakonnet River and Mount Hope Bay where peaks increase to approximately >0.5 m/s; however, these peaks are not experienced the majority of the time.

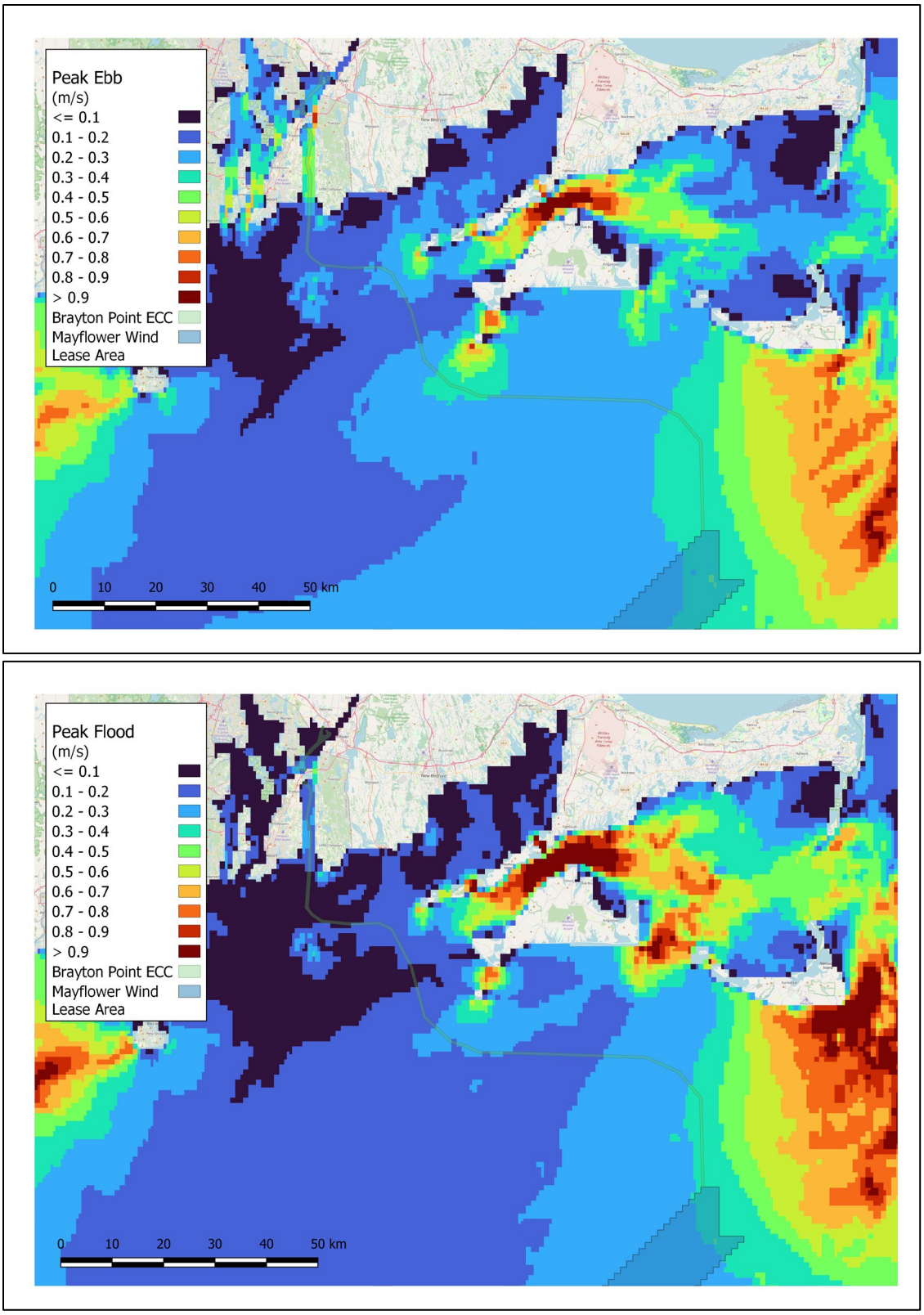

FIGURE 3-11. PEAK EBB (TOP) AND FLOOD (BOTTOM) CURRENT SPEEDS.

3.6 PROJECT SCENARIO

The three-dimensional time varying current fields of validated hydrodynamic model were stored and used in the sediment transport modeling. The near bottom currents at a set of stations aligned with different KPs were queried to assess the current regime along the ECC that will be relevant to the sediment transport. A map showing the current roses at the specific locations is presented in Figure 3-12 and a summary of statistics of the current speeds at these locations is provided in Table 3-8. The current roses show that the bottom speeds are relatively weak, and less than 0.15 m/s more than half the time at most stations except KP22 and KP140. The latter two stations are areas of relatively higher current speeds within the Sakonnet River and offshore near the Lease Area, respectively. The directions differ along the ECC in response to the changing circulation patterns which are shaped by the shoreline and offshore bathymetric features, however at all locations the tidal influence is dominant and the currents shift in direction continuously.

TABLE 3-8. SUMMARY OF CURRENT SPEED STATISTICS ALONG THE ECC.

	Current Speed Statistics (values in m/s)							
	KP5	KP22	KP38	KP50	KP63	KP82	KP108	KP140
Minimum	0.00	0.00	0.00	0.00	0.00	0.00	0.00	0.00
Maximum	0.56	1.16	0.30	0.30	0.30	0.55	0.37	0.45
Percentiles								
5	0.02	0.04	0.01	0.02	0.05	0.06	0.04	0.10
10	0.03	0.07	0.02	0.04	0.06	0.07	0.05	0.12
25	0.06	0.12	0.03	0.06	0.09	0.11	0.08	0.16
50	0.09	0.19	0.04	0.08	0.12	0.15	0.11	0.21
75	0.12	0.25	0.07	0.12	0.15	0.21	0.16	0.26
90	0.15	0.30	0.12	0.15	0.18	0.26	0.20	0.31
95	0.17	0.33	0.18	0.17	0.20	0.31	0.23	0.34

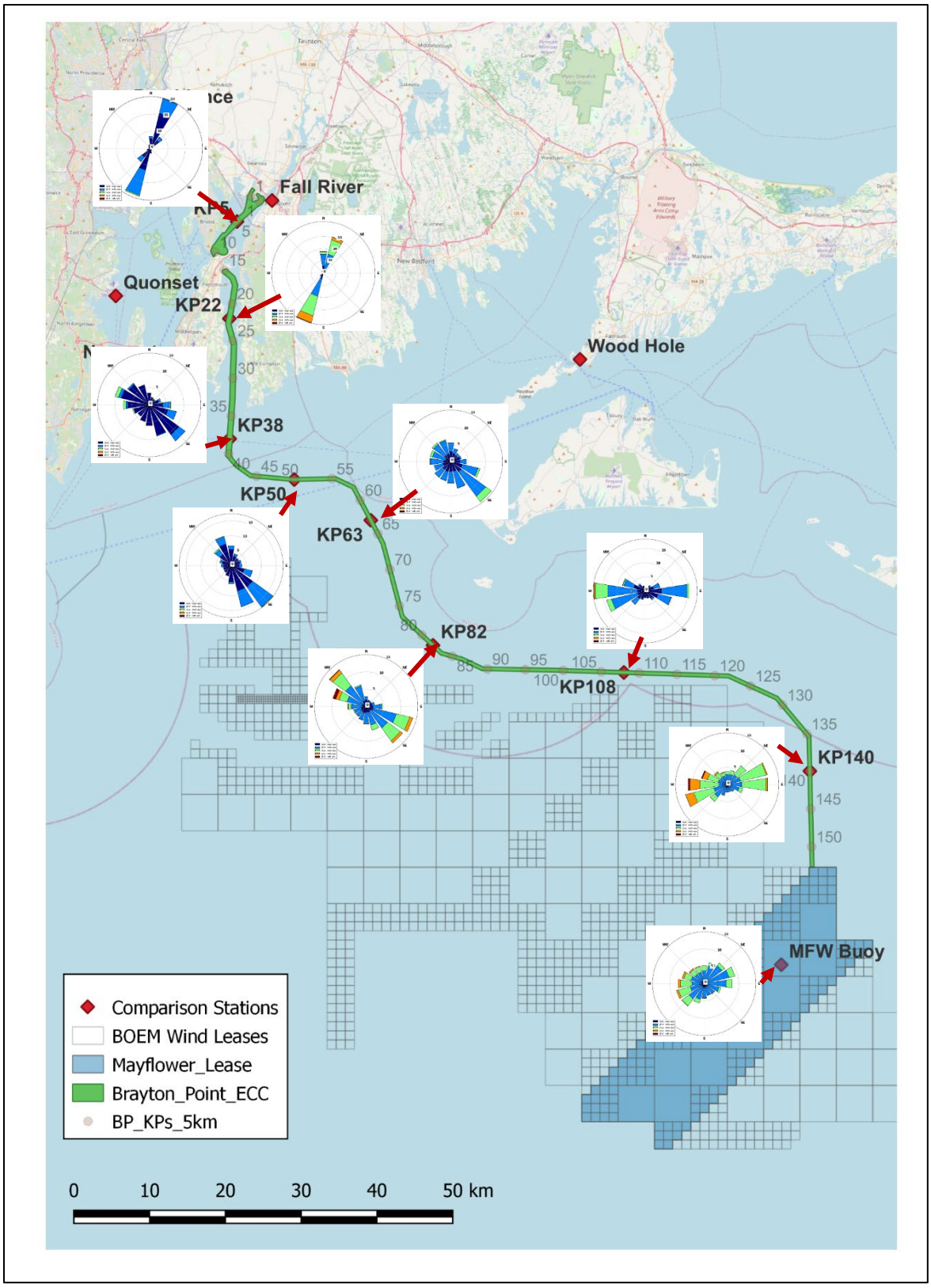

FIGURE 3-12. CURRENT ROSES FROM MODEL PREDICTED BOTTOM CURRENTS AT POINTS ALONG ECC.

4 SEDIMENT TRANSPORT MODELING

The goal of this study was to determine the effects of proposed cable burial activities, evaluated in terms of water column concentrations of suspended sediment and sediment deposition patterns and thickness. The model application focused on "excess" sediment concentrations and did not incorporate natural background concentrations. The concentrations are therefore considered excess above any background levels. The effects were assessed through sediment dispersion, transport, and deposition modeling. This section provides a description of the sediment model application to the Brayton Point ECC development assessment and the resulting model predictions.

4.1 BRAYTON POINT EXPORT CABLE CORRIDOR DESCRIPTION

The planned Brayton Point export cable ECC connecting the Lease Area to land at Somerset, MA can be considered as two basic parts for modeling purposes: the portion of the ECC in Mount Hope Bay and the rest of the ECC extending from the head of the Sakonnet River to Lease Area. For the following analyses, the ECC will be further divided into four segments for discussion purposes: Mount Hope Bay, the Sakonnet River, Offshore Segment 1 (from the Sakonnet River entrance at KP34 to KP78) and Offshore Segment 2 (from KP78 to the north end of the Lease Area at KP152). A map of the Brayton Point ECC showing the four sections and the HDD sites is presented in Figure 4-1.

Starting at the Brayton Point terminus of the ECC, the submarine portion of the cables run from an HDD connection point used to bring the cables from shore, roughly 325 m (1,066 ft) offshore of the Brayton Point landfall, 9.5 km (5 nm) in a southwest direction to another HDD offshore exit point approximately 285 m (935 ft) offshore of the northern end of Aquidneck Island near the Mount Hope Bay entrance just west of Common Fence Point. The cables will cross Aquidneck Island and exit the island via HDD connection point, approximately 340 m (1,116 ft) offshore of Island Park at the head of the Sakonnet River.

The three HDD connection pits will be referred to as the Brayton Point, Mount Hope Bay entrance north of Aquidneck Island, and south of Aquidneck Island at the north end of the Sakonnet River excavation pits, respectively. Each of the excavation pits are assumed to be 3.05 m wide x 6.1 m long x 4.3 m deep (10 ft x 20 ft x 14 ft) for the purpose of this analysis.

Each export cable then runs approximately 18 km (9.7 nm) down the length of the Sakonnet River to the entrance at Rhode Island Sound at KP34. The ECC continues south to KP40 then heads east across the mouth of Buzzards Bay to KP55, south again to KP80 and east across the north end of the MA/RI lease areas to KP130 and finally south to the Mayflower Wind Lease Area at KP 152.

Each of the cable ECC segments and the HDD exit point sites were evaluated individually to determine the re-suspended sediment concentration in the water column, the deposition pattern and dimensions (spread and thickness), at and around the cable burial or HDD excavation site activities. The total surface area of the burial trench, based on the assumed 1 m (3.3 ft) wide trench, is presented in Table 4-1. The surface area associated with each HDD pit excavation is also presented in the table, as well as the amount of time in each the excavation activities take for each segment assuming continuous operation in that segment at the 200 m/hr advance rate.

TABLE 4-1. DISTANCE AND SURFACE AREA OF EACH TRENCH SECTION.

Section	Approximate Distance	Trench Surface Area (based on 1.0 m [3.3 ft] trench width)	Duration of Excavation Activities (hrs)
Mount Hope Bay	9.5 km (5.9 mi)	0.95 ha (2.4 ac)	47.5
Sakonnet River	18 km (11.2 mi)	1.8 ha (4.5 ac)	90
Offshore Segment 1	44 km (27.3 mi)	4.4 ha (10.9 ac)	220
Offshore Segment 2	74 km (46.0 mi)	7.4 ha (18.3 ac)	370
HDD Connection Pit	3.05 m x 6.1 m (10 ft x 20 ft)	0.00186 ha (0.0046 ac)	1

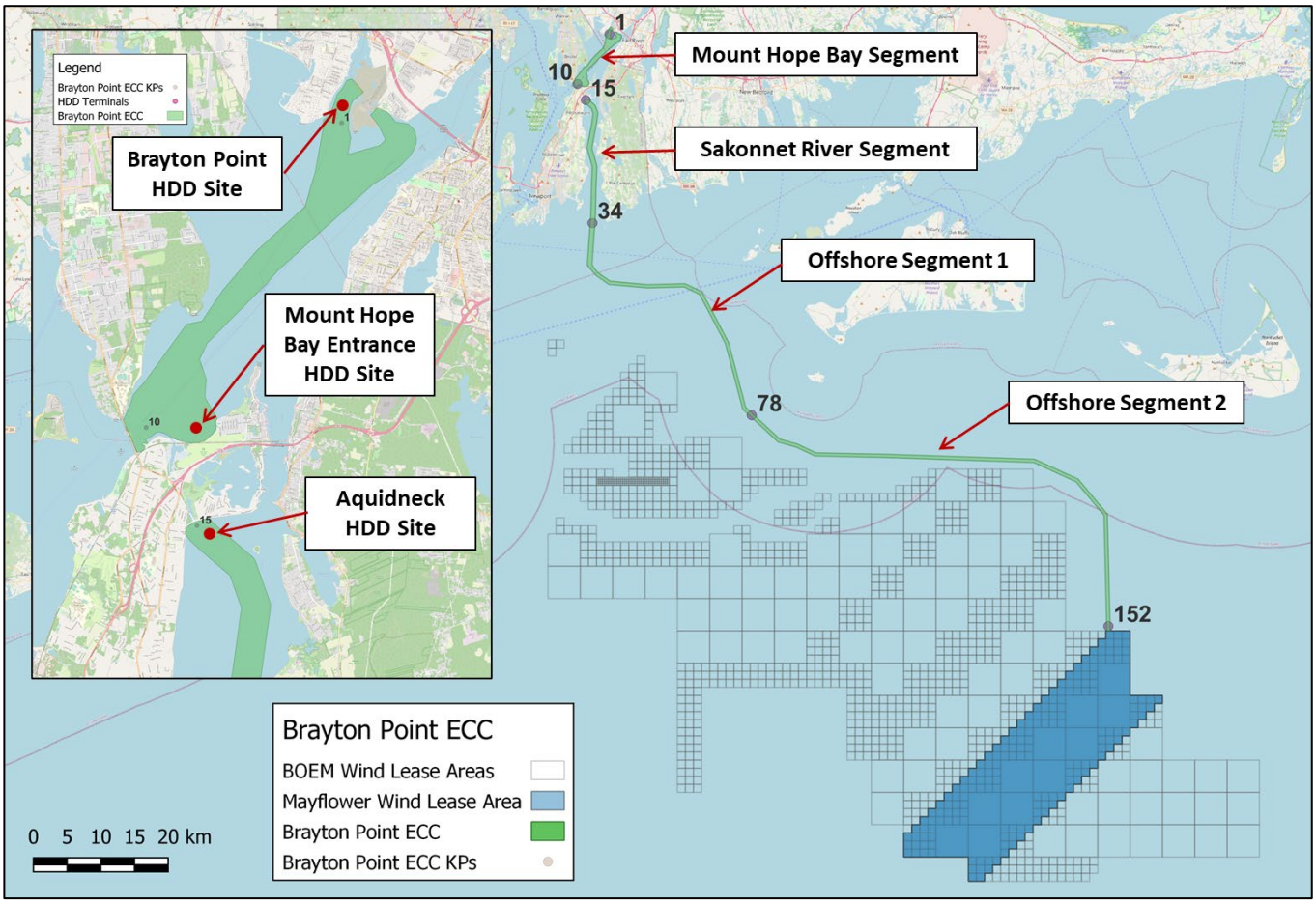

FIGURE 4-1. MAP OF THE BRAYTON POINT ECC SHOWING THE SEGMENTS USED FOR RESULTS DISCUSSION AND THE LOCATIONS OF THE HDD CONNECTION SITES ANALYZED.

4.2 SEDIMENT SOURCE TERMS

Two different subsea excavation techniques are likely to be employed for the cable burial trenching and the HDD pit excavation construction activities. For the cable burial activities, mechanical plow or jetting sediment excavation methods were assumed, while suction dredging was assumed for the HDD pit excavation. Losses (i.e. sediments resuspended to the water column) from each of these activities were represented in the D-WAQ PART model by characterizing the source strength, vertical distribution, and grain-size distribution of the sediment load. Details describing the parameterization of each method are provided below.

The cable burial activities were simulated with an advance rate of 200 m/hr (656 ft/hr). The trench dimensions were specified as 3 m (9.8 ft) deep by 1 m (3.3 ft) wide for the length of the export cables, resulting in a production rate of 600 m^3/hr (21,189 ft^3/hr) for the cable burial. An excavation production rate of 90 m^3/hr (3,178 ft^3/hr) was specified for the HDD pits suction dredging.

Using the source term specifications and the grain size distributions along the ECC, a loading time series was developed for each of the components listed in Table 4-1. The loading was subdivided into five-minute production segments, calculated as the cross-sectional area of the trench times the distance travelled by the jetting equipment in one time step (i.e. 50 m^3 [1766 ft^3] and 16.67 m [54.7 ft]) for injection into the water column over the entire length of the export cables.

Each five-minute load was comprised of six grain size mass components based on the local grain size distribution along that segment of the ECC, a loss rate of 25 percent, the production volume, the volume mass/moisture content ratio and the sediment density and released into the water column. The vertical distribution of the sediments resuspended was centered at 1.5 m (4.9 ft) above the bottom, whereby the majority of the sediment is released close to the seabed. The 25 percent release volume is a conservative value for these types of operations based on previous experience but is used in the absence of contractor data for the specific jetting or mechanical equipment to be used for the actual cable burial in the Sakonnet River, Mt. Hope Bay and Rhode Island Sound.

Suction dredge equipment was specified to be used to excavate the HDD connection pit at each of the sea-to-shore transition points in Mount Hope Bay and in the Sakonnet River. A suction dredger uses a vacuum to excavate a sediment slurry from the seabed and the fluidized sediment is released through a discharge pipe to a spoil area on the seafloor nearby. Contractor estimates indicate that the dredger can operate at a production rate of 90 m3/hr. For implementation in the modeling, it is assumed that 100 percent of the fluidized sediment will be lost to the water column as it is released from the discharge pipe (i.e. sediment will be side-cast adjacent to the excavation site). The discharged sediment is initialized within the model at a single point in the water column, 1.5 m (4.9 ft) above the seafloor. A summary of the export cable burial and the HDD pit excavation activities simulation parameters are presented in Table 4-2and Table 4-3, respectively.

TABLE 4-2. SUMMARY OF EXPORT CABLE BURIAL ACTIVITIES SIMULATED.

Export Cable Burial Activities	
Excavation method	Mechanical or jet trenching
Advance Rate	200 m/hr (656 ft/hr)
Production Rate (Based on 1 m wide x 3 m deep trench)	600 m^3/hr (21,189 ft^3/hr)
Release amount	25 percent
Release height	Centered 1.5 m (4.9 ft) above local seabed
Total Duration	727.5 hrs (30.3 days)

TABLE 4-3. SUMMARY OF HDD PIT EXCAVATION ACTIVITIES SIMULATED.

Export Cable Burial Activities	
Excavation method	Suction dredge
Production Rate (Based on 10 ft x 20 ft, 14 ft deep pit)	90 m^3/hr (3178 ft^3/hr)
Release amount	100 percent
Release height	Centered 1.5 m (4.9 ft) above local seabed
Total Duration (3 pits)	3 hrs (0.125 days)

4.3 EXPORT CABLE CORRIDOR SEDIMENT CHARACTERISTICS

The sediment loading also takes into account the spatial variability of the sediments characteristics along the ECC with respect to the grain size distributions and the water content. For this assessment sediment surface grab samples were taken along the ECC. The samples were obtained as part of site investigation field studies performed for the Project (AECOM, 2022). A total of 36 samples were taken of which 23 were on the Brayton Point ECC and were used to characterize the sediments for the modeling. The remaining samples were taken as controls for use in the lab analysis. The samples were processed to determine the grain size distribution from both sieve and hydrometer and to provide the moisture content and specific gravity.

The grain size analysis was used to determine the percent of sediments in the six different sediment classification bins as defined in Table 2-1 using the Wentworth grade scale. The moisture content and specific gravity were estimated from the data and used to determine the percent of the trench that would be considered solids and to define the sediment density in the model. Since seabed sediments have moisture (water), this means that the trench volume is not entirely comprised of sediment.

The sediment characteristics along the Brayton Point ECC which were used in the modeling are presented in Figure 4-2. In Mount Hope Bay the figure shows that the sediments contain large fraction (over 50 percent) of silt and clay with the remainder divided roughly evenly among the 4 sand bins. At the mouth of the Sakonnet River (southern end) and moving into Rhode Island Sound the predominant sediment fraction is fine sand mixed with coarse and medium sand. Along the Brayton Point ECC to the west of Martha's Vineyard the sediments contain fine and very fine sand but become medium to coarse south of Martha's Vineyard and remain a mix of predominantly fine and medium sand for the remaining segments to the Lease Area. The tabulated details of the

grain size distributions can be found in Appendix 1 - Brayton Point ECC Surface Sediment Grab Sample Grain Size Distribution.

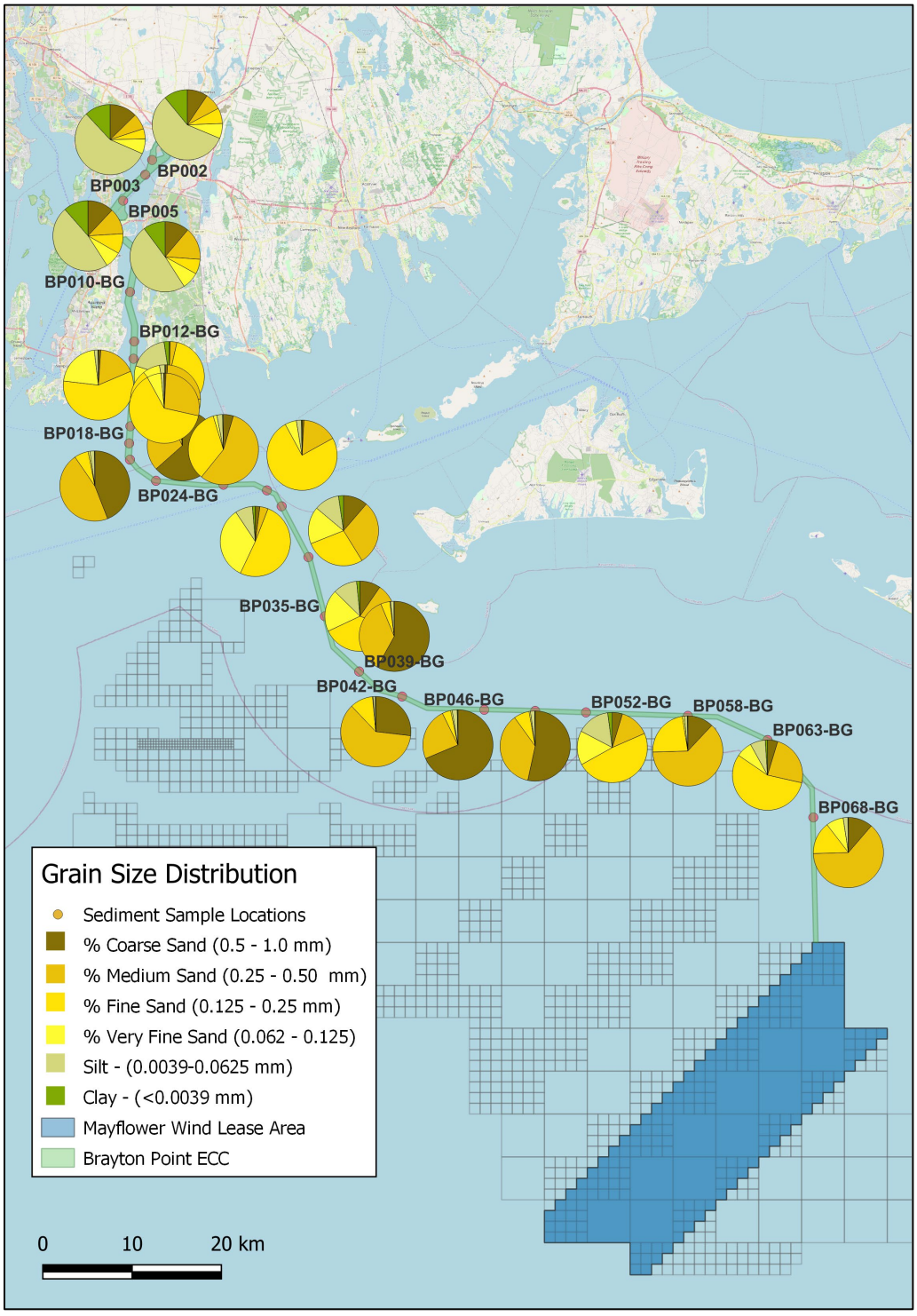

FIGURE 4-2. GRAIN SIZE DISTRIBUTION ALONG THE BRAYTON POINT EXPORT CABLE CORRIDOR. (MAYFLOWER WIND, 2021A)

The grain size distributions were parsed into segments with a dividing line at the mid-point between sediment samples for use in the model. The load development assumed a constant sediment grain size distribution based on the sample between midpoints. There was no additional information available on the transition of sediment characteristics (grain size fractions) between measurements so the modeling did not interpolate between samples. A hard transition was therefore made to the next segment's values at each of the mid-points between samples.

4.4 BRAYTON POINT ECC SEDIMENT MODEL APPLICATION

Based on the ECC, trench dimensions, and near surface sediment data, the model was run for each segment described in the preceding sections. The model was used to predict the trajectory and fate of the resuspended sediment resulting from the jetting and suction excavation activities.

At each time step sediment particles are released into the water column in proportion to the spatially varying sediment class distribution as determined from the surface grab samples analyzed. For each sediment class over 1,250,000 particles were released over the loading period of the simulations. Each particle is advected laterally by tidal currents as predicted by the Delft3D hydrodynamic model application (described in Section 1) at every time step in the model. The three-dimensional currents vary time and space and therefore the sediment model is predicting the sediment transport and deposition for a single discrete event. For this study a start date was chosen for a time period that would be likely to embark on the cable burial operations and was coordinated with a time when there was in-situ data for model validation as presented in Section 1. The final selected dates placed the simulation between November and December 2020.

At each time step of the model simulation sediment concentrations in the water column were calculated both on the hydrodynamic model grid as well as on a rectangular grid measuring approximately 20 m by 20 m (65 ft x 65 ft) in the horizontal and 1 m (3.28 ft) in the vertical dimension. For each model time step, water column concentrations of total suspended sediments were calculated based on the mass of sediment per unit volume of water for each class of sediments and stored in terms of mass per cubic meter.

Concentrations are calculated on a grid of finite dimension and therefore provide a concentration average, based on the cell volume and mass within that cell, at each time step and thus in reality there may be some highly localized peaks above the model predicted concentrations, directly above the cable burial tool representative of a jet / mechanical trenching.

Individual sediment particles also have a downward (fall) velocity which is variable depending on both the particle size of the sediment class (settling velocity) and the environmental conditions. There is some upward movement potential associated with the parameterized vertical mixing but the general trend is for the particles to settle to the seabed where larger particles settle faster than smaller ones. Once a sediment particle has settled onto the bottom it remains as placed (no-resuspension is assumed).

Deposited mass was calculated based on particle deposition locations overlain on the same rectilinear 20 m by 20 m (65 ft x 65 ft) grid. The deposition for each cell calculated by the model are also averages across finite grid cell area. There may be some highly localized points (i.e., in line with the jetting) where deposition accumulations

exceed that of the predicted deposition as output by the model. The mass in each cell across the seabed is stored at each time step (therefore always accumulating) in units of mass per square meter.

The model was also used to simulate the sediment dispersion from the HDD pit suction dredging. Three HDD-associated sediment release scenarios were modeled, corresponding to the Brayton Point, Mount Hope Bay and Aquidneck HDD connection offshore sites. Based on specifications provided by Mayflower Wind, 80 m^3 (2,825 ft^3) of sediment were to be entrained in the suction device and discharged at a nearby site over a period of approximately 1 hour.

A similar methodology was applied for these cofferdam infilling scenarios as was done for the jet/mechanical trenching scenarios concerning the sediment type, with the same sediment classification being used and the sediment distribution being determined based on the closest grab sample. The same 20 m by 20 m (65 ft by 65 ft) horizontal grid was used to calculate concentration and deposition output. A five-minute time step was used for all of the HDD simulations.

The results of the model simulations are presented in the following sections. The sections address the potential impacts for the Mount Hope Bay jetting, the Sakonnet River jetting, the two offshore jetting activities and the HDD activities, respectively.

4.5 SEDIMENT TRANSPORT MODEL RESULTS

The D-WAQ PART model was used to perform simulations for each construction activity. All modeling assumed continuous operation for each phase of the construction. Note that reported concentrations are those predicted above the background concentration in the study area.

The results from the model runs are presented below in maps showing the predicted TSS concentrations and subsequent deposition for each activity. Specifically, two sets of graphics were developed for each scenario:

(i) A map of time-integrated maximum instantaneous TSS concentrations (mg/L), which shows peak TSS for any cell at any time step in the model domain throughout full water column.
(ii) Seabed deposition (thickness in mm) following the modeled activity.

The results are depicted in multiple figures for the scenario. The subsections below discuss the figures for the scenario result and summarize the results in tabular form. Two main sections address the water column TSS concentrations and the deposition thickness resulting from the sediments settling to the seabed. The results in each of those sections are divided into 3 sub-sections representing the impacts on two Narragansett Bay segments, (Mount Hope Bay and the Sakonnet River), two offshore segments, (the portion of the ECC between KP34 and KP78, and the portion on the ECC between KP78 and KP152), and the HDD pit excavation activities impacts, respectively.

4.6 WATER COLUMN CONCENTRATION

The water column concentrations presented are the maximum TSS concentration above background anywhere in the water column at each 20 m x 20 m (65 ft x 65 ft) concentration grid cell over the total duration of the cable installation. Ambient TSS load and concentrations have been monitored in Mount Hope Bay for many years, related to concerns for impacts of the three waste water treatment plants that discharge into the bay and rivers feeding the bay (EPA, 2016, Abdelrhman 2016, Desbonnet et.al., 1992). Ambient TSS concentrations were observed ranging regularly from 2 mg/L to 19 mg/L, with a mean of in the range of 11 mg/L (FERC, 2005).

4.6.1 Mount Hope Bay and Sakonnet River Sediment Concentrations, KP0 - KP34

A map of the maximum water column TSS associated with the cable installation activities in the Mount Hope Bay (KP0 – KP10) and Sakonnet River (KP15 – KP34) portions of Narragansett Bay are presented in Figure 4-3 and Figure 4-4. The transport and dispersion of resuspended sediments in the two water bodies are similar.

Mount Hope Bay is an enclosed partially mixed estuary with a dynamic tidal regime, effectively transporting and dispersing the resuspended sediments over a wide area as can be seen in the figure. The level of maximum concentrations predicted in the estuary was primarily a result of the relatively high concentrations of silt and clay in the sediments as seen in the grain size distribution data (Figure 4-2 and Appendix 1 - Brayton Point ECC Surface Sediment Grab Sample Grain Size Distribution). The small grain size of the silt and clay particles mean that they settle more slowly than sand classes allowing additional time for transport and spreading through tidal circulation.

Mount Hope Bay has two openings, (to the south and southwest), and is open to the tidally influenced Taunton River at the head of the bay in the northeast corner. The tidal dynamics drive the currents along a predominantly southwest-northeast axis which aligns with the majority of the Brayton Point ECC, transporting the resuspended sediments along the ECC axis. The higher TSS concentrations are consequently seen to follow the ECC as well. The exception is the area near the southwest entrance to the bay where the ECC turns south towards the HDD connection north of Aquidneck Island. Along that section of the ECC the suspended sediments (and the maximum TSS concentrations) were transported perpendicular to the ECC.

The Sakonnet River is similarly an enclosed partially mixed estuary with a dynamic tidal regime, transporting and dispersing the resuspended sediments over a wide area. The river also has relatively high concentrations of silt and clay in the sediments as seen in the grain size distribution. For the most part the tidal currents along the length of the estuary are aligned with the ECC except near the head of the Sakonnet River where the ECC is in a southeast-northwest direction. In that area the tidal currents are oblique to the ECC and some higher TSS concentrations are seen to extend farther from the cable installation centerline. There is also a section of higher speed currents over the portion of the ECC that run past Fogland Point, midway along the river, where maximum TSS concentrations follow the currents off the ECC centerline.

Figures 4-3 and 4-4 show a time-integrated picture of the modeled maximum concentration over the entire trenching simulation; concentrations are not at the level shown all at once, but occur over time as the cable installation progresses. As an example, the concentration in the Sakonnet River at an instant in time is presented in Figure 4-5. In the figure, the sediment plume is seen being transported to the north, away from the trenching operation but is dispersed and diminishes to near background levels within a few kilometers. At any given location, the high concentrations dimmish rapidly and the low concentrations diminish to background in only a few hours.

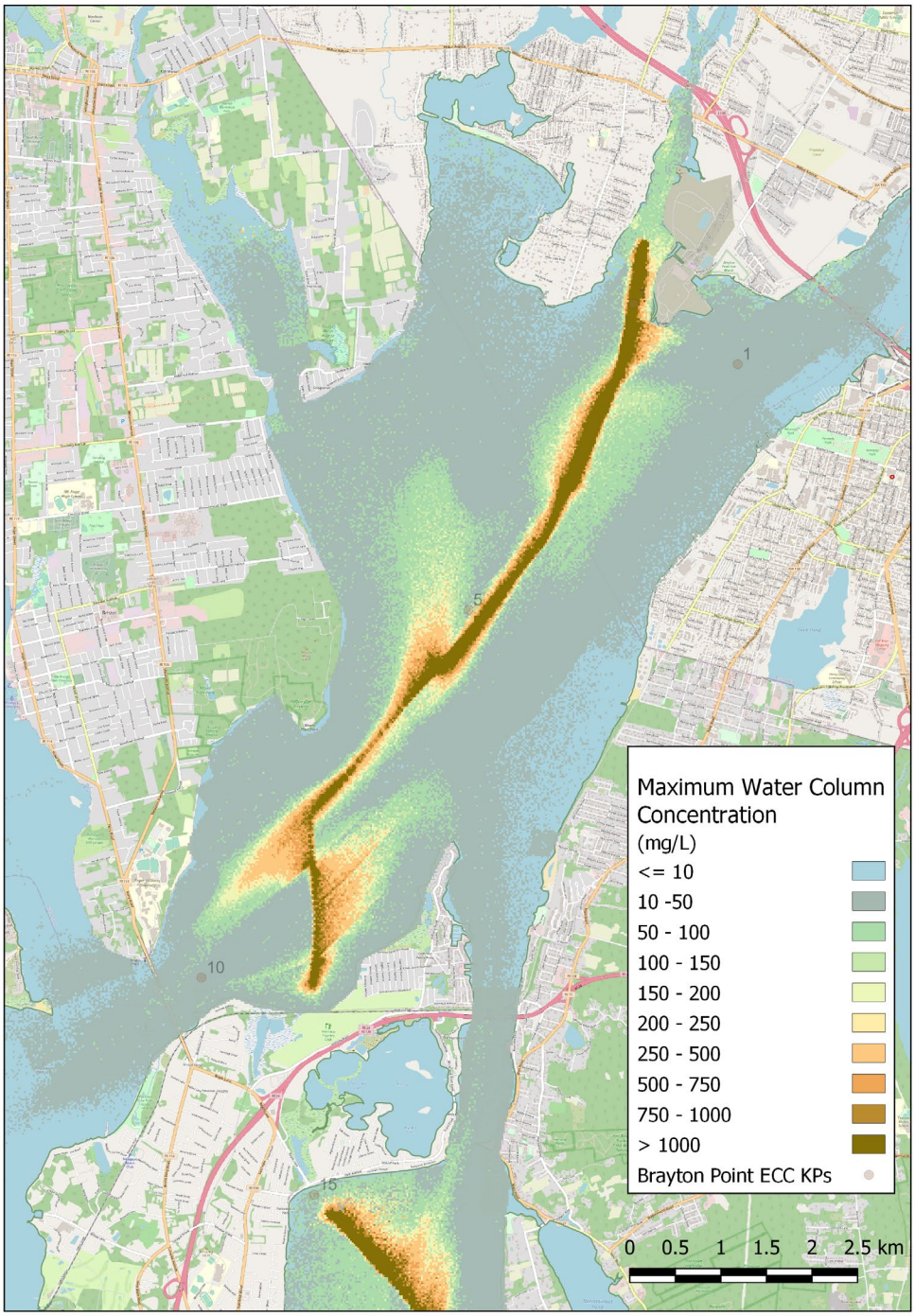

FIGURE 4-3. MAP OF MAXIMUM SEDIMENT CONCENTRATION IN THE MOUNT HOPE BAY PORTION OF THE EXPORT CABLE INSTALLATION, KP0 TO KP10.

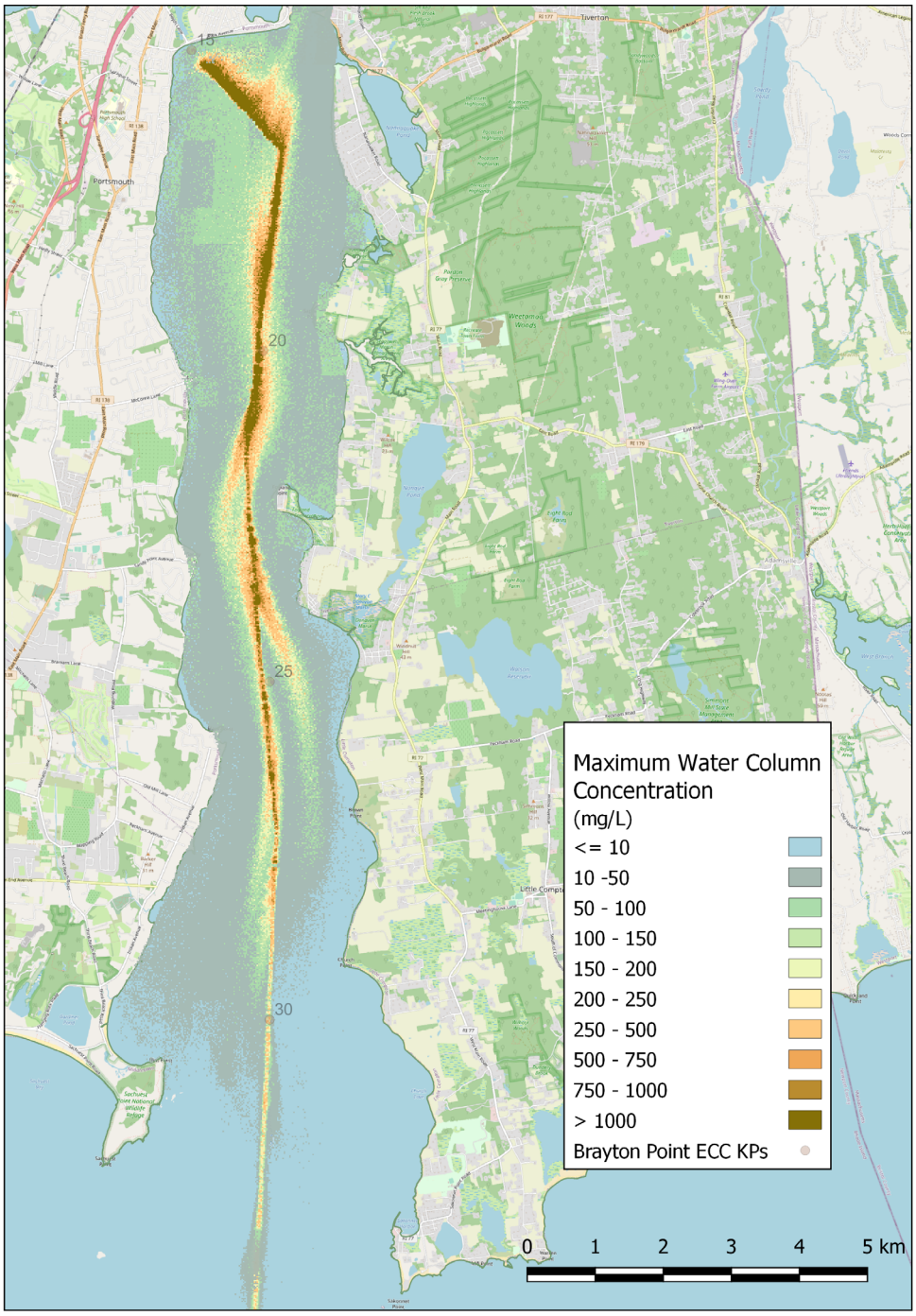

FIGURE 4-4. MAP OF MAXIMUM SEDIMENT CONCENTRATION IN THE SAKONNET RIVER PORTION OF THE EXPORT CABLE INSTALLATION, KP15 TO KP34.

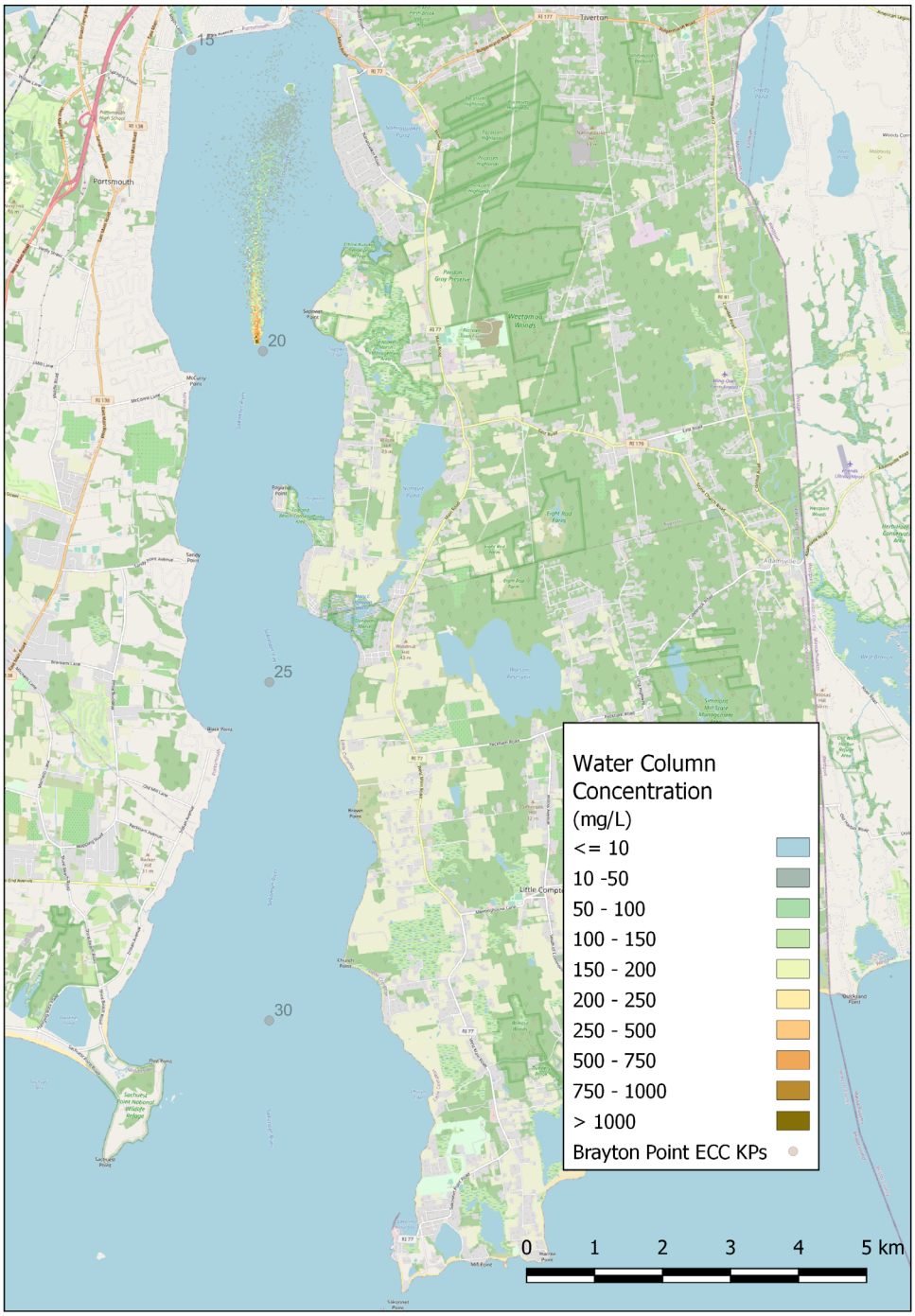

FIGURE 4-5. MAP OF AN EXAMPLE INSTANTANEOUS SEDIMENT CONCENTRATION AT IN THE SAKONNET RIVER PORTION OF THE EXPORT CABLE INSTALLATION, KP15 TO KP34.

The maximum water column TSS concentration results are summarized in Table 4-4, describing the area coverage at selected TSS concentration threshold and the distance that the TSS concentration extends from the cable installation centerline. While the lower concentration numbers in the table indicate that 10 mg/L could be observed at a maximum distance of 4.4 km (2.7 mi) from the ECC in Mount Hope Bay and up to 3.3 km (2.1 mi) from the ECC in the Sakonnet River, the more biologically keyed threshold of 100 mg/L was contained within approximately 1.2 km (0.74 mi) and 0.62 km (0.38 mi) for Mount Hope Bay and the Sakonnet River, respectively. The area coverage of the threshold TSS concentration levels of 100 mg/L maximum TSS concentration in Mount Hope Bay and the Sakonnet River were 542 ha (1340 ac) and 668 ha (1650 ac), respectively.

TABLE 4-4. AREA COVERAGE FOR SELECTED TSS CONCENTRATION THRESHOLDS IN MOUNT HOPE BAY AND THE SAKONNET RIVER (KP0 – KP34).

TSS Threshold (mg/L)	Mount Hope Bay Area Coverage (ha) KP0 - KP10	Maximum Distance from Indicative ECC Centerline (km)	Sakonnet River Area Coverage (ha) KP15 - KP34	Maximum Distance from Indicative ECC Centerline (km)
10	3625	4.40	3477	3.37
50	1015	1.83	1330	1.46
100	542	1.16	668	0.61
150	402	0.99	488	0.44
200	334	0.74	391	0.39
250	293	0.57	321	0.22
500	184	0.32	175	0.0
>1000	101	0.15	84	0.0

4.6.2 Offshore Sediment Concentrations, KP34 - KP152

The maximum water column TSS concentrations from the cable installation process offshore, between the mouth of the Sakonnet River and the Mayflower Wind Lease Area are presented in Figure 4-6 and Figure 4-8 and a summary table of TSS concentration areal coverage and distance from the installation centerline is presented in Table 4-5. The results are noticeably different than those of the Mount Hope Bay and Sakonnet River areas. The segment of the ECC extending directly south from the mouth of the Sakonnet showed a fairly small signature of even the 10 mg/L TSS concentration level between KP34 and KP45. A signature tidal oscillation was seen but again small through KP45 but increasing towards KP78. In addition, the higher TSS concentrations remained close to the centerline from the Sakonnet River entrance through KP55. It can be seen from the grain size distribution (Figure 4-2) that the amount of slit and clay is only a small fraction of the total sediment distribution and larger sized particle dominate indicating that the settling would be faster and therefore less transport occurred through that area.

The small grain size fractions increase in their proportion of the distribution between KP55 and KP78 which led to more transport and dispersion and greater area coverage away from the ECC. The areal coverage at the selected TSS concentration thresholds for the Offshore Segment 1 portion of the cable installation route were similar if not lower in each case than those of the Mount Hope Bay and Sakonnet River areas although the length of the ECC through this segment is more than 2 times as long as the Sakonnet River and 4.5 times as long as the Mount Hope

Bay segment. The 10 mg/L TSS concentration extended up to 2.2 km (1.3 mi) away from the cable installation centerline but the 100 mg/L threshold concentration is contained within 0.37 km (0.23 mi).

The Offshore Segment 2 segment (KP78 – KP152) of the export cable installation impacts are presented in Figure 4-8. There was a length of relatively low impact between KP78 and KP100 in this segment which was due to the predominance of large sediment grain sizes. The TSS concentrations and their extent were low in the area. This is true for most of the offshore segments of the ECC, where concentrations of 100mg/L were predicted to be within 50 m (160 ft) of the centerline, and to decreased quickly.

In the stretch of the ECC to the east of KP100 the grain size distribution changes to favor smaller particle sizes again and the 10 mg/L TSS concentration limit extent increased to a maximum distance of 1.65 km (1 mi) commensurately. The 100 mg/L concentration limit reaches 0.37 km (0.23 mi) as in the previous segment, but the higher concentration thresholds are all contained in smaller areas closer to the ECC centerline.

The effects of the rotary tidal current oscillations observed in the Mayflower Wind metocean buoy currents and the hydrodynamic model predicted currents can be seen in the 10 mg/L concentration footprint in Figure 4-8. Rather than a rectilinear (back and forth motion) tidal pattern in the sediment concentrations, the concentrations can be seen to make an almost helical pattern between KP100 and KP152. The currents are fairly strong in that region but the grain size distribution shows a predominance of larger sizes which resulted in lower water column concentrations.

TABLE 4-5. AREA COVERAGE FOR SELECTED TSS CONCENTRATION THRESHOLDS FOR THE OFFSHORE EXPORT CABLE SEGMENTS (KP34 – KP152).

TSS Threshold (mg/L)	Offshore Segment 1 Area Coverage KP34 - KP78 (ha)	Maximum Distance from Indicative ECC Centerline (km)	Offshore Segment 2 Area Coverage KP78 - KP152 (ha)	Maximum Distance from Indicative ECC Centerline (km)
10	3408	2.18	6629	1.65
50	1163	0.75	1354	0.71
100	662	0.37	585	0.37
150	437	0.23	340	0.17
200	312	0.13	216	0.10
250	232	0.09	148	0.09
500	80	0.0	32	0.0
>1000	11	0.0	3	0.0

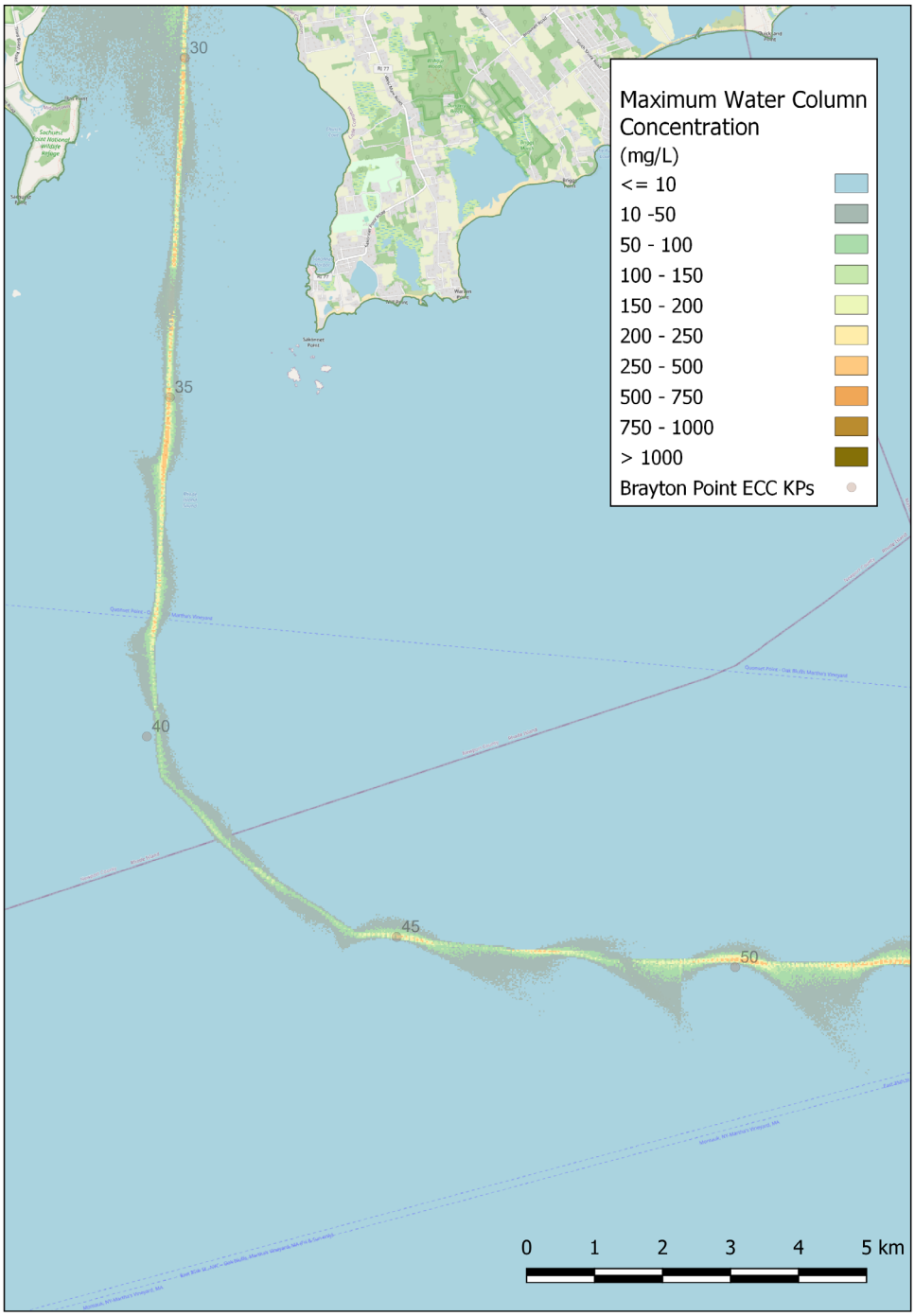

FIGURE 4-6. MAP OF MAXIMUM SEDIMENT CONCENTRATION ASSOCIATED WITH THE OFFSHORE EXPORT CABLE INSTALLATION, KP34 TO KP55.

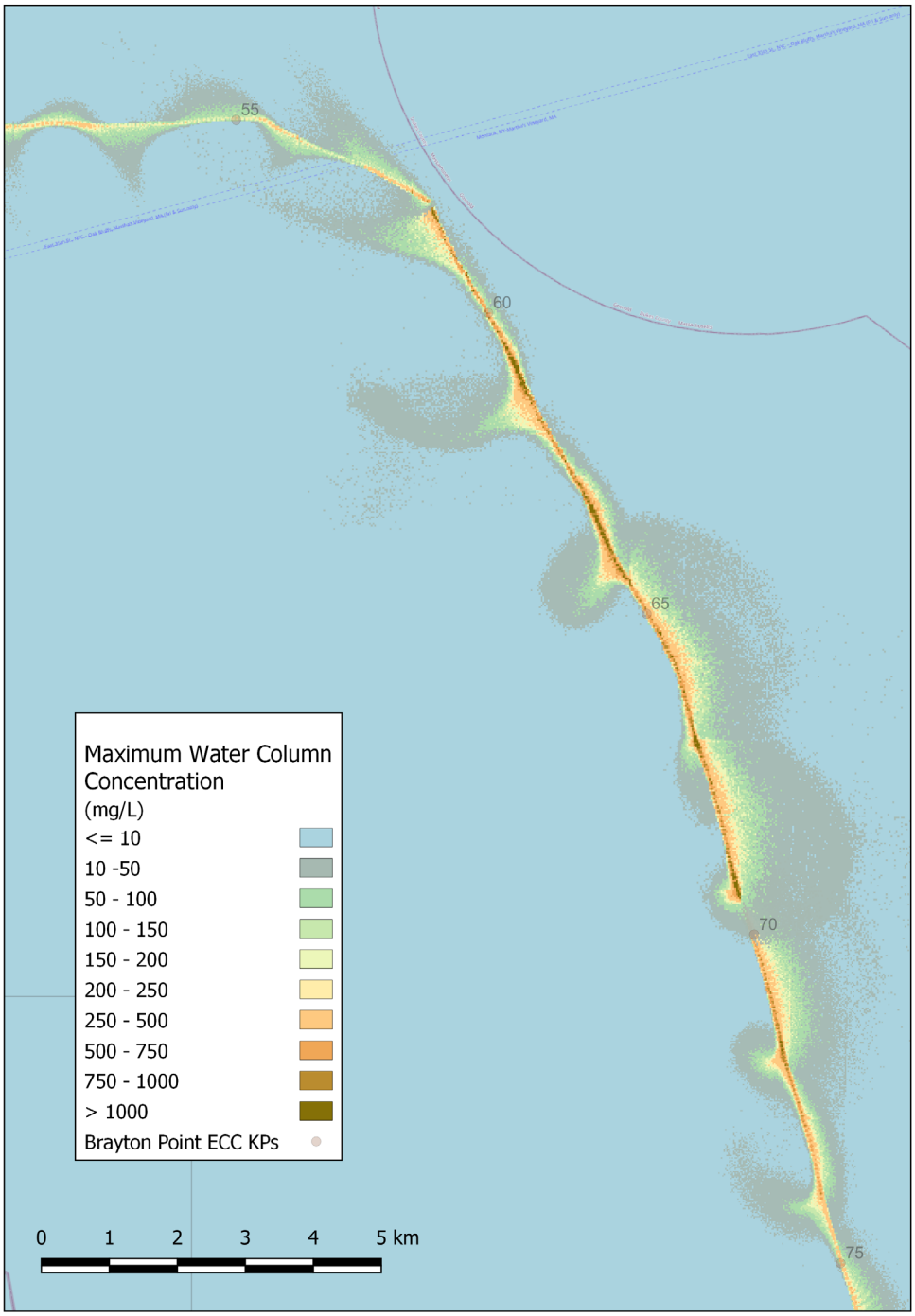

FIGURE 4-7. MAP OF MAXIMUM SEDIMENT CONCENTRATION ASSOCIATED WITH THE OFFSHORE EXPORT CABLE INSTALLATION, KP55 TO KP78.

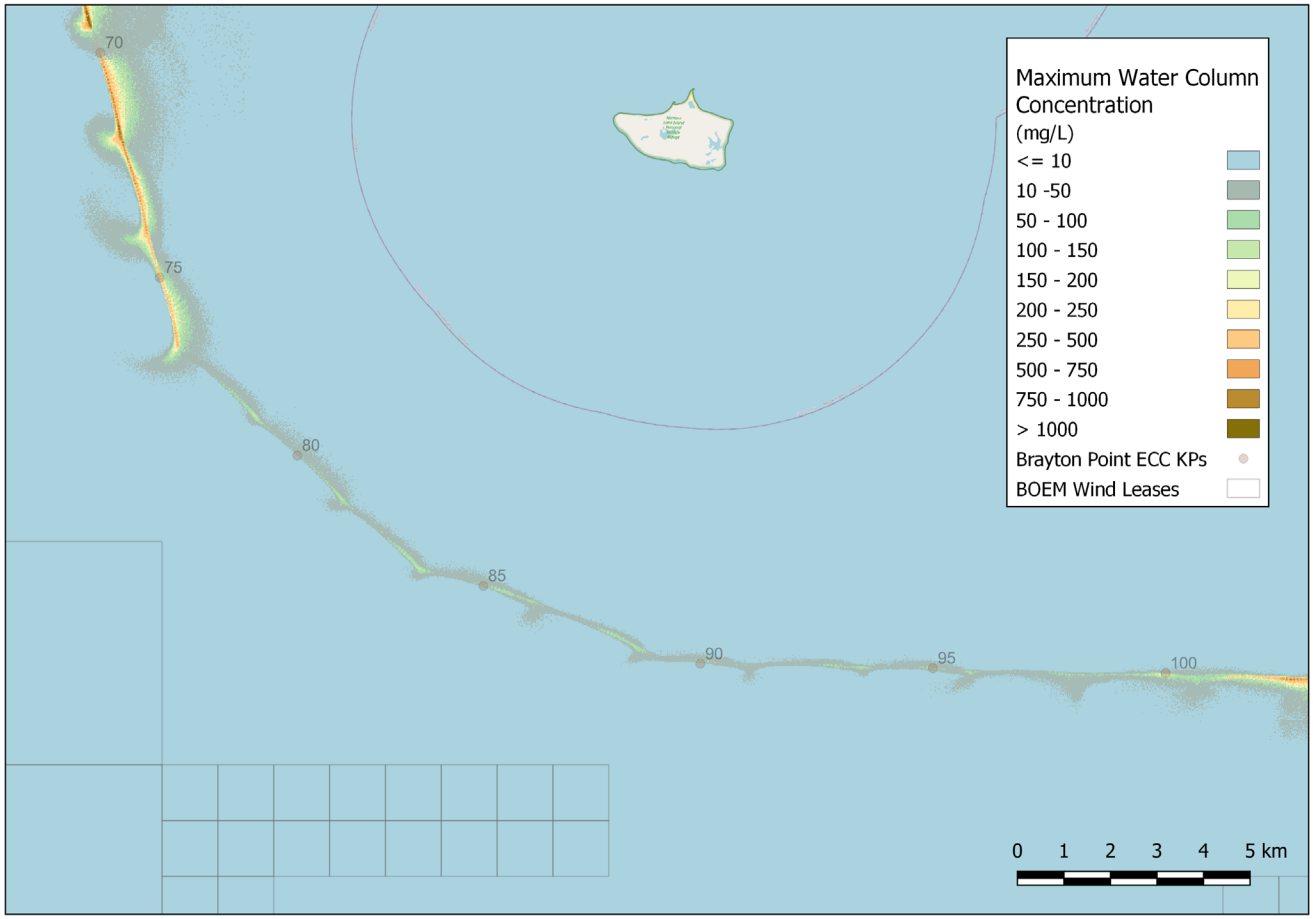

FIGURE 4-8. MAP OF MAXIMUM SEDIMENT CONCENTRATION ASSOCIATED WITH THE OFFSHORE EXPORT CABLE INSTALLATION, KP78 TO KP105.

Reviewing Table 4-6 in light of Table 4-4 and Table 4-5, it can be seen that half or more of the impacts were experienced in the Mount Hope Bay and Sakonnet River segments, at less than 30 km (19 mi), (20 percent of the total length), as opposed to 118 km (73 mi) for the offshore segments. This was particularly true of the higher TSS concentration levels examined.

It is of interest to understand how the resuspended TSS and associated concentrations disperse over time. This provides an additional metric to better understand the physical impacts and their environmental consequences. A summary of the duration of the TSS plume after the cessation of the installation activities at selected concentration levels for each of the ECC segments examined above is presented in Table 4-7.

The duration of the water column concentrations in Mount Hope Bay were fairly slow to decrease as the relatively higher currents in the bay appear to have kept the sediment suspended longer than in slower current areas. The same was true of the Sakonnet River although to a lesser extent where the higher concentrations settled out quickly.

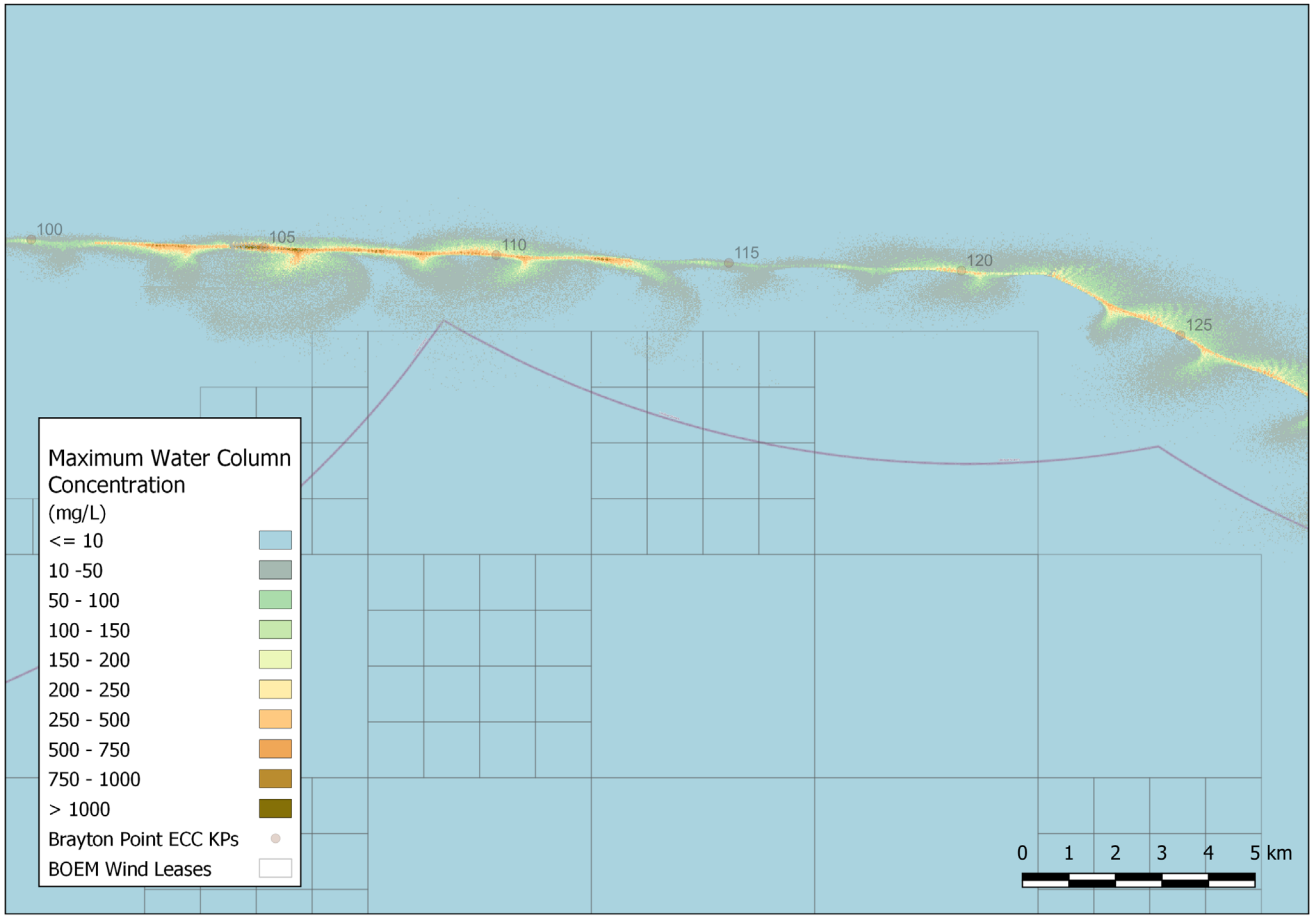

FIGURE 4-9. MAP OF MAXIMUM SEDIMENT CONCENTRATION ASSOCIATED WITH THE OFFSHORE EXPORT CABLE INSTALLATION, KP105 TO KP125.

TABLE 4-6. SUMMARY OF TOTAL AREA COVERAGE FOR SELECTED TSS CONCENTRATION THRESHOLDS OVER THE LENGTH OF THE ECC.

TSS Threshold (mg/L)	Total Area Coverage KP0 - KP152 (ha)
10	17140
50	4863
100	2457
150	1668
200	1253
250	993
500	470
>1000	199

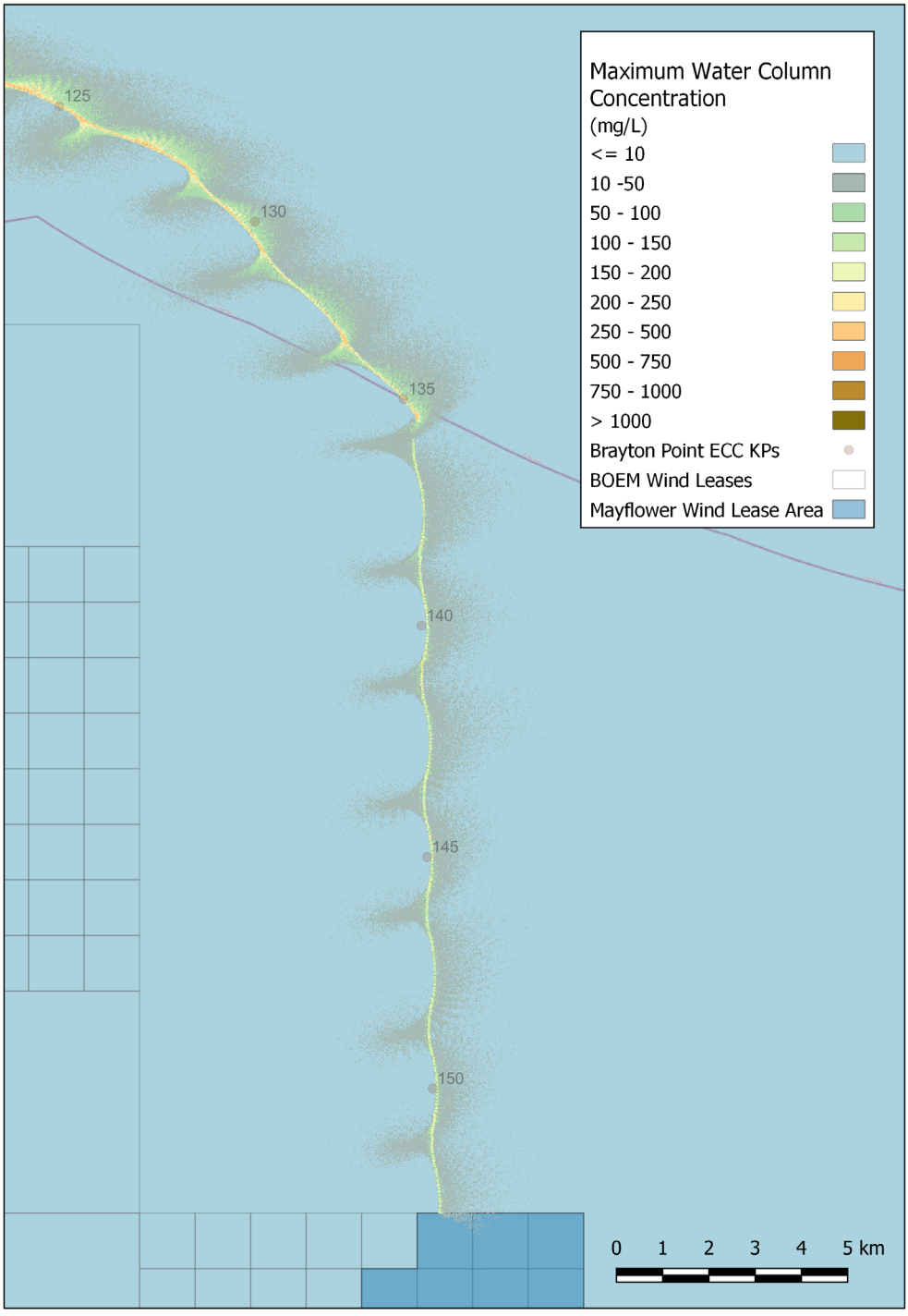

FIGURE 4-10. MAP OF MAXIMUM SEDIMENT CONCENTRATION ASSOCIATED WITH THE OFFSHORE EXPORT CABLE INSTALLATION, KP125 TO KP152.

The offshore segments cleared more rapidly than in Mount Hope Bay and the Sakonnet River but the very fine sand and silt content in Offshore Segment 1 between KP55 and KP78 increase the duration at the selected concentration threshold levels evaluated in comparison to the remainder of the offshore route.

In all areas excluding Mount Hope Bay and a portion of Offshore Segment 1, the TSS concentration fell below the 100 mg/L threshold in less than 20 minutes. These results indicate that the water column TSS concentration impacts from the export cable installation activities were contained to within or near the Brayton Point ECC and were short lived.

TABLE 4-7. TIME FOR TSS CONCENTRATIONS TO DROP BELOW SELECTED LEVELS ALONG THE ECC AFTER THE END OF THE CABLE INSTALLATION ACTIVITIES

TSS Concentration (mg/L)	Mount Hope Bay KP0 - KP10 (min)	Sakonnet River KP10 – KP34 (min)	Offshore Segment 1 KP34 – KP78 (min)	Offshore Segment 2 KP78 – KP152 (min)
10	2980	1465	725	255
50	860	465	215	95
100	280	20	175	35
150	160	20	115	15
200	140	20	95	15
250	120	20	95	15
500	100	0	35	0
>1000	60	0	15	0

4.6.3 HDD Pit Excavation Sediment Concentrations

The impacts of the HDD excavation were examined in the same manner as the cable installation impacts. Figure 4-11 shows the model predicted extent of the maximum water column TSS concentration at each of the HDD sites overlain on the ECC. The Brayton Point HDD pit results shown on the map in the left figure indicate that the impacts of the dredging activities there were almost entirely contained within the ECC. The same is almost true for the Mount Hope Bay entrance and the Aquidneck pit excavation activities though a short tail of 10 mg/L TSS concentration extends across the ECC centerline in each reaching a maximum of 1 km (0.62 mi) from the Mount Hope Bay pit and 0.88 km (0.55 mi) from the Aquidneck pit. The 100 mg/L threshold TSS concentration was contained within 0.33 km (0.2 mi) and was within the ECC boundaries in all cases. It should be noted that for the Mount Hope Bay and Aquidneck sites there is a tidal influence that transports the sediment plume in one direction (towards the east in this case). At other stages of the tide the plume is likely to be directed in the opposite direction, albeit with similar levels of impact.

The areal coverage of the 10 mg/L or higher TSS concentration ranged from a low of 18 ha (45 ac) at the relatively low energy Brayton Point site up to 28 ha (70 ac) at the high energy Mount Hope Bay site near the entrance to Mount Hope Bay. The 100 mg/L TSS concentration threshold covered no more than 5.4 ha (13 ac) at any of the sites.

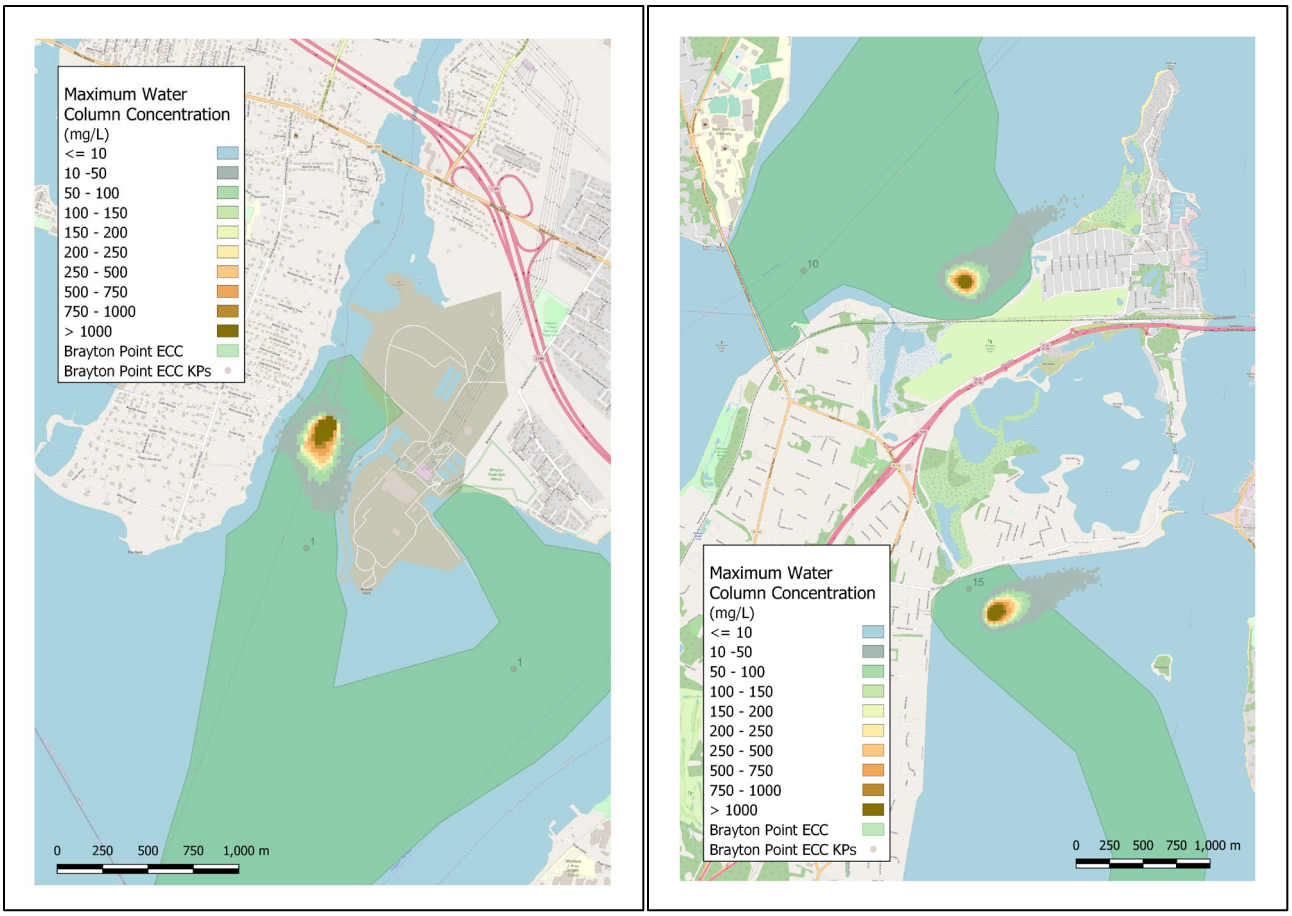

FIGURE 4-11. MAP OF MAXIMUM SEDIMENT CONCENTRATION ASSOCIATED WITH THE EXCAVATION ACTIVITIES AT THE THREE HDD CONNECTION PITS AT BRAYTON POINT (LEFT MAP), AND MOUNT HOPE BRIDGE AND AQUIDNECK ISLAND (RIGHT MAP).

TABLE 4-8. AREA COVERAGE FOR SELECTED TSS CONCENTRATION THRESHOLDS FOR THE THREE HDD PIT EXCAVATION ACTIVITIES.

TSS Threshold (mg/L)	Brayton Pt HDD Pit Area Coverage (ha)	Maximum Distance from Release (km)	Mount Hope Bay HDD Pit Area Coverage (ha)	Maximum Distance from Release (km)	Aquidneck HDD Pit Area Coverage (ha)	Maximum Distance from Release (km)
10	18.5	0.53	28.5	1.08	22.5	0.88
50	7.1	0.38	7.0	0.21	7.5	0.31
100	5.2	0.32	4.6	0.14	5.4	0.25
150	4.4	0.29	3.6	0.11	4.4	0.21
200	3.8	0.27	2.9	0.11	3.7	0.20
250	3.3	0.25	2.6	0.10	3.2	0.18
500	2.4	0.21	1.6	0.08	2.1	0.15
>1000	1.4	0.17	0.8	0.05	1.2	0.10

The amount of time required for the water column TSS concentration to drop below the 100 mg/L threshold was less than 100 min at all of the HDD pit areas (Table 4-9). The concentrations sank below the selected thresholds relatively quickly, the lower concentrations or 10 mg/L and 50 mg/L persisted for several hours at the high energy Mount Hope Bay site.

TABLE 4-9. TIME FOR TSS TO DROP BELOW SELECTED LEVELS AT THE HDD SITES AFTER THE END OF THE RELEASE

TSS Concentration (mg/L)	Brayton Pt-HDD Duration (min)	Mount Hope Bay-HDD Duration (min)	Aquidneck-HDD Duration (min)
10	280	400	300
50	140	160	120
100	100	100	100
150	80	100	80
200	80	80	80
250	60	80	60
500	40	40	40
>1000	20	40	40

4.7 SEDIMENT DEPOSITION ON THE SEABED

The ultimate fate of the resuspended sediments is to resettle onto the seabed. Depending on the amount and type of sediments resuspended and the local current regime they can settle close to or far from the resuspension point at the cable installation operations. These factors also affect the sedimentation depth, i.e. how thick a layer the deposited sediments can create. As with the water column concentrations the farther the sediments are transported the more area they cover when settling, but at a lower thickness than if the entire mass settles near the resuspension point.

This is an important factor in determining the potential for impacts due to smothering of organisms that live near or on the seabed. Each of the segments described above were examined to determine the seabed deposition depth and areal coverage, the results of which are presented in the following sections.

4.7.1 Mount Hope Bay and Sakonnet River Sediment Deposition, KP0 to KP34

The model- predicted deposition thickness and area coverage settled sediments associated with the export cable installation operations in Mount Hope Bay and the Sakonnet River are presented in Figure 4-12 and Figure 4-13, respectively. Referring to the figures there is a very clear line of deposition that follows the ECC because the majority of sediment resuspended fell back to the seabed fairly quickly, and therefore in line with the cable route. There is a minor exception to the quick deposition in the area of the Mount Hope Bay entrance where the strong

currents run in and out of the bay perpendicular to the ECC at that point. As seen in the water column concentrations, a portion of the sediments were transported away from the ECC with the currents and therefore settled elsewhere as well. In that they were transported, they were also dispersed and the sediment deposition thickness in that area was consequentially smaller.

A summary of the deposition thickness and footprint area coverage statistics is presented in Table 4-10. The highest deposition thicknesses were contained primarily within a 20 m (65 ft) corridor around the ECC centerline. The 1 mm (0.04 in) deposition depth extended to a maximum of 124 m (406 ft) and 161 m (528) and the 0.5 mm (0.02 in) depth extended to 267 m (876) and 202 m (663) in Mount Hope Bay and the Sakonnet, respectively. Thinner deposits are found at larger distances related to the silt and clay particles that have low fall velocities and therefore experience greater travel distances. Depositions exceeding 1 mm (0.4 in) cover a maximum area of 58 ha (143 ac) in the Sakonnet and 42 ha (104 ac) in Mount Hope Bay for a combined total of 100 ha (247 ac) in the two.

TABLE 4-10. AREA COVERAGE FOR SEABED SEDIMENTATION THICKNESS THRESHOLDS IN MOUNT HHOPE BAY AND THE SAKONNET RIVER (KP0 – KP34).

Thickness Threshold (mm)	Mount Hope Bay Area Coverage KP0 - KP10 (ha)	Maximum Distance from Indicative ECC Centerline (m)	Sakonnet River Area Coverage KP15 - KP34 (ha)	Maximum Distance from Indicative ECC Centerline (m)
0.5	91	267	127	202
1	42	124	58	161
1.5	28	85	43	122
2	22	64	39	87
5	12	15	35	24
>10	1	<10	20	<10

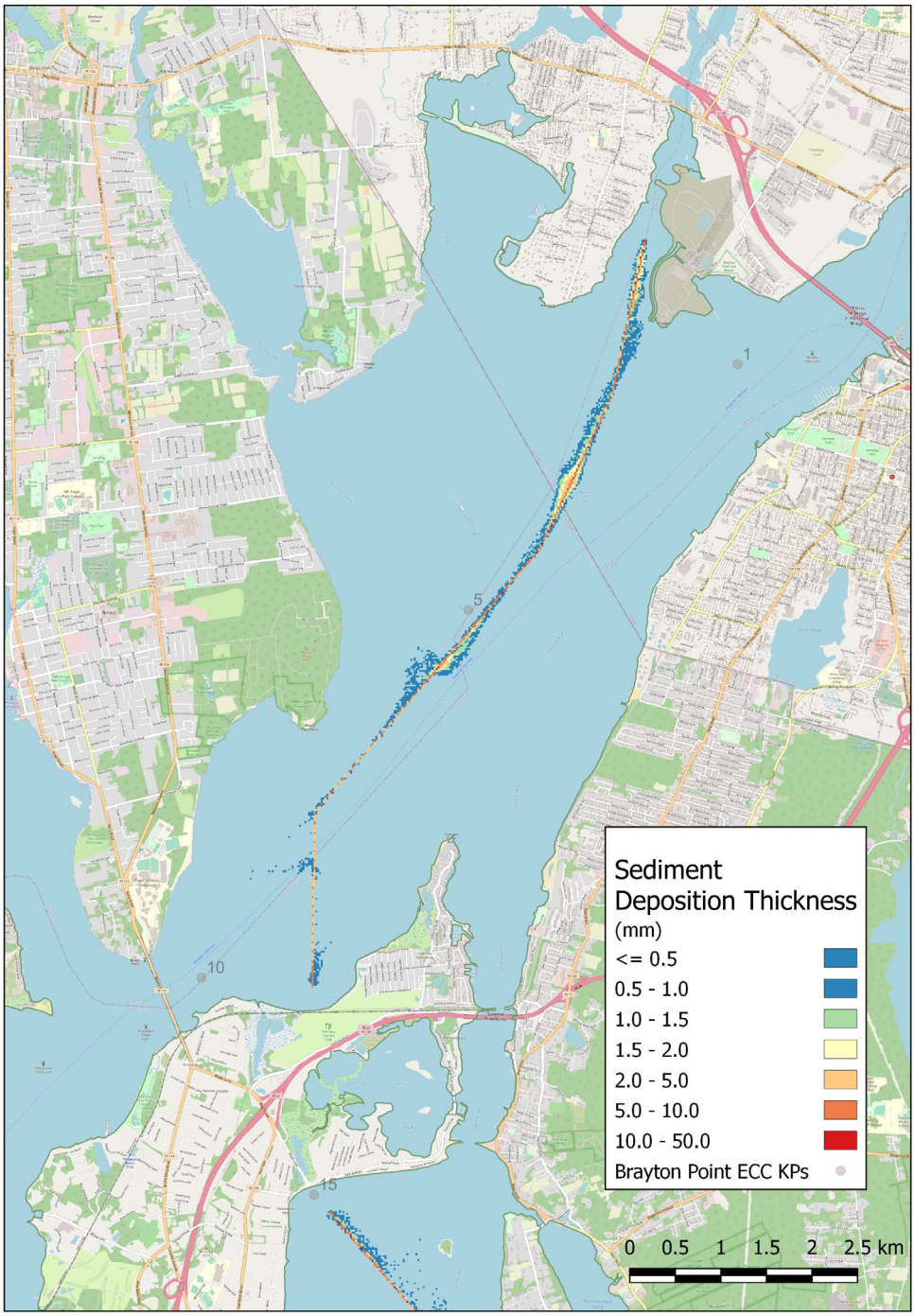

FIGURE 4-12. MAP OF MAXIMUM SEABED SEDIMENT DEPOSITION THICKNESS IN THE MOUNT HOPE BAY PORTION OF THE EXPORT CABLE INSTALLATION, KP0 TO KP10.

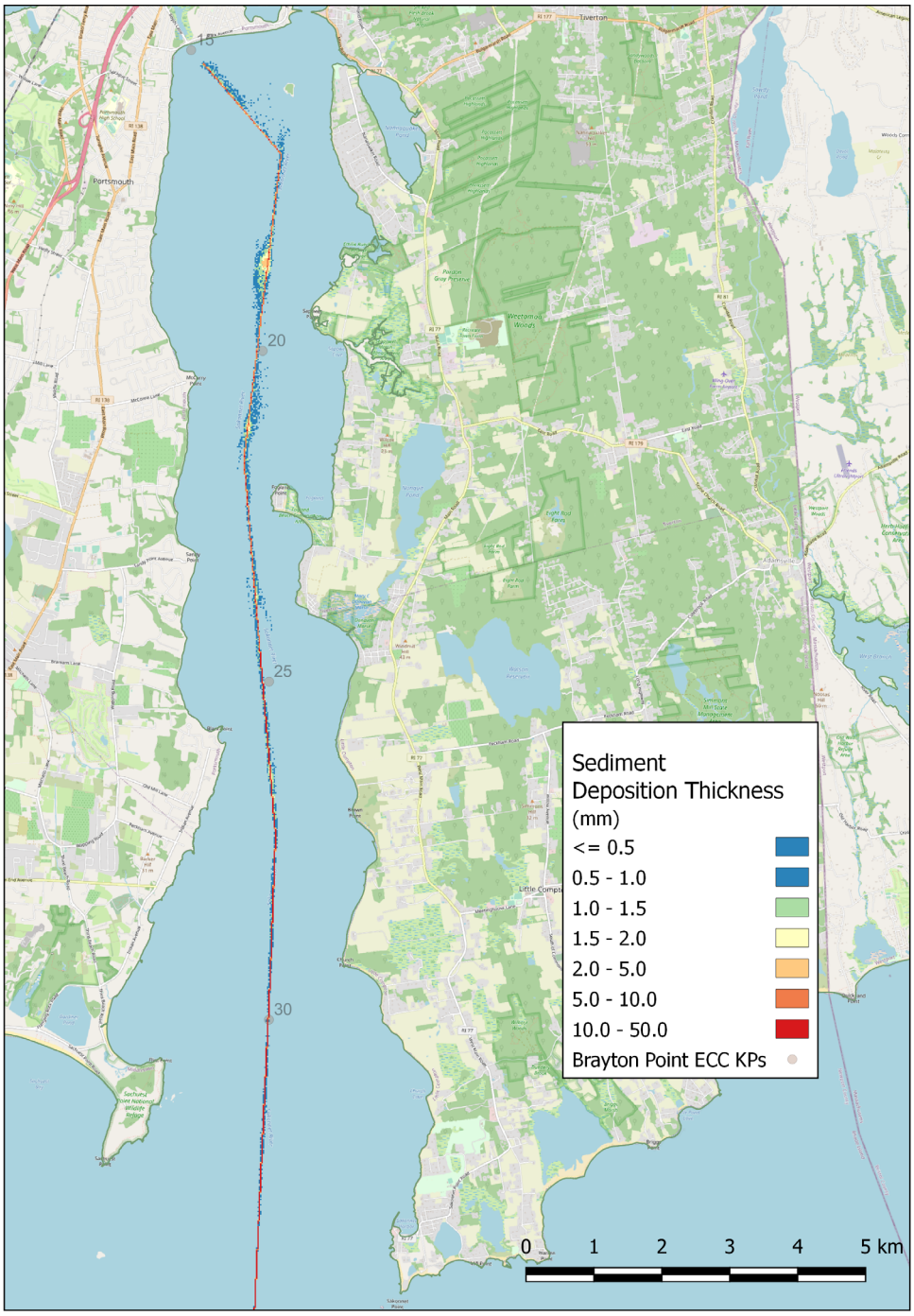

FIGURE 4-13. MAP OF MAXIMUM SEABED SEDIMENT DEPOSITION THICKNESS IN THE SAKONNET RIVER PORTION OF THE EXPORT CABLE INSTALLATION, KP15 TO KP34 .

4.7.2 Offshore Sediment Deposition, KP34 to KP152

The model- predicted deposition thickness and area coverage settled sediments associated with the export cable installation operations offshore are presented in Figure 4-14 and Figure 4-15 for Offshore Segment 1 and Figure 4-16 through Figure 4-18 for Ofshore Segment 2. The deposition coverage along the offshore segments of the export cable installation process was smaller than in the Mount Hope Bay and Sakonnet River segments.

Suspended sediment falling quickly to the seabed and resulting in the line of deposition following the ECC was even more pronounced offshore. There was little deposition outside of the 20 m (65 ft) installation corridor and none outside of the ECC boundaries. The maximum extent of the deposition footprint in the offshore areas was in the region of KP105 where the 0.5 mm (0.02 in) thickness extended 179 m (587 ft) but the maximum 1 mm (0.04 in) thickness extended 59 m (194) from the installation centerline in the area around KP58. A summary of the deposition thickness and footprint area coverage statistics is presented in Table 4-11.

Depositions exceeding a 1 mm (0.4 in) thickness covered a maximum area of 165 ha (407 ac), seen in the Offshore Segment 2 segment and 96 ha (237 ac) in the Offshore Segment 1 River segment for a total area coverage of 261 ha (645 ac) for the entire 118 km (64 nm) length of the offshore ECC. The area covered by 0.5 mm (0.02 in) or greater thickness was 179 ha (442 ac) and 134 ha (331 ac) for the Offshore Segment 2 and Offshore Segment 1 segments, respectively. The total for the entire offshore length of the export cable covered with a deposition thickness of 0.5 mm (0.02 in) or more was 313 ha (773 ac).

TABLE 4-11. AREA COVERAGE FOR SEABED SEDIMENTATION THICKNESS THRESHOLDS ALONG THE OFFSHORE EXPORT CABLE SEGMENTS (KP34 – KP152).

Thickness Threshold (mm)	Offshore Segment 1 Area Coverage KP34 - KP78 (ha)	Maximum Distance from Indicative ECC Centerline (m)	Offshore Segment 2 Area Coverage KP78 - KP152 (ha)	Maximum Distance from Indicative ECC Centerline (m)
0.5	134	88	179	179
1	96	59	165	50
1.5	93	46	163	31
2	92	31	161	28
5	81	<10	121	<10
>10	7	<10	16	<10

The total area coverage at selected deposition thicknesses over the entire length (KP0 to KP152) of the ECC is presented in Table 4-12.

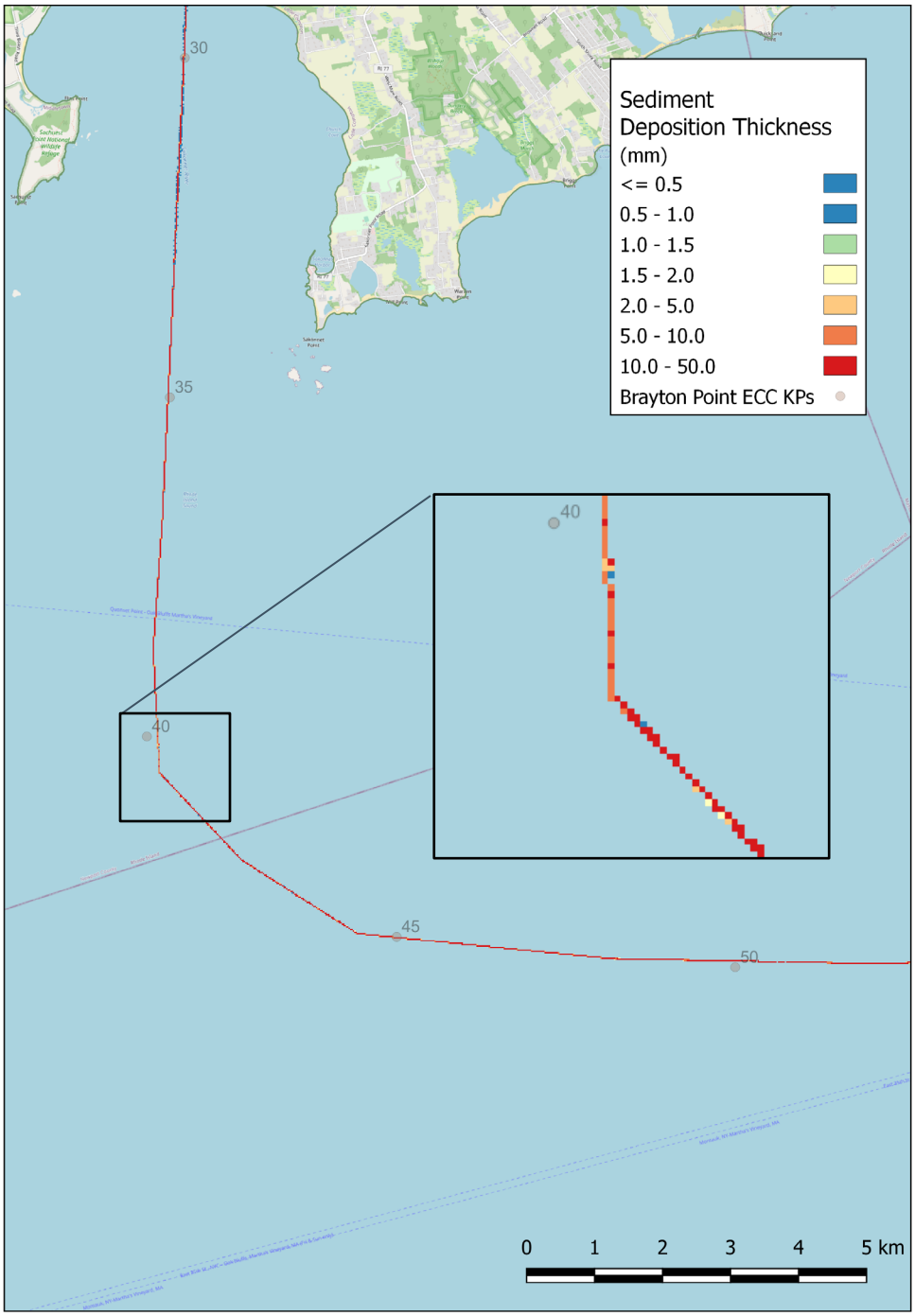

FIGURE 4-14. MAP OF MAXIMUM SEABED SEDIMENT DEPOSITION ALONG THE FIRST PART OF OFFSHORE SEGMENT 1 OF THE EXPORT CABLE INSTALLATION, KP34 TO KP55.

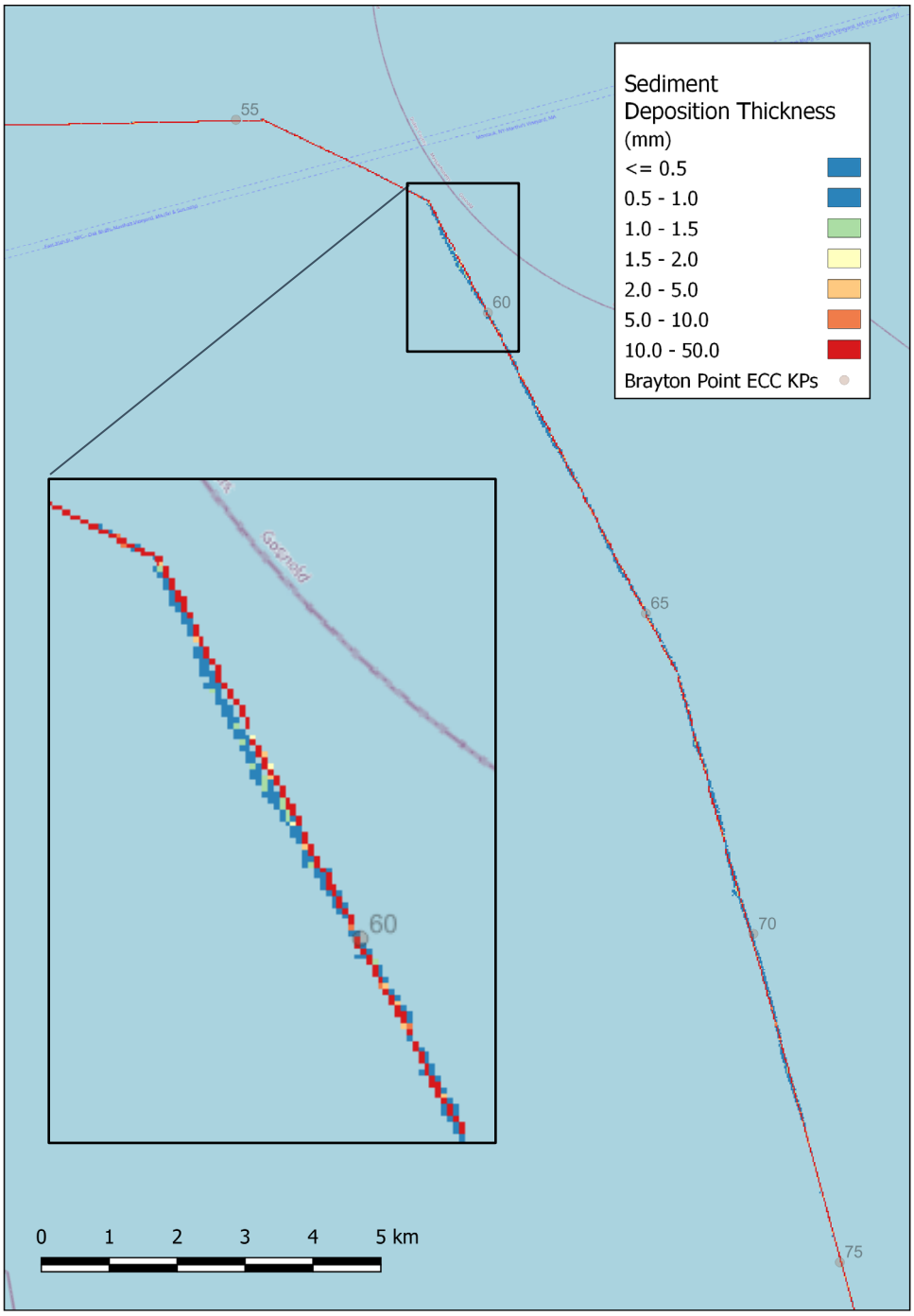

FIGURE 4-15. MAP OF MAXIMUM SEABED SEDIMENT DEPOSITION ALONG THE SECOND PART OF OFFSHORE SEGMENT 1 OF THE EXPORT CABLE INSTALLATION, KP55 TO KP78.

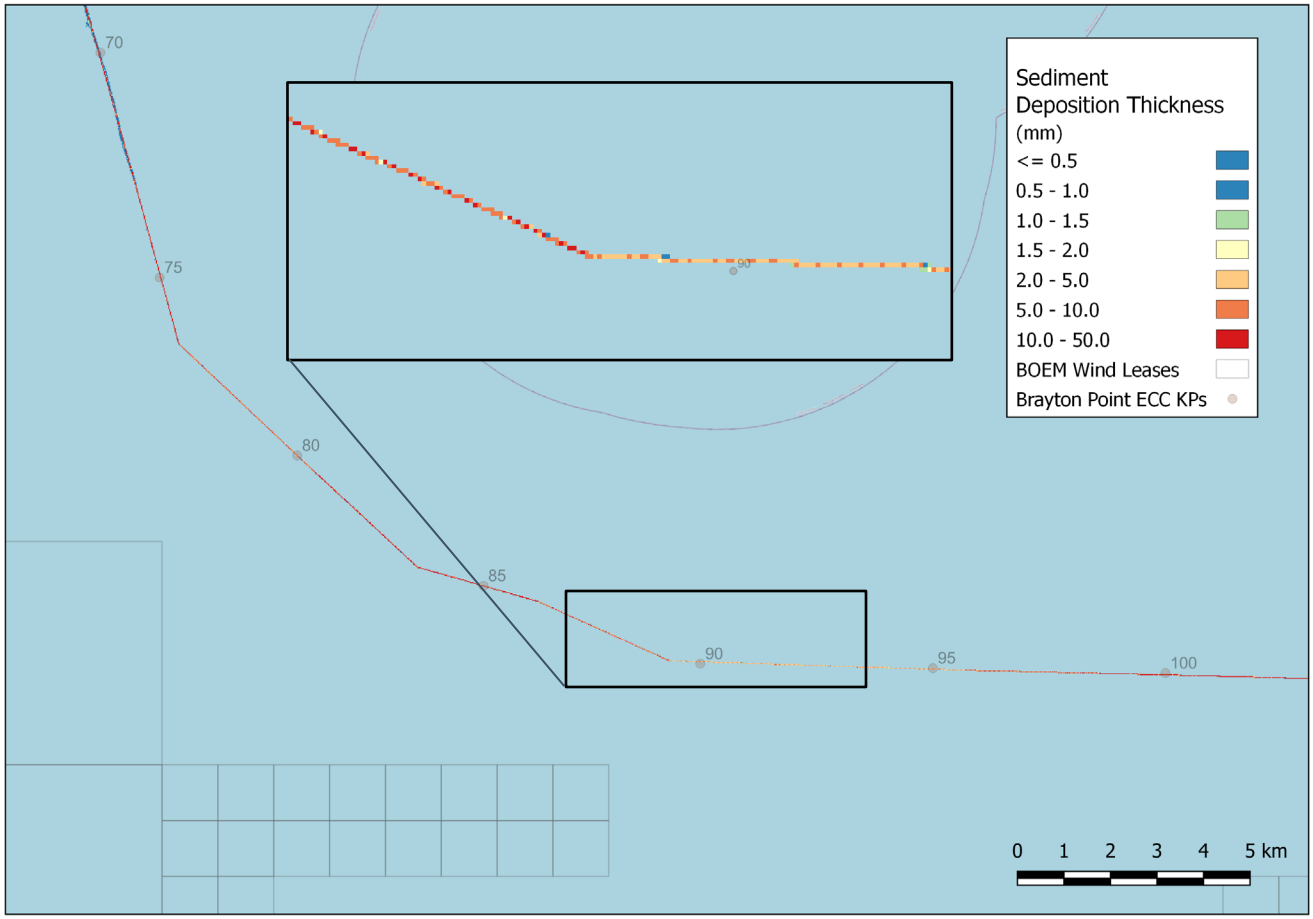

FIGURE 4-16. MAP OF MAXIMUM SEABED SEDIMENT DEPOSITION ALONG THE FIRST THIRD OF OFFSHORE SEGMENT 2 OF THE EXPORT CABLE INSTALLATION, KP78 TO KP105.

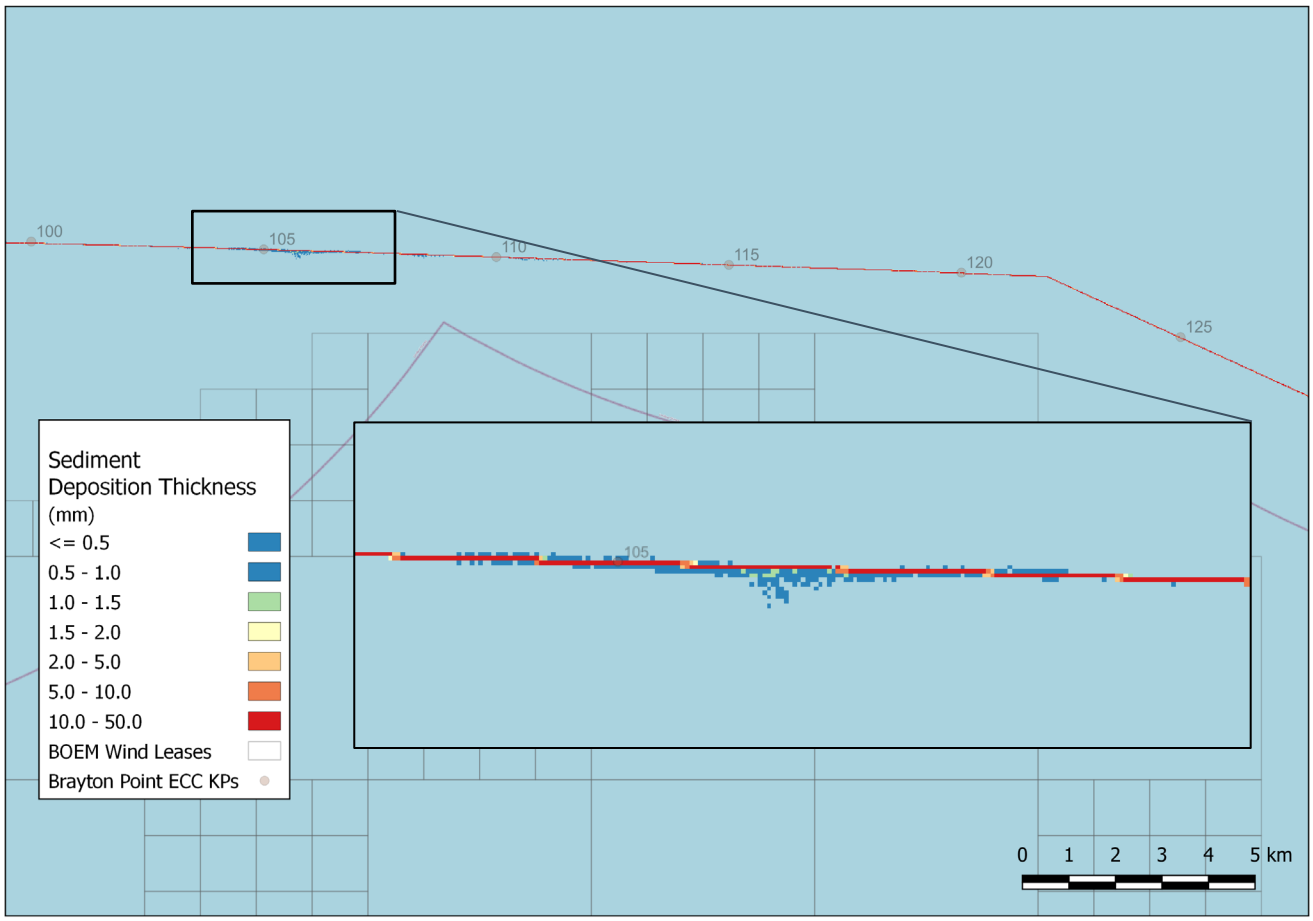

FIGURE 4-17. MAP OF MAXIMUM SEABED SEDIMENT DEPOSITION ALONG THE MIDDLE THIRD OF OFFSHORE SEGMENT 2 OF THE EXPORT CABLE INSTALLATION, KP105 TO KP125.

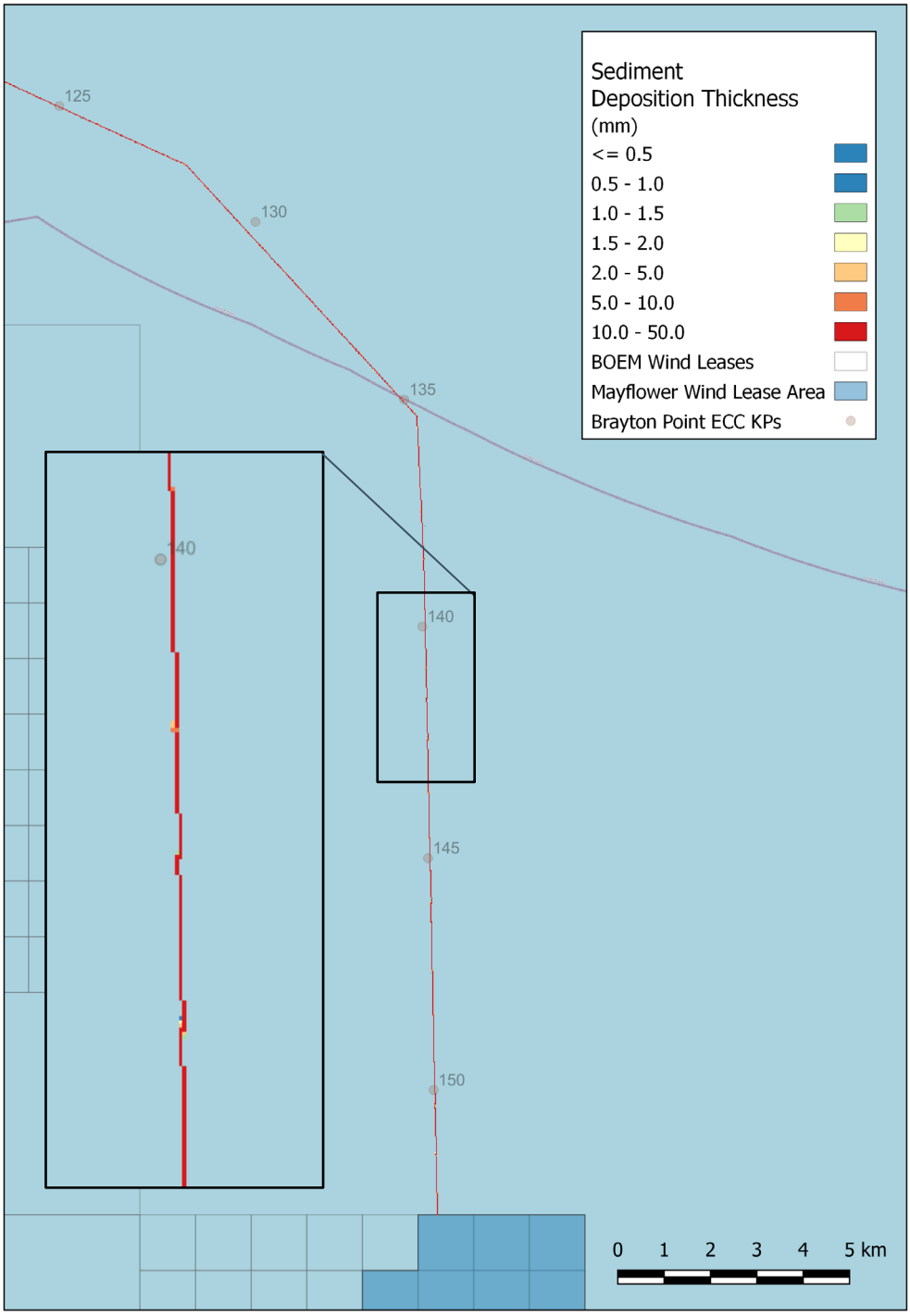

FIGURE 4-18. MAP OF MAXIMUM SEABED SEDIMENT DEPOSITION ALONG THE LAST THIRD OF OFFSHORE SEGMENT 2 OF THE EXPORT CABLE INSTALLATION, KP125 TO KP152.

TABLE 4-12. SUMMARY OF TOTAL AREA COVERAGE FOR SELECTED SEDIMENT DEPOSITION THRESHOLDS OVER THE LENGTH OF THE EXPORT CABLE CORRIDOR.

Deposition Thickness (mm)	Total Deposition Coverage KP0 - KP152 (ha)
0.5	531
1	361
1.5	326
2	315
5	223
>10	23

4.7.3 HDD Pit Excavation Sediment Concentrations

The deposition patterns and depths resulting from sediment resuspension from the HDD pit excavation activities are shown in Figure 4-19. A summary of the deposition thickness and footprint area statistics is presented in Table 4-13. As shown in Figure 4-9, the deposition footprint is small and completely contained within the ECC for all three of the HDD sites. The distance from the excavation site of the 1 mm (0.04 in) thickness threshold was less than a maximum of 95 m (312 ft), at the Brayton Point site but was only 42 m (138 ft) and 57 m (187 ft) at the Mount Hope Bay and Aquidneck sites, respectively. The 0.5 mm (0.02 in) thickness coverage extended to a maximum of 158 m (518 ft) from the Brayton Point site, 56 m (183 ft) from the Mount Hope Bay site and 102 m (335 ft) from the Aquidneck site.

The areal coverage of the 1 mm (0.4 in) threshold thickness or greater were small, at 0.5 ha (1.2 ac), 0.28 ha (0.69 ac) and 0.36 ha (0.89 ac) for the Brayton Point, Mount Hope Bay and Aquidneck sites, respectively. The lower threshold thickness of 0.5 mmm (0.02 in) area coverages were 1 ha (2.5 ac), 0.46 ha (1.1 ac) and 0.92 ha (2.3 ac) at the Brayton Point, Mount Hope Bay and Aquidneck sites, respectively. The numbers indicate that the sediment deposition at the HDD sites had limited impact on the surrounding seabed areas and are well within the ECC in all cases as can be seen in the figures as well.

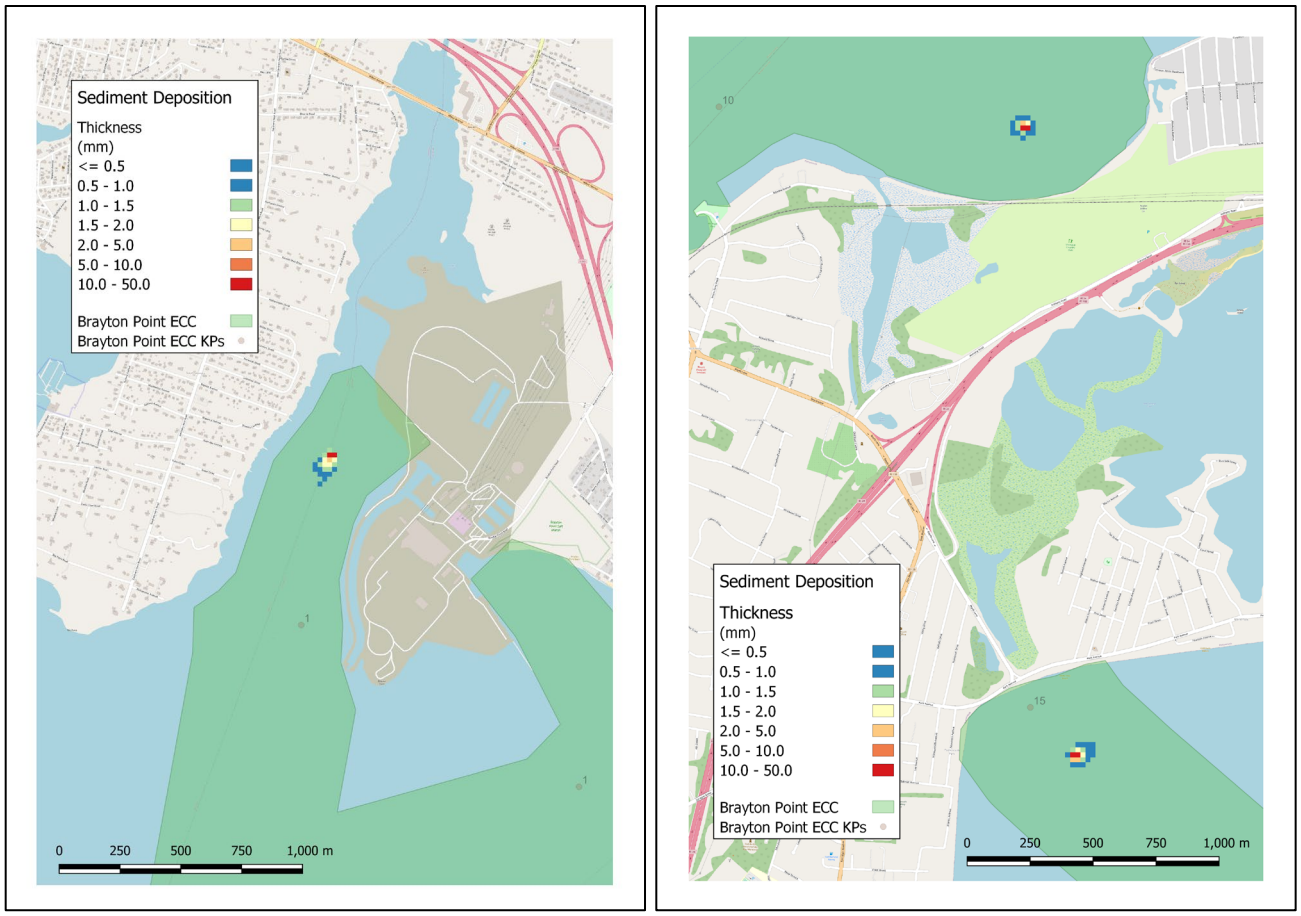

FIGURE 4-19. MAP OF MAXIMUM SEABED SEDIMENT DEPOSITION ASSOCIATED WITH THE EXCAVATION ACTIVITIES AT THE THREE HDD CONNECTION PITS AT BRAYTON POINT (LEFT MAP), AND MOUNT HOPE BRIDGE AND AQUIDNECK ISLAND (RIGHT MAP).

TABLE 4-13. AREA COVERAGE FOR SEABED SEDIMENTATION THICKNESS THRESHOLDS FOR THE THREE HDD PIT EXCAVATION ACTIVITIES.

Thickness Threshold (mm)	Brayton Pt HDD Pit Area Coverage (ha)	Maximum Distance from Release (m)	Mount Hope Bay HDD Pit Area Coverage (ha)	Maximum Distance from Release (m)	Aquidneck HDD Pit Area Coverage (ha)	Maximum Distance from Release (m)
0.5	1.0	158	0.76	56	0.92	102
1	0.5	95	0.28	42	0.36	57
1.5	0.3	76	0.16	41	0.24	50
2	0.1	52	0.12	31	0.16	43
2.5	0.1	42	0.08	29	0.12	31
5	0.1	42	0.08	29	0.08	31
>10	0.1	42	0.08	29	0.08	31

5 DISCUSSION AND CONCLUSIONS

The results of the sediment dispersion modeling study indicated that the water column concentration and the sediment deposition pattern and thickness were most heavily influenced by the properties of the trench sediments disturbed during the cable burial operations and localized current velocities. The dimensions of the trench, the advance rate and the loss rate to the water column, specified the total amount of sediments re-suspended, but the response was short lived for all but the finest grade sediments (silts and clays). A conservative loss rate of 25 percent was assumed for the cable burial operations.

A hydrodynamic model application over the area stretching from the New York Bight to Cape Cod with a fine resolution nested grid for Narragansett Bay was applied to predict the three- dimensional currents and circulation that were used in the sediment model to transport the resuspended sediments. Wind observations from the Mayflower Wind metocean buoy and from the NOAA weather station at Quonset Point were used along with TPXO model tide data to drive the hydrodynamic model. The model- predicted surface elevations and currents were successfully validated using NOAA tide and current stations and the vertical profile of currents at the Mayflower Wind metocean buoy. This procedure assured that the sediment transport from the currents were a reasonable reflection of actual currents that the cable installation operations will likely encounter in the study area.

Surface sediment grab sample data was collected along the ECC at 23 sites used in the modeling. The data showed that the Mount Hope Bay and Sakonnet River segments were mostly characterized by high fractions of the fine grade silt and clay sediment classes (greater than 50 percent), through Mount Hope Bay and the Sakonnet River segments. Offshore, the sediments tended to have higher fractions of fine sand to coarse sand classes with an occasional pocket of silt or very fine sand.

In regions with large clast sizes, sediments re-suspended from the cable burial operations quickly dropped back to the sea floor keeping TSS concentrations low and localized; concentrations above ambient background were limited to within a few meters of the burial tool. The deposition area coverage was small as a result. This was true for most of the offshore segments of the ECC where concentrations of 100mg/L were predicted to be within 50 m (160 ft) of the route and decreased rapidly (less than 15 minutes). The segments of the ECC between KP32 and KP45 and between KP78 and KP100 are particular examples of this, where the currents were low and the sediment grain size distribution favored the larger materials. The sections of the offshore route that were seen to have higher fractions of the fine grade sediments exceeded that response in the model predictions showing the 100 mg/L concentration extending to greater than 300 m (984 ft). These areas are seen between KP55 and KP78 and again in the area of KP100 to KP110.

The sediment deposition footprint resulting from the cable installation activities occurred relatively locally. Along the majority of the route a large fraction of the mass settles out quickly and does not get transported far by the currents. Deposition thicknesses of 1 mm (0.04 in) are generally limited to a corridor with a maximum width of 30 - 35 m (100 – 115 ft) around the cable centerline. In the areas where there are finer grain sediments, the 1mm (0.04 in) thickness contour distance can increase locally to 165 m (540 ft) from the ECC as seen in the area of KP105.

The fine grade materials tend to settle slowly compared to the larger grain size sediments, meaning that the resuspended silt, clay and even very fine sands tend to be transported farther with the tidal currents than the

coarser components and correspondingly higher water column concentrations and longer durations of plumes were predicted from the model. This was the case along the Mount Hope Bay and Sakonnet River segments of the ECC where much of Mount Hope Bay and the Sakonnet River were impacted at low concentration levels.

The higher-level suspended sediment concentrations (100 mg/L TSS and up) were somewhat contained in the Sakonnet River but covered a larger area in Mount Hope Bay. Near the Mt. Hope Bay Aquidneck landing, currents running perpendicular to the EC coupled with fine grade resuspended sediments, increased the overall material transport extending the maximum 100 mg/L concentration a little over 1 km (0.62 mi). Concentrations reached levels of 500 mg/L but were short lived and persisted for approximately 30 minutes to an hour. Concentrations in the range of 200 mg/L or more are not expected to endure for longer than about 2 hours, while the lowest concentrations, in the 10 mg/L range may last several hours after re-suspension.

The conditions creating suspended sediments at the HDD excavation sites were different than those investigated for the cable burial routes. The source was assumed to be at a single point and continuous over a 1- hour period, releasing 100 percent of the dredged material into the water column. The sediments at the three HDD sites were similar (each taken from the nearest surface grab sample site), where, excluding the rock/cobble component, they were comprised of approximately 50 percent silt and 11 percent clay and therefore the material settled relatively slowly to the seabed. Concentrations of 100 mg/L were transported to a maximum of 0.32 km (0.2 mi) from the HDD site but dissipated in a little over an hour. The area coverage of the 100 mg/L or greater level was contained within an average of 5 ha (12 ac).

The sedimentation footprint however was very small with a maximum coverage of the 1 mm (0.04 in) thickness contour of only 0.5 ha (1.2 ac), extending a maximum distance of 95 m (312 ft) and 1 ha (2.5 ac) for the 0.5 mm (0.02 in) thickness contour, extending a maximum distance of 158 m (518 ft) from the HDD site.

Since the time of completion of the sediment transport and dispersion study for the Brayton Point ECC cable burial, additional in-situ data has been collected and analyzed. This is of interest in the lower Mount Hope Bay and upper Sakonnet River areas in that the new data shows a marked divergence from the surface grabs at several points. For the reach of the ECC in Mount Hope Bay near the entrance to the East Passage of Narragansett Bay where the cable centerline is aligned in a north-south direction, perpendicular to the tidally driven currents, two new data points with vertical profiles of the sediments show considerably coarser material. The new data would replace the surface grabs in the southwestern end of the ECC to the HDD connection site on the north side of Aquidneck Island at the Mount Hope Bay entrance. The coarser material would have the effect of reducing the transport and deposition concentration and thickness maxima, respectively, as reported in Section 4 and therefore have less of an impact on the environment.

The same is true of the upper half of the Sakonnet River where three new vertical profiles of the sediment are available. The vertical profile sediment data at the northern end of the Sakonnet River was previously taken from a station more than a third of the distance towards the ocean. The new data shows lower fine grained (silt and clay) percentages particularly in the lower half of the trench. Again, the coarser material would have the effect of reducing the transport and deposition concentration and thickness maxima, respectively, predicted in the study based on the surface grab data also reducing the impacts.

In summary, despite conservative model assumptions, water column concentrations and seabed deposition thickness and extent from the cable burial operations and HDD exit pit dredging remain generally localized and of short duration.

6 REFERENCES

Abdelrhman 2016. Quantifying Contributions to Light Attenuation in Estuaries and Coastal Embayments: Application to Narragansett Bay, Rhode Island. Estuaries Coast. 2017 Jul;40(4):994-1012. DOI: 10.1007/s12237-016-0206-x.

AECOM, 2022. Benthic Community Structure Analysis – Summer, 2021. Prepared by: AECOM, February 2022 as part of the Mayflower Wind Construction and Operations Plan.

CERC (Coastal Engineering Research Center), 1984. Shore Protection Manual, Volume 1. US Army Corps of Engineers.

Codiga, D.L and D.S Ullman. (2010). Characterizing the Physical Oceanography of Coastal Waters Off Rhode Island, Part 1: Literature Review, Available Observations, and A Representative Model Simulation in the Rhode Island Ocean SAMP study area (p. 14). Technical Report 2.

Crowley, D. and D. Mendelsohn, 2010. Hydrodynamics of Block Island Sound (HYDROMAP tidal simulations) for the Rhode Island Ocean Special Area Management Plan. In: Ocean Special Area Management Plan, Vol. 2, Technical Report #6, Appendix A. University of Rhode Island, Narragansett, Rhode Island.

Deltares, 2018a. Delft3D-FLOW User Manual. 3.15 ed. Deltares, Boussinesqweg 1, 2629 HV Delft, P.O. 177, 2600 MH Delft, The Netherlands

Deltares, 2018b. D-WAQ-PART User Manual. 2.15 ed. Deltares, Boussinesqweg 1, 2629 HV Delft, P.O. 177, 2600 MH Delft, The Netherlands

Desbonnet, A., D. Lazinsky, S. Codi, C.Baisden, and L. Cleary, 1992. An Action Plan for the Taunton River Watershed: Assessment and Recommendations. Report of the U. Mass. Boston to the National Oceanic and Atmospheric Administration. Funded by grant NOAA Award No.· NA90AA-H-CZB42.

Egbert, G. D. and S. Y. Erofeeva, 2002. Efficient Inverse Modeling of Barotropic Ocean Tides. Journal of Atmospheric and Oceanic Technology, Volume 19, February, 2002, pp 183 – 204.

EPA, 2016. Modeling Total Suspended Solids (TSS) Concentrations in Narragansett Bay, by Mohamed A. Abdelrhman. U.S. Environmental Protection Agency Atlantic Ecology Division NHEERL ORD, 27 Tarzwell Drive Narragansett, RI 02882 USA National Health and Environmental Effects Research Laboratory Office of Research and Development Narragansett, RI 02882 USA. EPA/600/R-16/195, August 2016.

Federal Energy Regulatory Commission (FERC), 2005. Final Environmental Impact Statements - Weaver's Cove LNG Terminal, (pp 4-70). Federal Energy Regulatory Commission, Public Reference Room, 888 First Street NE; Room 2A, Washington, DC 20426. May, 2005. https://cms.ferc.gov/final-environmental-impact-statements-weavers-cove-lng-terminal (Last accessed 22 Feb, 2022).

Mayflower Wind Construction and Operations Plan, 2021a. Appendix M: Final Benthic and Shellfish Resources Characterization Report Prepared by: AECOM, 9 Jonathan Bourne Drive Pocasset, MA 02559. February 2021

NOAA, 1999. NOAA National Geophysical Data Center. 1999: U.S. Coastal Relief Model Vol.1- Northeast Atlantic. NOAA National Centers for Environmental Information. https://doi.org/10.7289/V5MS3QNZ. Accessed [10/21/2021].

NOAA, 2007. Tidal Analysis and Prediction. NOAA Special Publication NOS CO-OPS 3, 2007. Bruce B. Parker, Ph.D. Silver Spring, Maryland. July 2007.

Shelley, R. C., 1988. Applied Sedimentology. Academic Press, Inc., San Diego, CA, 92101.

Spaulding, M. L., & Gordon, R. B. (1982). A nested NUMERICAL tidal model of the Southern New England Bight. Ocean Engineering, 9(2), 107-126.

Spaulding, M. and C. Swanson, 2008. Circulation and Transport Dynamics in Narragansett Bay. 10.1007/978-0-387-35299-2_8. In: Science for Ecosystem-based Management: Narragansett Bay in the 21st Century, 2008, Eds: Desbonnet, A. and B. Costa-Pierce. Springer Series on Environmental Management, Springer, New York, NY.

Spaulding, M. L., and F. M. White, Circulation dynamics in Mt. Hope Bay and the lower Taunton river. In: Residual Currents and Long-Term Transport, vol. 38, Coastal and Estuarine Studies, edited by R. T. Cheng, pp. 494 – 510, Springer-Verlag, New York, 1990.Wentworth, C. K., 1922. A scale of grade class terms for clastic sediments. J. Geol. 30, 377-392.

APPENDIX 1 - BRAYTON POINT ECC SURFACE SEDIMENT GRAB SAMPLE GRAIN SIZE DISTRIBUTION

SampleID	Easting	Northing	Longitude	Latitude	%Coarse Sand (0.5-1.0 mm)	%Medium Sand (0.25-0.50 mm)	%Fine Sand (0.125-0.25 mm)	%VeryFine Sand (0.062-0.125 mm)	%Silt-(0.0039-0.0625 mm)	%Clay (<0.0039 mm)
21SU-MW0521-BP002	316865.8	4618773.5	-71.20092	41.69969	7.3	6	5.5	5.3	44.5	8.4
21SU-MW0521-BP003	316084.7	4617116.5	-71.20979	41.68460	10.4	6	3.9	5.6	46.4	9.8
21SU-MW0521-BP005	313608.3	4614216.1	-71.23862	41.65792	8.2	8.2	6.3	5.2	32.5	7.8
21SU-MW0521-BP010-BG	314381.2	4604007.4	-71.22618	41.56621	8.8	11.8	5.4	6.2	38.5	8
21SU-MW0521-BP012-BG	314848.1	4598463.4	-71.21887	41.51642	0.4	3.1	48.1	28.2	17.6	2.4
21SU-MW0521-BP013-BG	314775.6	4596531.2	-71.21915	41.49902	1.1	17.4	57.9	21.1	1.7	0.2
21SU-MW0521-BP017-BG	314420.4	4588971.3	-71.22108	41.43089	1	23.4	63.6	7.8	2.4	0.3
21SU-MW0521-BP018-BG	314287.3	4587062.6	-71.22208	41.41368	0.8	27.7	63.5	6.5	1.3	0.2
21SU-MW0521-BP019-BG	314377.4	4585235.9	-71.22045	41.39726	21.6	22.7	3.2	0.4	1	0.1
21SU-MW0521-BPT07-BG	317290.1	4582870.9	-71.18491	41.37664	59.6	28.1	4.7	0.4	0.9	0.2
21SU-MW0521-BP024-BG	324846.7	4582428.0	-71.09448	41.37433	4.6	56.2	34.5	1.7	2.6	0.4
21SU-MW0521-BPT08-BG	329719.7	4581796.7	-71.03607	41.36969	0.9	16.1	75.1	5.3	2.3	0.3
21SU-MW0521-BP028-BG	331367.1	4580016.0	-71.01589	41.35401	2.1	3.8	50.9	33.5	8	1.3
21SU-MW0521-BPT09-BG	334364.8	4574333.1	-70.97852	41.30347	10.9	28.8	26.8	16.5	11.2	2.2
21SU-MW0521-BP035-BG	336209.3	4567713.5	-70.95472	41.24425	8.7	19.5	33.7	17.6	10.1	1.4
21SU-MW0521-BP039-BG	340050.6	4561525.3	-70.90729	41.18931	37.1	22.8	2.7	0.2	1	0.1
21SU-MW0521-BP042-BG	344859.7	4558726.7	-70.84926	41.16505	25.6	58.1	10.1	0.2	1	0.2
21SU-MW0521-BP046-BG	354060.6	4557245.5	-70.73928	41.15342	20.8	7.3	1.2	0.2	0.7	0.1
21SU-MW0521-BP049-BG	359766.8	4557113.7	-70.67128	41.15324	43.9	30.1	5.9	0.5	1.6	0.2
21SU-MW0521-BP052-BG	365453.9	4556948.1	-70.60349	41.15271	4.5	13.2	46.5	15.1	14.6	2
21SU-MW0521-BP058-BG	376862.7	4556558.9	-70.46749	41.15102	12	62.4	22.9	0.9	1.4	0.2
21SU-MW0521-BP063-BG	385790.7	4553858.8	-70.36062	41.12801	4.5	22.8	53.6	7.1	6.7	1
21SU-MW0521-BP068-BG	390918.1	4545193.7	-70.29801	41.05068	11.3	63.1	15	8	2.2	0.2
21SU-MW0521-A080-BG	390041.4	4563662.8	-70.31175	41.21689	0.2	0.4	48.4	48.8	2.3	0.2
21SU-MW0521-BPALT02	317652.6	4618421.7	-71.19136	41.69671	0.15	20.9	14.25	7.5	46.8	10.6
21SU-MW0521-C01-BG	383725.7	4562652.0	-70.38688	41.20691	0.2	3.3	91.3	2.8	2.3	0.3
21SU-MW0521-C02-BG	386552.5	4562690.3	-70.35318	41.20765	0.2	24.6	67.6	3.9	3.4	0.6
21SU-MW0521-C03-BG	385169.1	4561339.7	-70.36942	41.19529	0.2	0.6	82.1	15	2.2	0.3
21SU-MW0521-C04-BG	383714.5	4560170.0	-70.38654	41.18455	0.2	3.6	86.5	6.7	2.9	0.4
21SU-MW0521-C05-BG	386499.5	4560086.7	-70.35333	41.18420	0.2	5.7	87.2	3.2	3.6	0.4

SampleID	Easting	Northing	Longitude	Latitude	%Coarse Sand (0.5-1.0 mm)	%Medium Sand (0.25-0.50 mm)	%Fine Sand (0.125-0.25 mm)	%VeryFine Sand (0.062-0.125 mm)	%Silt-(0.0039-0.0625 mm)	%Clay (<0.0039 mm)
21SU-MW0521-C05-BG-DUP	386499.5	4560086.7	-70.35333	41.18420	0.2	4.1	90.4	3.1	2.3	0.3
21SU-MW0521-C16-BG	325252.4	4589128.9	-71.09157	41.43474	0.2	0.3	32	66	1.8	0.2
21SU-MW0521-C17-BG	322854.2	4587722.4	-71.11984	41.42155	0.2	0.4	18.4	78.5	2.5	0.4
21SU-MW0521-C17-BG-DUP	322854.2	4587722.4	-71.11984	41.42155	0.2	0.4	22.5	74.1	2.8	0.4
21SU-MW0521-C19-BG	386562.5	4562674.3	-70.35306	41.20751	0.2	0.4	25.5	71.6	2.4	0.3
21SU-MW0521-C20-BG	386562.5	4562674.3	-70.35306	41.20751	0.2	0.4	31.3	65.8	2.3	0.3